Application of optimization algorithms in the design of a superconducting A.C. generator rotor

Safi, Sabah K.

APPLICATION OF OPTIMIZATION ALGORITHMS IN THE DESIGN OF A SUPERCONDUCTING A.C. GENERATOR ROTOR

by

Sabah K. Safi

A Thesis submitted in partial fulfilment of the requirements for the degree of Master of Science

School of Engineering and Applied Science

The University of Durham

1990

Declaration

I confirm that no part of the material offered has previously been submitted by me for a degree in this or any other University.

Copyright

ACKNOWLEDGEMENTS

I would like, first of all, to express my many thanks and sincere gratitude to my supervisor, Dr Jim R. Bumby for his guidance and enthusiam during this work.

This work also brings to mind people whose attitudes and efforts has contributed to my educational pursuit: my parents who convinced me of the value of education and my wife who patiently endured my many hours of study.

Finally, a word of appreciation for my fellow graduate students who helped to create an environment which was both enjoyable and broadening.

ABSTRACT

The superconducting a.c. generator is expected to be the optimum choice among a.c. generation systems in future because of its reduced size, high efficiency, high terminal voltage and its contribution to the stability of the power system. Such machines also exhibit unique design problems which remain unsolved. The optimal selection of the basic design parameters is a current problem of interest. This thesis is intended as a contribution in this direction, and a general design strategy has been developed for the superconducting a.c. generator.

Elements of the design process include magnetic field analysis, losses, and mechanical performance all which of are discussed in the thesis.

An analytical model has been developed to help determine the distribution of magnetic flux density inside the superconducting machine. This model takes into account the number, and the geometric structure, of the winding slots and allows the rotor of the superconducting machine to be designed with optimum magnetic field distribution.

A general design strategy has been developed for the superconducting a.c. generator rotor for predicting the optimum design. The design optimization process incorporates "direct search" and random-shrinkage methods. Two direct search methods of minimization have been compared on mathematical functions and also on machine design problems. The best method is highlighted and discussed.

A general computer program package is presented that will optimize and analyse machine design problems. The package is organised in such a way that future addition or deletion of performance specifications, constraints, optimization methods and design process elements are readily implemented.

CONTENTS

LIST OF FIGURES

FIGURES

LIST OF TABLES

Symbols

A	vector potential	
B_c	critical magnetic flux density	(T)
B_r	radial component of flux density	(T)
B_θ	tangential component of flux density	(T)
C_o	constant	
d_x	core loss per unit mass	(kw/kg)
E	Young's modulus	(GP_a)
f_{os}	over speed factor	
$F(\bar{x})$	objective function to be minimized	
$g(\bar{x})$	inequality constraints, feasible when $g(\bar{x}) \geq 0$	
$h(\bar{x})$	equality constraints, feasible when $h(\bar{x}) = 0$	
i	number of equality constraints	
I	total number of equality constraints	
I	current	(A)
J	current density	(A/m^2)
$\widehat{J}_n$	peak current density of the nth order harmonic	(A/m^2)
$\widehat{K}_n$	peak linear current density of the nth harmonic	(A/m)
k_c	concentration factor	
k_g	geometry coefficient	
K_o	geometry factor	
k_{wn}	nth space harmonic winding factor	
l	straight part length	(m)
L	self inductance	(H)
m	number of inequality constraints	
M	total number of inequality constraints	
M	mutual inductance	(H)

n	harmonic number	
n	number of independent variables	
N	total number of independent variables	
N	number of conductors in series per pole pair	
p	number of pole pairs	
p_{co}	eddy current conducting losses	(W)
p_i	internal pressure	(P_a)
p_o	external pressure	(P_a)
$P(\bar{x}, r_k)$	modified objective function to be maximized	
Q	the ratio of tooth width to slot width $(\sigma_{ft}/\sigma_{fs})$	
r	radius	(m)
r_s	mean radius of armature winding	(m)
r_f	mean radius of field winding	(m)
R	r_{fo}/r_c	(m)
S	number of slot-pairs	(m)
S_r	apparent power	(VA)
t	winding thickness	(m)
T_c	critical temperature	(k)
$\bar{x}$	vector of independent variables	
x	r_c/r_{fi}	(m)
y	r_{fo}/r_{fi}	(m)
δ	skin depth of the iron screen	(m)
σ	winding spread angle	(rad)
σ_r	radial stress	(N/m^2)
σ_θ	tangential stress	(N/m^2)
ψ	flux linkage	
ψ	angular displacement of armature	(rad)
α	slot-pairs phase shift angle	(rad)

λ	effective length	(m)
μ_o	permeability of free space	
ρ	conductivity	(s/m)
ρ	rotor body density	(kg/m^3)
ρ_o	winding average density	(kg/m^3)
ρ_x	stator core mass density	(kg/m^3)
ω	angular frequency	(rad/s)
Ω	critical speed	(m/s)

subscripts

a	armature
as	armature slot-pairs
f	field
fs	field slot-pairs
i	inner radius
i	numbering of slot-pairs (1,2,3....S)
o	outer radius
r	radial
θ	tangential
x	environmental screen
z	axial

CHAPTER 1

INTRODUCTION

1.1 Introduction

In recent years the demand for electrical energy worldwide has almost doubled every ten years; a demand which has been met by building increasingly larger machine units. Economic advantages are realised in the capital and operational costs of both the prime mover and the generator as the unit rating increases. A point of diminishing return in economic advantages is reached for the generator above ratings of about 1300 MVA. The economy realised in conventional generators from increased unit rating is a result of the evolution of the generator cooling system permitting higher current densities in the rotor and stator windings. However higher current densities inevitably lead to increased losses in the windings. Thus any advance in the material utilization is limited by demand to keep generator efficiency at the present high level of 98.5% to 98.8%. Further, as the rated current for a given machine is increased, the per unit reactances of the machine are increased and inertia constant is decreased, both of which degrade the transient stability margin. To decrease synchronous reactance, air gap lengths must be increased resulting in the requirement for more excitation power and greater power losses in the field winding. Consequently very large rated machines with a well utilised armature can become less efficient and less economical than smaller machines in an operational sense [Woodson, et al, 1971]. The crossover occurs at rating of about 1300 MVA.

The capital cost advantage associated with higher rated units is off-set above 1300 MVA for conventional generators by construction and shipping considerations. The stator iron makes the larger machines heavy so that they

must be shipped in pieces and re-assembled at site. Rotor diameters are limited by mechanical stresses requiring length increases for increased power rating. Therefore weight increases, proportional to length, further complicate shipping and assembly. Lower rotor mechanical natural frequencies are another result of increased length.

Generators with a superconducting field winding do not require iron in the rotor or stator to produce high magnetic flux density and with no concern with iron saturation problems, the ampere-turns of the field winding can be increased to produce greater flux linkage of the armature winding.

Elimination of the stator iron has several beneficial effects. Firstly, the elimination of iron within the armature provides space for more armature conductors whilst also reducing the machine weight. Insulation problems in the armature are also reduced because of the absence of iron at ground potential so that machines can be designed for higher voltages. Secondly, machines without iron have lower reactances and rotational inertia reduced so that the transient stability margin is improved over the conventional machine [Maki, 1980].

The configuration for a superconducting a.c. generator is as shown in figure 1.1. The armature is at room temperature; it is similar to a conventional armature except for the absence of iron interleaved with the conductor bars. A winding scheme developed by Woodson [Woodson, 1971], permitts the use of much less insulation, and provides better utilisation of the armature space for carrying current. A laminated iron screen surrounds the armature to provide a uniform boundary for the magnetic field.

The low-temperature superconducting field winding is located inside a liquid helium space in the rotor and is maintained at 4.2 K. Surrounding the field winding is a thermal screen maintained at approximately 70 K to intercept thermal radiation from the room temperature parts. The outer

part of the rotor is a conducting electrical screen to intercept asynchronous magnetic field produced in the armature. If the superconducting field winding was exposed to these harmonic fluxes, losses would be produced and the field winding would be driven normal. The layer of steel beneath the electrical screen provides structural support for the screen when it is subjected to large electromechanical stresses under fault conditions.

Superconducting a.c. generators have been shown to process several operational and economic advantages over conventional machines such as higher efficiency, good performance stability, and smaller size [Bratoljic, 1973], [Appleton, et al, 1975], [Edmonds, 1976].

Since the successful operation of the first 45 KVA synchronous generator with rotating superconducting field winding at MIT in 1969 [Thullen, et al, 1971], the development of superconducting generators has received growing attention througthout the world. Meanwhile, several industrial organizations and laboratories have been carrying out theoretical and experimental design studies on different ratings of low temperature superconducting generators. [Luck and Thullen, 1973], [Kirtely and Furuyama, 1975], [Minnich, et al, 1979], [Parker, 1979], [Maki, et al, 1980], [Gillet, 1980], [Ross and Appleton, 1980], [Lambrech, 1981], [Sabrie, et al, 1983], [Yamaguchi, 1984].

In recent years the discovery of high temperature superconductors has reawakend interest in the power engineering application of superconductors and in the development of a high critical current density superconductor into a form suitable for use in power applications. Already three years after the discovery of these high temperature materials considerable progress in Germany, the USSR, the U.S.A, Japan and Britain has been made towards realising these goals [Kirtley, 1988].

Initial studies on the development of superconducting generators indicated that the high magnetic field capability of the superconducting field

winding would allow an increase in the magnetic flux density at the armature compared to that of the conventional machine [Woodson, et al,1971] and that there would be a dramatic reduction in both weight and volume compared to the conventional machine. Later research (i.e. theoretical and experimental) suggested that these gains may be somewhat less dramatic [Kirtley and Furuyama, 1975], [Maki, al et, 1980], [Gillet, 1980]. However, using theoretical and experimental analysis methods to determine the characteristic of superconducting machines, there is no way of ensuring optimum characteristic. This is an unfortunate restriction since superconducting generators can have considerable economic advantages over the conventional machine if an optimum design can be ensured. The usefulness of such theoretical and experimental design methods can only be guessed until a strict mathematical design technique is available. The use of mathematical optimization design methods on superconducting machines has not yet been applied. Consequently, the purpose of this research is to present the design philosophy and implementation of a strict mathematical optimization procedure in the design of superconducting a.c. generators.

1.2 Design tools and models

In section 1.1, it has been shown that the design features of the superconducting generator differ considerably from those of the conventional generator. This has resulted not only in models to simulate the physical phenomena involved in the new design concepts but also new analytical methods. The absence of iron in the active volume of the machine results in magnetic field solutions which differ from those for a conventional machine (i.e. the active volume of the machine is treated as free space containing a region of uniform current density with boundaries of fixed permeability). The

development of a two dimensional magnetic field analysis for a superconducting rotor winding is an example of this [Hughes and Miller, 1977], [Kirtley, 1971].

In addition, the reliability of the superconducting generator should not be less than that of a conventional generator. To attain such a high reliability has demanded the development of accurate methods of predicting the performance characteristics of the machine during the design stage. Some of the perfomance indicators of concern in the design of these machines are reactances, short-circuit forces and losses. To evaluate these quantities, the electromagnetic fields of the machine must be accurately predicted. Further problems of concern in the design of the machine are related to the magnitude and nature of high localized flux densities appearing around the field winding open edge (outermost slot). Localised flux concentration particularly in this region, can cause performance difficulties [Bumby, 1981]. In addition, as in conventional machines, apart from increasing the electric and mechanical stresses, raising the specific outputs of a machine has meant a greater demand being made on the magnetic circuit.

Although problems in such areas have been prominent for some time, it has been possible to produce analytic expressions to calculate the magnetic field distribution in and around the superconducting generator with simplified models of the machine geometry. Hughes and Miller [Hughes and Miller, 1979] derived expressions for electrical parameters of the machine based on the current sheet (i.e. assuming the winding has zero thickness). Kirtley [Kirtley, 1971] and Martinelli [Martinelli and Morini, 1980] extended these expressions to take into account the thickness of the windings. In this thesis, the work is extended to include the number and geometry of slots of both field and armature windings.

Stress analysis is of importance to design and optimization work in so far as it effects the geometric components. The inner rotor which contains a

liquid having a free surface in its internal space was quite a new case. Thus, the mechanism of stress analysis of the inner rotor will need to be considered in a fashion very different from the conventional rotor.

Some solutions to these problems are discussed in the following chapters.

1.3 Optimization in the design process: An informatics point of view

The design of a superconducting machine is normally accomplished by an interactive process such that a preliminary design is done based on a set of empirical assumptions. The dimensions are then used to determine the flux density distribution and consequently the performance of the machine. The final step involves the modification of the dimensions and assumed parameters to meet the desired specifications and constraints. The actual design process involving the selection of design parameters which meet the behaviour requirements are, in some sense, optimum but has mainly been left to the experience and intuition of the designer.

With advances over the past two decades in digital computers, the computer now plays a dominant role in the design process of superconducting machines. In the situation described above, the use of computers in machine design starts with their application to the determination of machine characteristics. In fact, any designer wants to achieve the design that is best according to some properties, while not violating any of the imposed design constraints. In order to verify whether these goals are really met, the characteristics of the machine design are determined by using theoretical and experimental analysis methods. Very probably the first design will lack some essential characteristics or violate some constraints. The design is modified by changing some of the design parameters (i.e. rotor dimensions). The design

is repeatedly re-calculated and re-analysed until significant improvements can no longer be obtained, or it is decided that continuing the search is useless.

In the situation described above, the computer is used only to derive parameters which are used in obtaining a satisfactory final design. A logical extension of this classical way of designing using computers is one in which the computer drives the parameters towards the final design. The analysis methods are then interactive with the optimization system which decides how to vary the design parameters in order to find the optimum with a minimum of effort. Furthermore, when a suitable mathematical optimization technique is used, this way of designing will be generally more efficient and the result really is an optimum. Besides, mathematical optimization is applicable to a higher dimensional space than the designer can manipulate. Therefore, using mathematical optimization techniques can be advantageous.

Some powerful methods are available for use in optimization [Himmelblau, 1972]. For machine applications, methods for constrained non-linear optimization problems are especially relevant. In recent years, research in this particular field has resulted in a number of efficient and reliable computer methods. Anderson [Anderson, 1967] used a Monte carlo random search method routine to optimize power transformers and generators. Ramarathnam [Ramarathnam et al,1973], Singh [Singh et al, 1983], Nagrial [Nagrial and Lawrenson, 1978], [Bharadwaj et al, 1979], and Pavithran [Pavithran et al, 1987] used the sequential unconstrained minimization technique by Fiacco [Fiacco and McCormick, 1968] to optimize the design of an induction motor. Minzies [Minzies et at, 1975] and Chidambaram [Chidambaram et al, 1982] used an optimization program based on a least p-th approximation method by Bandler [Bandler, 1972], for an optimized design of a large and small induction motor.

The use of direct search optimization is also rapidly expanding in

different fields of engineering design e.g. field analysis, power system studies, circuit analysis, structural engineering, chemical engineering etc. They are very useful methods for finding the minimum of an objective function where derivatives can not be evaluated easily which is often the case in practical design problems. These techniques are iterative in nature and may use considerable computer time depending on the problem complexities so that an efficient and reliable routine is essential. Moreover, some optimization methods may solve simple mathematical functions, but fail to produce an acceptable solution to complex engineering problems. All the existing optimization methods have been developed to solve unconstrained problems (i.e. no constraint on the parameters), but most of the design problems place limits on the values of different parameters. There are no universal methods available for solving constrained non-linear problems. In practice a constrained design problem is transformed to an unconstrained one and then solved using some efficient method for unconstrained optimization. Special care is required in selecting the proper minimization method to reach a solution at reasonable cost. With this in mind, the principle reason for the selection of search methods of minimization will be discussed in detail in chapter 4.

1.4 Design optimization of superconducting machines

An optimum design for the superconducting a.c. generator can be defined in many ways depending on the performance requirements. The objective of this study is to examine the essential feature in the design optimization of a superconducting generator. The principle objective function of the design problem is to maximize the magnetic power of the inner rotor. This is achieved by applying non-linear mathematical programming methods. However, the objective function is formulated in terms of all the parameters

(or variables) associated with the machine magnetic circuit. These parameters are also used to formulate some important design peformance indices which act as inequality design constraints.

1.5 Research presentation

This thesis consists of six chapters. Chapter two discusses the magnetic field analysis applicable to the electromagnetic design of the superconducting machine. This includes a two dimensional field analysis by the most common types of models and a study which compares the differences involved in their adaption to the calculation of the magnetic field. This chapter also describes a new method for magnetic field calculation which takes into account the geometric structure of the slots.

The third chapter presents the design procedure. This chapter describes in detail the main behavioural requirements such as material stresses, critical speed, superconductor performance and stator core saturation. In addition, some analytical methods are developed to represent the behavioural constraints such as stresses due to critical speed and maximum flux density allowed in the stator core.

The fourth chapter is devoted to the study of direct search methods of minimization for machine design. This chapter also discusses general non-linear programming applied to the design problem, its formalution, it's relation to other types of programming and its selection for optimal solution. Further sections in this chapter describe the direct search methods used in the minimization (or maximization) procedure. These methods are compared on standard mathematical functions and also on design problems. Different penalty function approaches are studied in conjunction with efficient optimization routines. The results illustrate the behaviour of the direct search

and the shrinkage methods when applied to test and design problems. The final section of this chapter draws the work to a conclusion by examining the performance of the direct search methods in general terms to provide a basis for the study of optimum design of the superconducting a.c. generator.

The next chapter deals with the optimization of the rotor structure for a superconducting a.c. generator. This chapter presents the mathematical formulation of rotor design in the context of an unconstrained optimization problem in conjunction with a penalty function. This problem is solved using the methods of pattern search [Hook and Jeeves, 1961] and simplex search [Nelder and Mead, 1965]. A comparative study of the synthesis based on these procedures is given. In addition, a design optimization package developed to solve the design problem is presented. An overview of the package structure is given, and this is followed briefly with an outline of the constituent routines.

In the final chapter, the main conclusions of this study are drawn together and recommendations for futher work made.

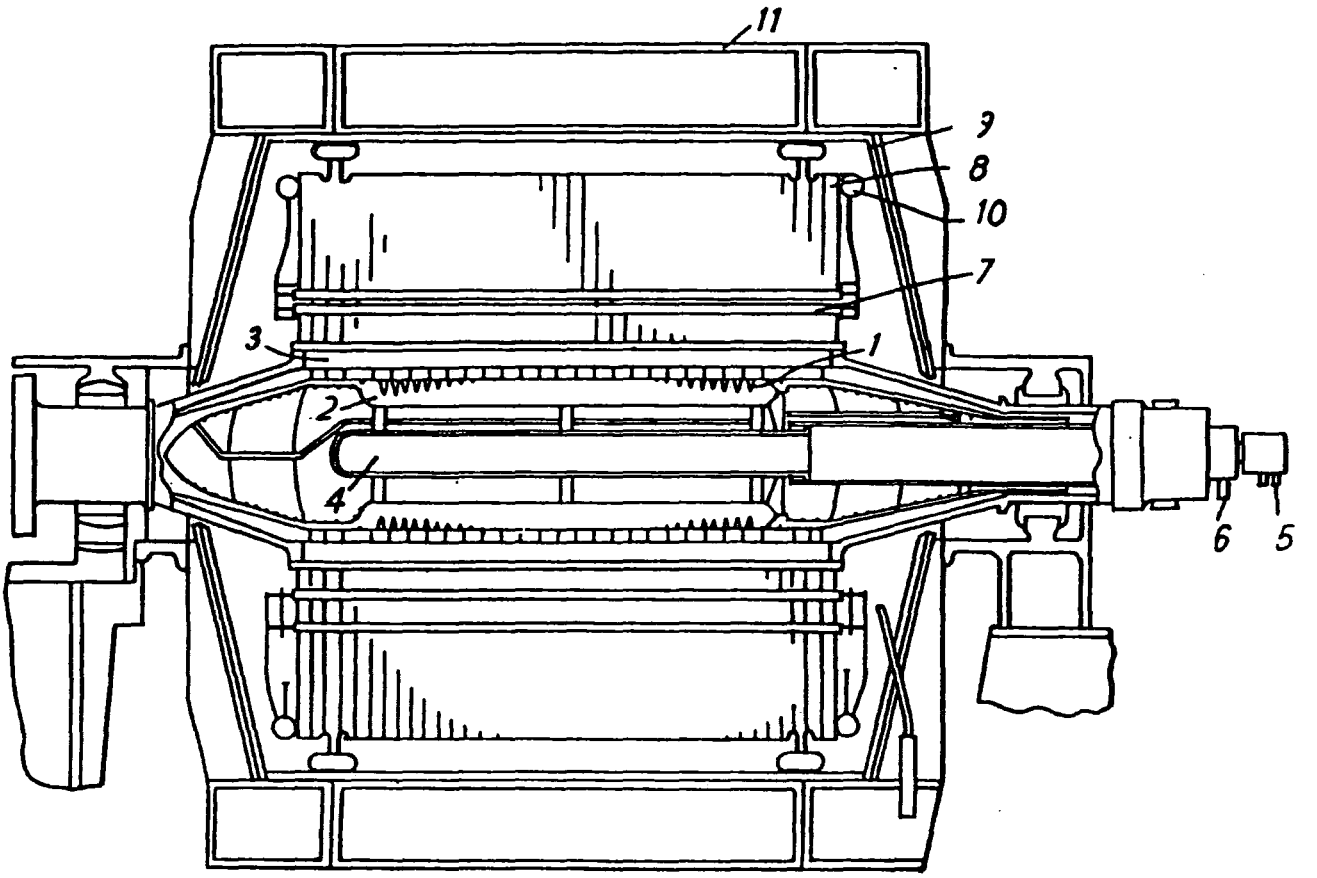

Figure 1.1 Longtudinal section of a generator with superconducting field winding

(1) superconducting winding

(2) inner rotor

(3) rotor screen

(4) refrigerator

(5) helium

(6) vac connection

(7) stator winding

(8) inner stator structure

(9) copper screen

(10) water mainfold

(11) outer stator casting.

CHAPTER 2

FIELD ANALYSIS OF A SUPERCONDUCTNG GENERATOR

2.1 Introduction

The concept of electromagnetic interaction between the mutually coupled rotor and stator magnetic fields remains the basis of operation any superconducting machine regardless of its configuration. The calculation of the the output voltage waveform, power, inductances as well as the magnetic forces, all depend on a knowledge of the magnetic field distribution. Thus it is essential to study the magnetic field distribution in a superconducting a.c. generator where concern is directed towards the optimum design criteria and improved performance of the machine.

Perhaps the greatest constraint on the design of a synchronous machine with either a low, or high, temperature superconducting field winding is related to the superconductivity state. All superconductors exhibit a limitation on the conductor current density, this maximum current density being a function of the flux density at the winding. As a consequence of this, the maximum permitted current density in the superconducting field winding is limited because there are localised field concentrations around the winding resulting from space harmonics which tend to concentrate the flux density around the outermost slot [Bumby, 1981]. If the superconducting field winding is located in slots, it cannot be arranged freely without being affected by the geometric structure of the slots themselves. Consequently, it is important to determine the maximum magnetic field within the field winding, so that the behaviour of the superconducting wire can be predicted more accurately. At the same time the field winding configuration must produce a sinusoidally distributed flux density at the armature winding to minimise harmonic voltages in the

armature.

In the past magnetic fields at the rotor and stator winding have been analysed on the basis of either a current sheet model [Hughes and Miller, 1977], or by assuming the current density is uniformly distributed over the winding spread angle and thickness [Kirtley, 1976], [Martinelli and Morini, 1980]. These models of the rotor and stator windings, although producing useful information, are based on simplifications concerning the geometry of the machine winding such that the finer points of the geometrical structure are overlooked. This chapter describes a new model, which permits the evaluation of the magnetic fields relative to the number and geometry of the slots. This approach has some similarities to the method adopted by Martinelli and Morini [Martinelli and Morini, 1981]. In their work Martinelli and Morini assumed the field winding to be distributed uniformly in all slots, assuming equal ampere-turns in all slots. The work presented here avoids such an assumption allowing the use of graded windings and different slot geometries to be studied if required.

The new model is believed to be a useful contribution to the study of the magnetic field distribution inside superconducting machines. It can be applied without limitations to rotors with different winding arrangements. To show the effectiveness of the proposed method the model is applied to the analysis of the space harmonic magnetic fields produced by different structures of field winding with axial slots. The investigation shows that the magnitude of harmonic flux density components can be affected not only by choosing a suitable spread angle for the winding but also by the aspect ratio of the slot to tooth width.

2.2 Field Analysis by Former Methods

2.2.1 Model of Analysis

Before describing the development of the new model, it is appropriate to summarize the performance of former models and give an indication of the magnetic fields computed using such models. The expressions for the magnetic field components produced by former methods have been used as a starting point from which to develop the new model proposed in this chapter. Former methods employ one of two types of model. These models are briefly described below:-

(a). Thin cylindrical current sheet model. In this model the thickness of the winding is ignored and all the current is assumed concentrated in a thin current sheet situated at the mean winding radius. The vector potential produced by current sheet is analyzed in Appendix 1.

(b). Thickness model. Here the winding is represented by its actual thickness and therefore it is necessary to integrate the vector potential given by the current sheet model with respect to the winding thickness to derive the actual electromagnetic fields. The results of such an integration are shown in Appendix 1. These field expressions are presented in table 2.1.

The electrical parameters of this machine are coefficient of the flux-current relationship.

$$\begin{pmatrix} \psi_a \\ \psi_b \\ \psi_c \\ \psi_f \\ \psi_{kd} \\ \psi_{kq} \end{pmatrix} = \begin{pmatrix} L_a & M_{ab} & M_{ab} & M_{af} & M_{ad} & M_{aq} \\ M_{ab} & L_a & M_{ab} & M_{bf} & M_{bd} & M_{bd} \\ M_{ab} & M_{ab} & L_a & M_{cf} & M_{cd} & M_{cq} \\ M_{af} & M_{bf} & M_{cf} & L_f & M_{fd} & 0 \\ M_{ad} & M_{bd} & M_{cd} & M_{fd} & L_d & 0 \\ M_{aq} & M_{bq} & M_{cq} & 0 & 0 & \end{pmatrix} \times \begin{pmatrix} i_a \\ i_b \\ i_c \\ i_f \\ i_{kd} \\ i_{kq} \end{pmatrix} \quad 2.1$$

These inductances are found by an additional integration of the flux

linkage produced by the fields listed in table 2.1 over the area of the winding (see appendix 1). These are represented by self and mutual inductance of set windings in the configuration of the machine which are given in table 2.2.

Included in the expression for each parameter is an effective length. This effective length may differ between windings in the same machine, and may in fact not correspond to any physical length in the machine.

Since the two dimensional work is used to describe a three dimensional effect with end effects not accounted for, provision for them must be included in the effective length, λ.

2.2.2 Field Solution by Former Models

The analytical expressions for the magnetic fields derived from the above models are used to compute the flux density distribution produced by the superconducting rotor of a two pole 1300 MVA superconducting generator shown in figure 2.1. The main parameters for this generator are tabulated in table 2.3

The radial variation of flux density produced by both the current and the thickness models are shown in figures 2.2, 2.3 and 2.4. These graphs are used as a basis for predicting and comparing the flux density distribution produced at no-load by the superconducting field winding. Figure 2.2 compares the peak value of the fundamental component of radial flux density calculated using the above models. Both the thickness and current sheet models give similar results with the only significant difference between the two being near the winding where the current sheet model is observed as being less accurate. This should be expected as the superconducting field winding is represented by a current sheet of zero thickness whereas the thickness model takes into account the winding thickness, thus giving a more accurate result for the magnetic field at the winding. However, the main features of the two models

are reported in figures 2.3 and 2.4 which show, in more detail, how the methods compare at no-load. These figures show the variation of both radial and tangential flux density components at angle of 0,15,30 and 45 degrees relative to the rotor axis and the influence space harmonics have on the field distribution. Because of the space harmonics, there is a definite increase in the radial flux density component as the angle is changed from 0 to 30 degrees with a significant concentration of flux density at 30°, the outermost edge of a 120° phase spread winding. Typically this flux density concentration is 1.32 times the value at $\theta = 0$. Further away from the winding the space harmonics rapidly diminish such that they have negligable influence on the magnetic field calculation. Similar flux concentrations have been reported previously [Bumby, 1981] and, as they are due to the geometrical design of the winding, this chapter extends the analysis to evaluate what effect the design of the actual slots, or conductor distribution, will have on the flux distribution.

2.3 Theoretical Approach to the New Model

2.3.1 Representation of a new model

The new model proposed in this section assumes a winding to be built up from an independent set of slot pairs, each pair having independent currents. In this way field windings can be thought of as being distributed into several slot-pairs per pole-pair each shifted in space relative to each other by some angle α as shown in figure 2.5. The new two dimensional model allows the field winding to fall into many paired slots which may be of any size or shape.

2.3.2 The magnetic field analysis by the new model

The magnetic field calculation is based on each paired slot so that the field winding becomes an aggregate of the many different slots involved. Assume that the field winding under consideration has several slots per pole. In this case the winding has, for every pole pair, S slot pairs separated by geometric angle (α) such that the calculated resultant of magnetic flux density is obtained by adding the magnetic flux density produced by the each slot pair i.e. $B_1(B_{r_1}, B_{\theta_1})$, $B_2(B_{r_2}, B_{\theta_2})$, $\ldots$, $B_s(B_{r_s}, B_{\theta_s})$. The radial and tangential flux density components for each slot pair are calculated using the thickness model equations but with the winding spread replaced by the spread angle of each individual slot. In addition the equations for each slot pair are phase shifted from the reference axis by the shift angle (α). Using the principle of superposition, the radial and tangential flux densities due to each of the winding slots-pairs are added vectorially, to obtain the resultant components, such that for the field winding:

$$B_{r_f}(r,\theta) = \sum_{i=1}^{S} \sum_{\substack{n=1 \\ n=odd}}^{\infty} B_{i_{r,n}}(r) cosnp(\theta \pm \alpha_i) \tag{2.2}$$

$$B_{\theta_f}(r,\theta) = \sum_{i=1}^{S} \sum_{\substack{n=1 \\ n=odd}}^{\infty} B_{i_{\theta,n}}(r) sinnp(\theta \pm \alpha_i) \tag{2.3}$$

Whilst for the armature winding

$$B_{r_a}(r,\theta) = \sum_{i=1}^{S} \sum_{n=1}^{\infty} B_{i_{r,n}}(r) cosnp(\theta \pm \alpha_i - \psi) \tag{2.4}$$

$$B_{\theta_a}(r,\theta) = \sum_{i=1}^{S} \sum_{n=1}^{\infty} B_{i_{\theta,n}}(r) sinnp(\theta \pm \alpha_i - \psi) \tag{2.5}$$

The full derivation of these equations is presented in Appendix 1 whilst the results generated by these equations are presented in table 2.4.

2.3.3 Inductances calculation by the new model

To determine the inductances of the slotted winding, the procedure is the same as in the thickness model with the exception of the geometrical angle (α). In this case, the magnitude of the winding flux linkages are derermined by combining the flux linkages of slot-pairs. As a result, the self and mutual inductances are

self-inductance for the field winding

$$L_{f_s} = \sum_{i=1}^{S} \sum_{n=1}^{\infty} L_{i_{f_s}}(n) \times cosnp(\alpha_i) \tag{2.6}$$

self-inductance for the armature winding

$$L_{a_s} = \sum_{i=1}^{S} \sum_{n=1}^{\infty} L_{i_{a_s}}(n) \times cosnp(\alpha_i) \tag{2.7}$$

Maximum inductance between armature winding

$$M_{ab_s} = \sum_{i=1}^{S} \sum_{n=1}^{\infty} L_{i_{a_s}}(n) \times cosnp(\alpha_i + \psi - \frac{2\pi n}{3}) \tag{2.8}$$

Maximum inductance between armature and field winding

$$M_{af_s} = \sum_{i=1}^{S} \sum_{n=1}^{\infty} L_{i_{af_s}}(n) \times cosnp(\alpha_i + \psi) \tag{2.9}$$

2.3.4 Validation of the new model

Using the 1300 MW generator data in table 2.3, the new model is validated by assuming there is no space between the rotor slots so that the radial flux density distribution can be compared with that calculated by the thickness model, figure 2.6. As expected both models agree in value and shape which confirms the validity of the new model.

2.4 The Influence of Slot Configuration on Magnetic Field

2.4.1 General consideration

As was noted in section 2.2.2 the geometry of the winding configuration can influence the magnetic field distribution within the winding itself and, as this can be critical to the safe operation of the superconductor, requires further investigation. As the aim of the designer is to minimise harmonic fields within the winding itself while producing a sinusoidal distribution at the armature correct selection of winding geometry is vital. Usually a winding spread angle of 120° is used as this eliminates the third harmonic component in the flux density waveform and, as flux density reduces with radius as $((r_f/r)^{np+1})$, this eliminates a major cause of harmonic distortion at the armature. However, the effect on field concentration within the winding itself is much less clear as is the effect the individual geometry may have on any flux concentrations. This section, is aimed at exploring such effects.

To analyse such slot geometry effects the magnitude of the flux density components have been determined for different values of Q, where Q is the ratio of tooth width to slot width ($Q = \sigma_{ft}/\sigma_{fs}$). The data for the 1300 MVA generator tabulated in table 2.3 is used for the study. Magnetic fields are calculated at no-load.

2.4.2 Comparison Between New and Former Models

To indicate the type of problems that may occur with the simpler analytical models figure 2.7 and 2.8 present results for the radial and tangential magnetic field components calculated by the three models and show how these vary with both radius and circumferential position. In calculating these distributions all the influencing harmonics have been included whilst for the new model a tooth width to slot width ratio of $Q = 1/5$ has been used. In

addition figure 2.9 shows more clearly how the peak radial and tangential components of no-load flux density compare at $\theta = 0$ and $\theta = 90°$ respectively. All the results show that the calculated magnetic field in regions signifcantly removed from winding coincide whereas significant differences are to be found in the region of the winding itself. The results also indicate that the difference between the new model and the thickness model is lower than the difference which appears between the thickness and the current sheet models. All the differences are due to the errors introduced into the calculations by the progressively simplifying assumptions made regarding the geometry of the winding in moving from the new model, through the thickness model to the current sheet. From the results, it can be seen that the new model has better accuracy than former models.

Because of the importance of flux concentration in reliable operation of the superconductor figures 2.10 and 2.11 show the radial and tangential components of flux density (B_r, B_θ) as a function of radius around the outermost slot of the rotor as computed by different models. As explained in section 2.2 the flux build up is due to the certain odd-space harmonics produced by the field winding configuration and, as can be seen, the current sheet model tends to overestimate the flux density whereas the thickness model underestimates compared to the new more detailed model.

2.4.3 Results and Discussion

In this analysis, four separate slot geometries, $Q = 0, 0.25, 0.33$ and 1 are considered for a field winding with an overall spread angle 120, 134, and 144 degrees respectively. In each case the winding is arranged in 12 slots. The harmonic component of both the radial and the tangential flux density is computed for each case and the results presented in table 2.5. This table is very instructive in obtaining an insight into the way the harmonic flux

density distribution depends on the structure of the superconducting rotor. All harmonics up to 7th have been shown in the table as beyond this they become individually negligible, firstly because their magnitude is very small and secondly because their windings factors are very low. From table 2.5 it is clear that a spread angle $\sigma_f = 120°$ completely eliminates the third harmonic whilst a spread angle of $\sigma_f = 144°$ eliminates the 5th harmonic. With a spread angle $\sigma_f = 134°$ the 3rd, 5th and 7th harmonic exist but may be used to reduce both the 3rd and 5th harmonic compared with $\sigma_f = 144°$ and $\sigma_f = 120°$ respectively.

Table 2.5 also demonstrates that the value of the various space harmonics is greatly dependent on Q, the width of tooth/slot-width. The ratio Q called the slot distribution factor, is always less than 1, and shows how the harmonic flux density of the magnetic field is affected by the width of the slot.

The circumferential and radial variation of flux density produced by the different winding configurations is shown in figures 2.12 and 2.13 respectively. Each figure comprises of six graphs, one for each of the Q factor stated above plus two additional intermediate values, whilst each graph consists of three curves, one for each of the three winding spreads used. Figure 2.12 shows how the radial flux density varies with tangential position at the mean winding radius and along with figure 2.13 clearly demonstrates the spacial oscillation of flux density due to the slot pitch. For any given winding spread angle as the ratio of tooth width/slot width increases so does the magnitude of this spacial distribution. This leads to an increase in the radial flux density at the outermost slot so that with a tooth width/slot width ratio of one the peak radial flux density is typically 11.6% greater than when the current density is assumed smeared over the full winding spread angle. Also apparent is the fact that as the winding spread is changed from

120° through 134° to 144° the peak radial flux density at outermost slot reduces. These variations in the peak radial and tangential flux density at the edge of the outermost slot is more clearly shown in figure 2.14 and 2.15 where the radial and tangential variation of this flux density are shown for the different winding spread angles and tooth width/slot width ratios. For completeness figures 2.16 and 2.17 show how the radial flux density ($\theta = 0$) and the tangential flux density ($\theta = 90°$) vary with radial position. As can be seen the tangential flux density changes direction in passing through the winding whilst both show the reduction with increasing radius so that at typical armature radius all the winding configurations produce similar levels of flux density.

2.5 Procedure of reducing harmonic content

As shown in the magnetic field analysis of appendix 1, the magnetic field distribution for any given harmonic varies directly with many principle factors such as the value of current flowing through the winding, the number of turns in the slots, the distribution factor, the geometric factor $(r_{fso}/r)^{np+1}$ and the relative position of the slot-pairs containing the field coils. Therefore, it is clear that when the new model is used, these factors can be employed to control the harmonic content of flux density waveform. As shown in the proceeding section, the rotor harmonics are caused mainly by the shape and configuration of the winding and solely eliminating a particular harmonic, does not necessarily reduce the undesirable flux concentration around the outermost slot.

2.6 Other applications

As the new model includes information on a large number of the important dimensions making up the magnetic circuit it renders valuable service in the design of cylindrical rotors for superconducting a.c. generators, especially in the optimization of their magnetic parameters. In a number of variants it is possible to study the effect on the magnetic field of

(1) the spread angle and the number of slots,

(2) changes in the slot geometry (or shape),

(3) separating and shorting the slots near the polar region,

(4) squeezing the slots near the neutral zone together.

(5) matching the depth of slots and height of the core to one another,

(6) omitting the central bore.

The use of the new model can also help to minimize the local flux concentration around the outermost slot and produce a valuable tool in diagnosing the problems which may be faced in the modification of the field winding design.

2.7 Summary and conclusions

In this chapter a model has been developed to help determine the distribution of the magnetic flux density inside a superconducting a.c generator. The model takes into account the number, and the geometric structure, of the winding slots and allows the rotor of the superconducting machine to be designed with optimum magnetic field distribution.

The results have shown that for a slotted winding of any given spread the maximum flux density at the outermost slot is influenced by the actual slot shape and ratio of tooth width/slot width used. Simply selecting a 120°

winding spread angle which eliminates the third spacial harmonic does not necessarily minimize the peak flux density at the winding.

It is recognized that although the two dimensional analysis agrees with that obtained from the three dimensional analysis in the centre part of the winding they differ towards the winding ends. However, the average flux linkage can be obtained from a two dimensional analysis if appropriate length corrections are made to the machine windings. More analysis is required to fully define this problem.

Essentially the new method is an extension to earlier magnetic field models where the winding was assumed smeared uniformly over its complete spread angle. Now full account has been taken of the slot geometry used.

TABLE [2.1]
MAGNETIC FIELD DISTRIBUTIONS PRODUCED FOR THICKNESS MODEL
MAGNETIC FIELD DISTRIBUTIONS PRODUCED BY FIELD WINDING

When $np \neq 2$

FOR REGION [1] $r < r_{fi}$
$B_{r_f} = \sum_{\substack{n=1 \\ n=odd}}^{\infty} \left(\frac{\mu_o J_{fn}}{2(2-np)}\right) r \left(\frac{r}{r_{fo}}\right)^{np-2} \left[1 - \left(\frac{r_{fi}}{r_{fo}}\right)^{2-np} \pm \left(\frac{2-np}{2+np}\right) \left(\frac{r_{fo}}{r_{si}}\right)^{2np} \left(1 - \left(\frac{r_{fi}}{r_{fo}}\right)^{2+np}\right)\right] cosnp\theta$
$B_{\theta_f} = - \sum_{\substack{n=1 \\ n=odd}}^{\infty} \left(\frac{\mu_o J_{fn}}{2(2-np)}\right) r \left(\frac{r}{r_{fo}}\right)^{np-2} \left[1 - \left(\frac{r_{fi}}{r_{fo}}\right)^{2-np} \pm \left(\frac{2-np}{2+np}\right) \left(\frac{r_{fo}}{r_{si}}\right)^{2np} \left(1 - \left(\frac{r_{fi}}{r_{fo}}\right)^{2+np}\right)\right] sinnp(\theta)$
FOR REGION [2] $r_{fi} < r < r_{fo}$
$B_{r_f} = \sum_{\substack{n=1 \\ n=odd}}^{\infty} \left(\frac{\mu_o J_{fn}}{2(4-n^2p^2)}\right) r \left[-2np - (2-np)\left(\frac{r_{fi}}{r}\right)^{2+np} + (2+np)\left(\frac{r}{r_{fo}}\right)^{np-2} \pm (2-np)\left(\frac{r}{r_{si}}\right)^{np-2} \left(\frac{r_{fo}}{r_{si}}\right)^{2+np} \left(1 - \left(\frac{r_{fi}}{r_{fo}}\right)^{2+np}\right)\right] cosnp\theta$
$B_{\theta_f} = - \sum_{\substack{n=1 \\ n=odd}}^{\infty} \left(\frac{\mu_o J_{fn}}{2(4-n^2p^2)}\right) r \left[-4 + (2-np)\left(\frac{r_{fi}}{r}\right)^{2+np} + (2+np)\left(\frac{r}{r_{fo}}\right)^{np-2} \pm (2-np)\left(\frac{r}{r_{si}}\right)^{np-2} \left(\frac{r_{fo}}{r_{si}}\right)^{2+np} \left(1 - \left(\frac{r_{fi}}{r_{fo}}\right)^{2+np}\right)\right] sinnp\theta$
FOR REGION [3] $r_{fo} < r < r_{si}$
$B_{r_f} = \sum_{\substack{n=1 \\ n=odd}}^{\infty} \left(\frac{\mu_o J_{fn}}{2(2+np)}\right) r \left(\frac{r_{fo}}{r}\right)^{2+np} \left(1 - \left(\frac{r_{fi}}{r_{fo}}\right)^{2+np}\right) \left[1 \pm \left(\frac{r}{r_{si}}\right)^{2np}\right] cosnp\theta$
$B_{\theta_f} = \sum_{\substack{n=1 \\ n=odd}}^{\infty} \left(\frac{\mu_o J_{fn}}{2(2+np)}\right) r \left(\frac{r_{fo}}{r}\right)^{2+np} \left(1 - \left(\frac{r_{fi}}{r_{fo}}\right)^{2+np}\right) \left[1 \pm \left(\frac{r}{r_{si}}\right)^{2np}\right] sinnp\theta$

TABLE [2.1b]

When $np = 2$

FOR REGION [1] $r < r_{fi}$
$B_{r_f} = \left(\frac{\mu_o \widehat{J}_{f1}}{4}\right) r \left[-ln\left(\frac{r_{fi}}{r_{fo}}\right) \pm \left(\frac{1}{4}\right) \left(\frac{r_{fo}}{r_{si}}\right)^4 \left(1 - \left(\frac{r_{fi}}{r_{fo}}\right)^4\right)\right] cos2\theta$
$B_{\theta_f} = -\left(\frac{\mu_o \widehat{J}_{f1}}{4}\right) r \left[-ln\left(\frac{r_{fi}}{r_{fo}}\right) \pm \left(\frac{1}{4}\right) \left(\frac{r_{fo}}{r_{si}}\right)^4 \left(1 - \left(\frac{r_{fi}}{r_{fo}}\right)^4\right)\right] sin2\theta$
FOR REGION [2] $r_{fi} < r < r_{fso}$
$B_{r_f} = \left(\frac{\mu_o \widehat{J}_{f1}}{16}\right) r \left[1 - \left(\frac{r_{fi}}{r}\right)^4 + 4ln\left(\frac{r_{fo}}{r}\right) \pm \left(\frac{r_{fo}}{r_{si}}\right)^4 \left(1 - \left(\frac{r_{fi}}{r_{fo}}\right)^4\right)\right] sin2\theta$
$B_{\theta_f} = -\left(\frac{\mu_o \widehat{J}_{f1}}{16}\right) r \left[-1 + \left(\frac{r_{fi}}{r}\right)^4 + 4ln\left(\frac{r_{fo}}{r}\right) \pm \left(\frac{r_{fo}}{r_{si}}\right)^4 \left(1 - \left(\frac{r_{fi}}{r_{fo}}\right)^4\right)\right] cos2\theta$
FOR REGION [3] $r_{fo} < r < r_{si}$
$B_{r_f} = \left(\frac{\mu_o \widehat{J}_{f1}}{8}\right) r \left(\frac{r_{fo_i}}{r}\right)^4 \left(1 - \left(\frac{r_{fi}}{r_{fo}}\right)^4\right) \left[1 \pm \left(\frac{r}{r_{si}}\right)^4\right] cos2\theta$
$B_{\theta_f} = \left(\frac{\mu_o \widehat{J}_{f1}}{8}\right) r \left(\frac{r_{fo}}{r}\right)^4 \left(1 - \left(\frac{r_{fi}}{r_{fo}}\right)^4\right) \left[1 \pm \left(\frac{r}{r_{si}}\right)^4\right] sin2\theta$

TABLE [2.2]
SELF AND MUTUAL INDUCTANCES

FIELD-SELF INDUCTANCE (L_f)
$$L_f = \sum_{\substack{n=1 \\ n=odd}}^{\infty} \frac{16\mu_o\lambda_f}{n^3p\pi\sigma_f^2\left(4-n^2p^2\right)}\left[\frac{N_f \sin\frac{n\sigma_f}{2}}{\left(1-\left(\frac{r_{fi}}{r_{fo}}\right)^2\right)}\right]^2\left[\left(2-np\right)+\left(2+np\right)\left(\frac{r_{fi}}{r_{fo}}\right)^4-4\left(\frac{r_{fi}}{r_{fo}}\right)^{2+np}\pm 2\frac{2-np}{2+np}\left(\frac{r_{fo}}{r_{xi}}\right)^{2np}\left(1-\left(\frac{r_{fi}}{r_{fo}}\right)^{2+np}\right)^2\right]$$
ARMATURE SELF-INDUCTANCE (L_a)
$$L_a = \sum_{\substack{n=1 \\ n=odd}}^{\infty} \frac{16\mu_o\lambda_a}{n^3p\pi\sigma_a^2\left(4-n^2p^2\right)}\left[\frac{N_a \sin\frac{n\sigma_a}{2}}{\left(1-\left(\frac{r_{ai}}{r_{ao}}\right)^2\right)}\right]^2\left[\left(2-np\right)+\left(2+np\right)\left(\frac{r_{ai}}{r_{ao}}\right)^4-4\left(\frac{r_{ai}}{r_{ao}}\right)^{2+np}\pm 2\frac{2-np}{2+np}\left(\frac{r_{ao}}{r_{xi}}\right)^{2np}\left(1-\left(\frac{r_{ai}}{r_{ao}}\right)^{2+np}\right)^2\right]$$
FIELD TO ARMATURE MUTUAL INDUCTANCE (M_{af})
$$M_{af} = \sum_{\substack{n=1 \\ n=odd}}^{\infty} \frac{32\mu_o N_f N_a \lambda_{of} \sin\frac{n\sigma_f}{2}\sin\frac{n\sigma_a}{2}}{n^3p\pi\sigma_f\sigma_a\left(4-n^2p^2\right)}\left(\frac{r_{fo}}{r_{ao}}\right)^{np}\left[\frac{1}{\left(1-\left(\frac{r_{ai}}{r_{ao}}\right)^2\right)\left(1-\left(\frac{r_{fi}}{r_{fo}}\right)^2\right)}\right]\left(1-\left(\frac{r_{fi}}{r_{fo}}\right)^{2+np}\right)\left[\left(1-\left(\frac{r_{ai}}{r_{ao}}\right)^{2-np}\right)\pm\frac{2-np}{2+np}\left(\frac{r_{ao}}{r_{xi}}\right)^{2np}\left(1-\left(\frac{r_{ai}}{r_{ao}}\right)^{2+np}\right)\right]$$

Table 2.3
Electrical and physical data of a 1300 MVA turbo-generator rotor

Name	Symbol	Unit	Value
No. of pole pairs	p	-	1
Rated power	P_r	MW	1300
No-load field current	I_f	A	4984
No. of slots per pole	S	-	12
No. of conductors per pole	N_f	-	1720
Field winding inner radius	r_{fi}	m	0.395
Field winding outer radius	r_{fo}	m	0.455
Inner radius of iron screen	r_{zi}	m	1.4
Ratio of tooth width to slot width	Q	-	1/5

TABLE [2.4a]

When $np \neq 2$ **MAGNETIC FIELD DISTRIBUTIONS PRODUCED BY FIELD WINDING**

FOR REGION [1] $r < r_{fsi}$
$B_{r_f} = \sum_{i=1}^{S} \sum_{\substack{n=1 \\ n=odd}}^{\infty} \left(\frac{\mu_o \hat{J}_{fo_n}}{2(2-np)}\right) r \left(\frac{r}{r_{fso_i}}\right)^{np-2} \left[1 - \left(\frac{r_{fsi_n}}{r_{fso_i}}\right)^{2-np} \pm \left(\frac{2-np}{2+np}\right) \left(\frac{r_{fso_n}}{r_{si}}\right)^{2np} \left(1 - \left(\frac{r_{fsi_n}}{r_{fso_i}}\right)^{2+np}\right)\right] cosnp(\theta \pm \alpha_i)$
$B_{\theta_f} = -\sum_{i=1}^{S} \sum_{\substack{n=1 \\ n=odd}}^{\infty} \left(\frac{\mu_o \hat{J}_{fo_n}}{2(2-np)}\right) r \left(\frac{r}{r_{fso_i}}\right)^{np-2} \left[1 - \left(\frac{r_{fsi_n}}{r_{fso_i}}\right)^{2-np} \pm \left(\frac{2-np}{2+np}\right) \left(\frac{r_{fso_n}}{r_{si}}\right)^{2np} \left(1 - \left(\frac{r_{fsi_n}}{r_{fso_i}}\right)^{2+np}\right)\right] sinnp(\theta \pm \alpha_i)$
FOR REGION [2] $r_{fsi} < r < r_{fso}$
$B_{r_f} = \sum_{i=1}^{S} \sum_{\substack{n=1 \\ n=odd}}^{\infty} \left(\frac{\mu_o \hat{J}_{fo_n}}{2(4-n^2p^2)}\right) r \left[-2np - (2-np)\left(\frac{r_{fsi_n}}{r}\right)^{2+np} + (2+np)\left(\frac{r}{r_{fso_i}}\right)^{np-2} \pm (2-np)\left(\frac{r}{r_{si}}\right)^{np-2} \left(\frac{r_{fso_n}}{r_{si}}\right)^{2+np} \left(1 - \left(\frac{r_{fsi_n}}{r_{fso_i}}\right)^{2+np}\right)\right] cosnp(\theta \pm \alpha_i)$
$B_{\theta_f} = -\sum_{i=1}^{S} \sum_{\substack{n=1 \\ n=odd}}^{\infty} \left(\frac{\mu_o \hat{J}_{fo_n}}{2(4-n^2p^2)}\right) r \left[-4 + (2-np)\left(\frac{r_{fsi_n}}{r}\right)^{2+np} + (2+np)\left(\frac{r}{r_{fso_i}}\right)^{np-2} \pm (2-np)\left(\frac{r}{r_{si}}\right)^{np-2} \left(\frac{r_{fso_n}}{r_{si}}\right)^{2+np} \left(1 - \left(\frac{r_{fsi_n}}{r_{fso_i}}\right)^{2+np}\right)\right] sinnp(\theta \pm \alpha_i)$
FOR REGION [3] $r_{fso} < r < r_{si}$
$B_{r_f} = \sum_{i=1}^{S} \sum_{\substack{n=1 \\ n=odd}}^{\infty} \left(\frac{\mu_o \hat{J}_{fo_n}}{2(2+np)}\right) r \left(\frac{r_{fso_n}}{r}\right)^{2+np} \left(1 - \left(\frac{r_{fsi_n}}{r_{fso_i}}\right)^{2+np}\right) \left[1 \pm \left(\frac{r}{r_{si}}\right)^{2np}\right] cosnp(\theta \pm \alpha_i)$
$B_{\theta_f} = \sum_{i=1}^{S} \sum_{\substack{n=1 \\ n=odd}}^{\infty} \left(\frac{\mu_o \hat{J}_{fo_n}}{2(2+np)}\right) r \left(\frac{r_{fso_n}}{r}\right)^{2+np} \left(1 - \left(\frac{r_{fsi_n}}{r_{fso_i}}\right)^{2+np}\right) \left[1 \pm \left(\frac{r}{r_{si}}\right)^{2np}\right] sinnp(\theta \pm \alpha_i)$

When $np = 2$

FOR REGION [1] $r < r_{fsi}$
$B_{r_f} = \sum_{i=1}^{S} \left(\frac{\mu_o \hat{J}_{fo_1}}{4}\right) r \left[-ln\left(\frac{r_{fsi_n}}{r_{fso_i}}\right) \pm \left(\frac{1}{4}\right) \left(\frac{r_{fso_n}}{r_{si}}\right)^4 \left(1 - \left(\frac{r_{fsi_n}}{r_{fso_i}}\right)^4\right)\right] cos2(\theta \pm \alpha_i)$
$B_{\theta_f} = -\sum_{i=1}^{S} \left(\frac{\mu_o \hat{J}_{fo_1}}{4}\right) r \left[-ln\left(\frac{r_{fsi_n}}{r_{fso_i}}\right) \pm \left(\frac{1}{4}\right) \left(\frac{r_{fso_n}}{r_{si}}\right)^4 \left(1 - \left(\frac{r_{fsi_n}}{r_{fso_i}}\right)^4\right)\right] sin2(\theta \pm \alpha_i)$
FOR REGION [2] $r_{fsi} < r < r_{fso}$
$B_{r_f} = \sum_{i=1}^{S} \left(\frac{\mu_o \hat{J}_{fo_1}}{16}\right) r \left[1 - \left(\frac{r_{fsi_n}}{r}\right)^4 + 4ln\left(\frac{r_{fso_n}}{r}\right) \pm \left(\frac{r_{fso_n}}{r_{si}}\right)^4 \left(1 - \left(\frac{r_{fsi_n}}{r_{fso_i}}\right)^4\right)\right] sin2(\theta \pm \alpha_i)$
$B_{\theta_f} = -\sum_{i=1}^{S} \left(\frac{\mu_o \hat{J}_{fo_1}}{16}\right) r \left[-1 + \left(\frac{r_{fsi_n}}{r}\right)^4 + 4ln\left(\frac{r_{fso_n}}{r}\right) \pm \left(\frac{r_{fso_n}}{r_{si}}\right)^4 \left(1 - \left(\frac{r_{fsi_n}}{r_{fso_i}}\right)^4\right)\right] sin2(\theta \pm \alpha_i)$
FOR REGION [3] $r_{fso} < r < r_{si}$
$B_{r_f} = \sum_{i=1}^{S} \left(\frac{\mu_o \hat{J}_{fo_1}}{8}\right) r \left(\frac{r_{fso_n}}{r}\right)^4 \left(1 - \left(\frac{r_{fsi_n}}{r_{fso_i}}\right)^4\right) \left[1 \pm \left(\frac{r}{r_{si}}\right)^4\right] cos2(\theta \pm \alpha_i)$
$B_{\theta_f} = \sum_{i=1}^{S} \left(\frac{\mu_o \hat{J}_{fo_1}}{8}\right) r \left(\frac{r_{fso_n}}{r}\right)^4 \left(1 - \left(\frac{r_{fsi_n}}{r_{fso_i}}\right)^4\right) \left[1 \pm \left(\frac{r}{r_{si}}\right)^4\right] sin2(\theta \pm \alpha_i)$

TABLE [2.5]

FIELD WINDINGS AND THEIR INTERACTION WITH THE SPACE-HARMONIC FLUX DENSITY COMPONENTS

	Amplitude of Br_n														
	σ_f=120, (N°of slots)=12					σ_f=134, (N°of slots)=12					σ_f=144, (N°of slots)=12				
	Q=0					Q=0					Q=0				
	harmonic order					harmonic order					harmonic order				
	1	3	5	7	$\sum_{n=odd}^{50} B_r$	1	3	5	7	$\sum_{n=odd}^{50} B_r$	1	3	5	7	$\sum_{n=odd}^{50} B_r$
$r = r_f$	3.049	0.000	0.485	0.325	4.702	3.093	0.126	0.110	0.340	4.505	3.064	0.332	0.000	0.124	4.419
$r = r_s$	0.787	0.000	0.003	0.000	0.791	0.799	0.005	0.000	0.000	0.805	0.791	0.013	0.000	0.000	0.805
$r = r_x$	0.532	0.000	0.000	0.000	0.533	0.539	0.002	0.000	0.000	0.542	0.534	0.006	0.000	0.000	0.541

	Amplitude of Br_n														
	σ_f=120, (N°of slots)=12					σ_f=134, (N°of slots)=12					σ_f=144, (N°of slots)=12				
	Q=1/5					Q=1/5					Q=1/5				
	harmonic order					harmonic order					harmonic order				
	1	3	5	7	$\sum_{n=odd}^{50} B_r$	1	3	5	7	$\sum_{n=odd}^{50} B_r$	1	3	5	7	$\sum_{n=odd}^{50} B_r$
$r = r_f$	3.033	0.000	0.462	0.344	4.831	3.064	0.148	0.084	0.334	4.624	3.040	0.353	0.000	0.104	4.523
$r = r_s$	0.783	0.000	0.003	0.000	0.787	0.791	0.006	0.000	0.000	0.798	0.785	0.014	0.000	0.000	0.800
$r = r_x$	0.529	0.000	0.000	0.000	0.530	0.534	0.002	0.000	0.000	0.537	0.530	0.006	0.000	0.000	0.537

	Amplitude of Br_n														
	σ_f=120, (N°of slots)=12					σ_f=134, (N°of slots)=12					σ_f=144, (N°of slots)=12				
	Q=1/3					Q=1/3					Q=1/3				
	harmonic order					harmonic order					harmonic order				
	1	3	5	7	$\sum_{n=odd}^{50} B_r$	1	3	5	7	$\sum_{n=odd}^{50} B_r$	1	3	5	7	$\sum_{n=odd}^{50} B_r$
$r = r_f$	3.025	0.000	0.448	0.353	4.922	3.054	0.156	0.075	0.326	4.704	3.028	0.363	0.000	0.092	4.595
$r = r_s$	0.781	0.000	0.003	0.000	0.785	0.789	0.006	0.000	0.000	0.796	0.782	0.015	0.000	0.000	0.797
$r = r_x$	0.528	0.000	0.000	0.000	0.528	0.533	0.003	0.000	0.000	0.536	0.528	0.006	0.000	0.000	0.535

	Amplitude of Br_n														
	σ_f=120, (N°of slots)=12					σ_f=134, (N°of slots)=12					σ_f=144, (N°of slots)=12				
	Q=1					Q=1					Q=1				
	harmonic order					harmonic order					harmonic order				
	1	3	5	7	$\sum_{n=odd}^{50} B_r$	1	3	5	7	$\sum_{n=odd}^{50} B_r$	1	3	5	7	$\sum_{n=odd}^{50} B_r$
$r = r_f$	2.999	0.000	0.403	0.370	5.249	3.020	0.178	0.043	0.289	5.050	2.989	0.391	0.000	0.053	4.980
$r = r_s$	0.774	0.000	0.003	0.000	0.778	0.780	0.007	0.000	0.000	0.788	0.772	0.016	0.000	0.000	0.788
$r = r_x$	0.523	0.000	0.000	0.000	0.524	0.527	0.003	0.000	0.000	0.530	0.521	0.007	0.000	0.000	0.529

	Amplitude of B_{θ_n}														
	σ_f=120, (N°of slots)=12					σ_f=134, (N°of slots)=12					σ_f=144, (N°of slots)=12				
	Q=0					Q=0					Q=0				
	harmonic order					harmonic order					harmonic order				
Radial	1	3	5	7	$\sum_{n=odd}^{50} B_\theta$	1	3	5	7	$\sum_{n=odd}^{50} B_\theta$	1	3	5	7	$\sum_{n=odd}^{50} B_\theta$
$= r_f$	-0.211	0.000	0.010	-0.007	-0.206	-0.157	-0.012	0.008	0.004	-0.158	-1.119	-0.017	0.000	0.006	-0.130
$= r_s$	0.147	0.000	-0.001	0.000	0.145	0.110	0.010	-0.001	-0.000	0.118	0.083	0.014	0.000	-0.000	0.097
$= r_x$	0.000	-0.000	0.000	0.000	0.000	-0.000	-0.000	0.000	0.000	0.000	0.000	0.000	0.000	-0.000	0.000

	Amplitude of B_{θ_n}														
	σ_f=120, (N°of slots)=12					σ_f=134, (N°of slots)=12					σ_f=144, (N°of slots)=12				
	Q=1/5					Q=1/5					Q=1/5				
	harmonic order					harmonic order					harmonic order				
Radial	1	3	5	7	$\sum_{n=odd}^{50} B_\theta$	1	3	5	7	$\sum_{n=odd}^{50} B_\theta$	1	3	5	7	$\sum_{n=odd}^{50} B_\theta$
$= r_f$	-0.209	0.000	0.009	-0.007	-0.212	-0.155	-0.014	0.006	0.004	-0.167	-0.118	-0.118	0.000	0.005	-0.136
$= r_s$	0.146	0.000	-0.001	0.000	0.146	0.109	0.012	-0.001	-0.001	0.119	0.082	0.015	0.000	-0.000	0.098
$= r_x$	0.000	0.000	-0.000	0.000	0.000	0.000	0.000	-0.000	-0.000	0.000	0.000	0.000	0.000	-0.000	0.000

	Amplitude of B_{θ_n}														
	σ_f=120, (N°of slots)=12					σ_f=134, (N°of slots)=12					σ_f=144, (N°of slots)=12				
	Q=1/3					Q=1/3					Q=1/3				
	harmonic order					harmonic order					harmonic order				
Radial	1	3	5	7	$\sum_{n=odd}^{50} B_\theta$	1	3	5	7	$\sum_{n=odd}^{50} B_\theta$	1	3	5	7	$\sum_{n=odd}^{50} B_\theta$
$= r_f$	-0.209	0.000	0.009	-0.007	-0.216	-0.155	-0.015	0.006	0.004	-0.170	-0.117	-0.018	0.000	0.004	-0.139
$= r_s$	0.146	0.000	-0.001	0.000	0.147	0.108	0.012	-0.001	-0.000	0.120	0.082	0.015	0.000	-0.000	0.098
$= r_x$	0.000	0.000	-0.000	0.000	0.000	0.000	-0.000	-0.000	0.000	0.000	0.000	0.000	0.000	-0.000	0.000

	Amplitude of B_{θ_n}														
	σ_f=120, (N°of slots)=12					σ_f=134, (N°of slots)=12					σ_f=144, (N°of slots)=12				
	Q=1					Q=1					Q=1				
	harmonic order					harmonic order					harmonic order				
Radial	1	3	5	7	$\sum_{n=odd}^{50} B_\theta$	1	3	5	7	$\sum_{n=odd}^{50} B_\theta$	1	3	5	7	$\sum_{n=odd}^{50} B_\theta$
$= r_f$	-0.207	0.000	0.008	-0.008	-0.240	-0.153	-0.017	0.003	0.003	-0.192	-0.116	-0.020	0.000	0.002	-0.159
$= r_s$	0.145	0.000	-0.001	0.008	0.148	0.107	0.014	-0.000	-0.000	0.121	0.081	0.017	0.000	-0.000	0.099
$= r_x$	0.000	0.000	-0.000	0.000	0.000	0.000	0.000	-0.000	-0.000	0.000	0.000	0.000	0.000	-0.000	0.000

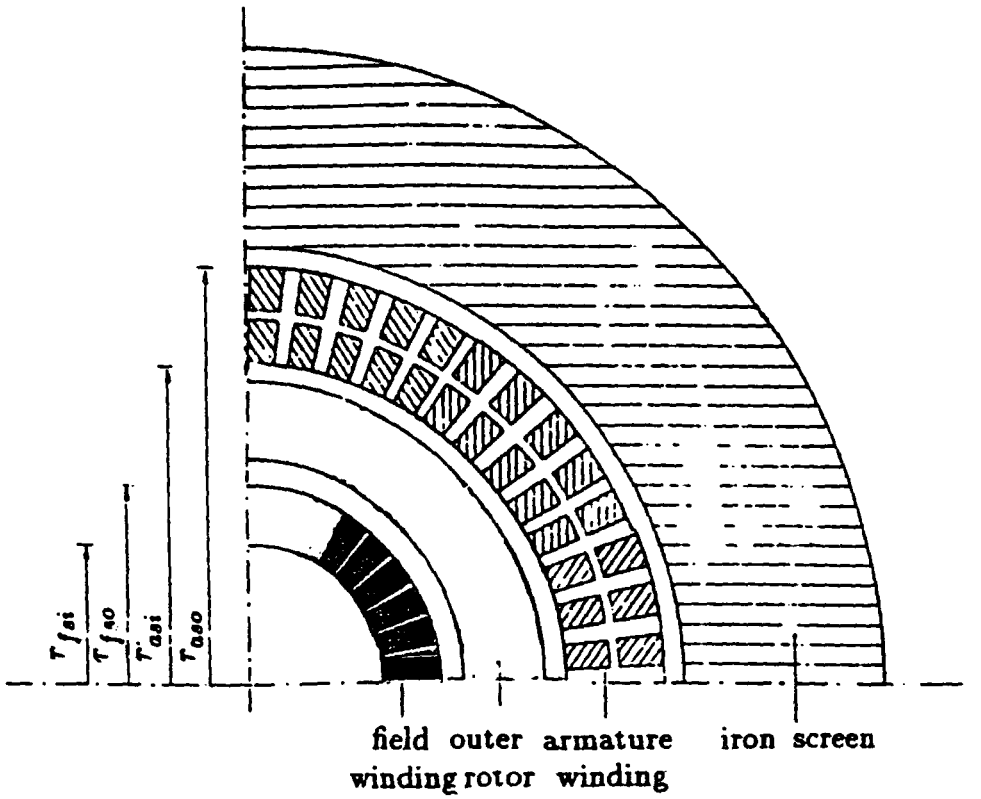

Fig. 2.1 Schematic diagram for superconducting generator.

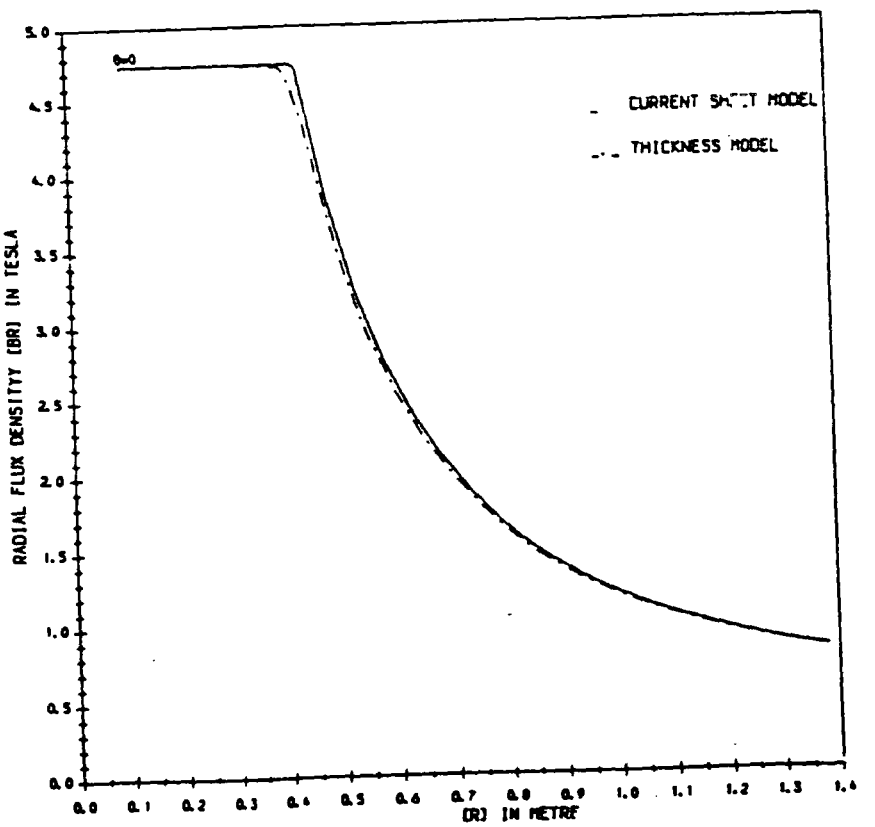

Fig. 2.2 Comprison of the fundamental component of radial flux density calculated by the current sheet and thickness

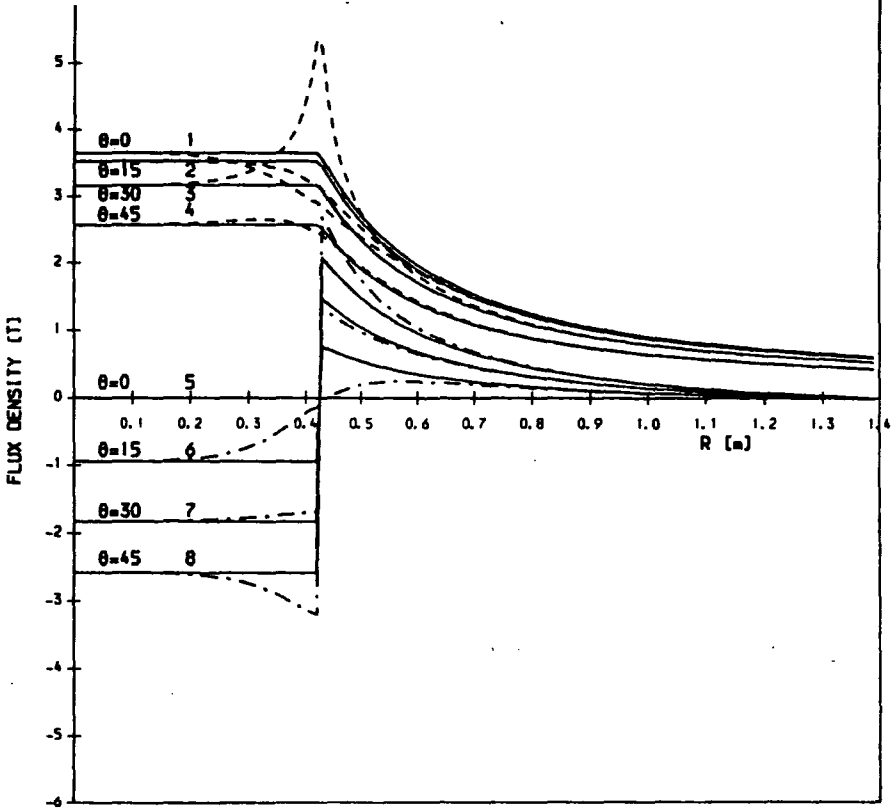

Fig 2.3 Radial variation of radial, B_r, and tangential, B_θ components of flux density produce by field winding using current sheet model at different circumferential positions and no-load

1,2,3,4 Radial flux density, B_r

5,6,7,8 Tangential flux density, B_θ

——— Fundamental component B_r and $B\theta$

– – – – $\sum_{n=1}^{n=49} B_r$

—·— $\sum_{n=1}^{n=49} B_\theta$

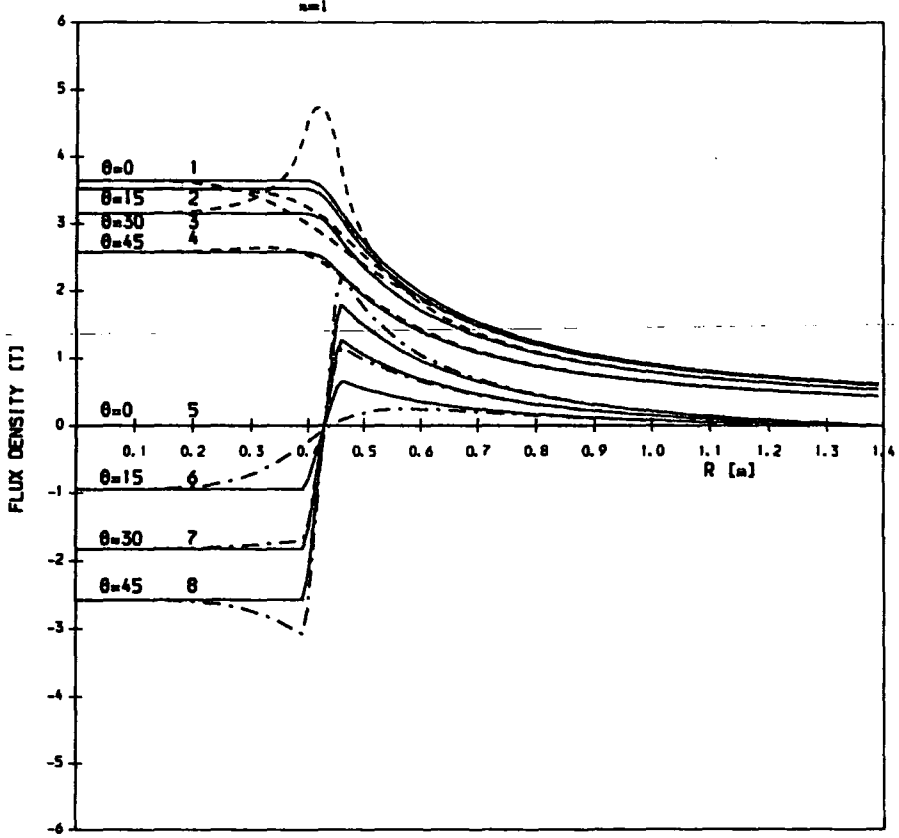

Fig 2.4 Radial variation of radial, B_r, and tangential, B_θ components of flux density produce by field winding using thickness model at different circumferential positions and no-load

1,2,3,4 Radial flux density, B_r

5,6,7,8 Tangential flux density, B_θ

——— Fundamental component B_r and $B\theta$

– – – – $\sum_{n=1}^{n=49} B_r$

—·— $\sum_{n=1}^{n=49} B_\theta$

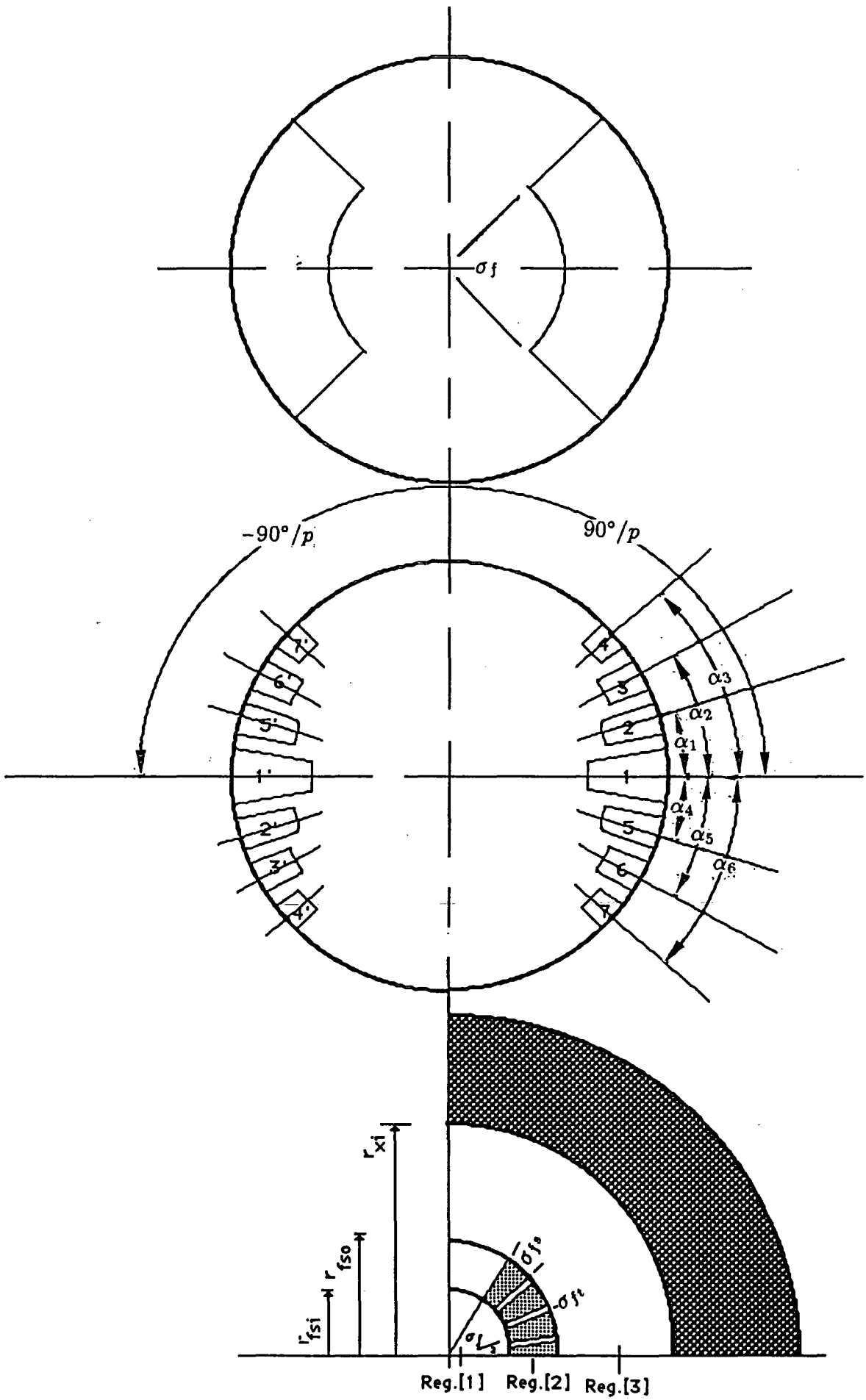

Fig. 2.5 Magnetic field calculation using a new model.

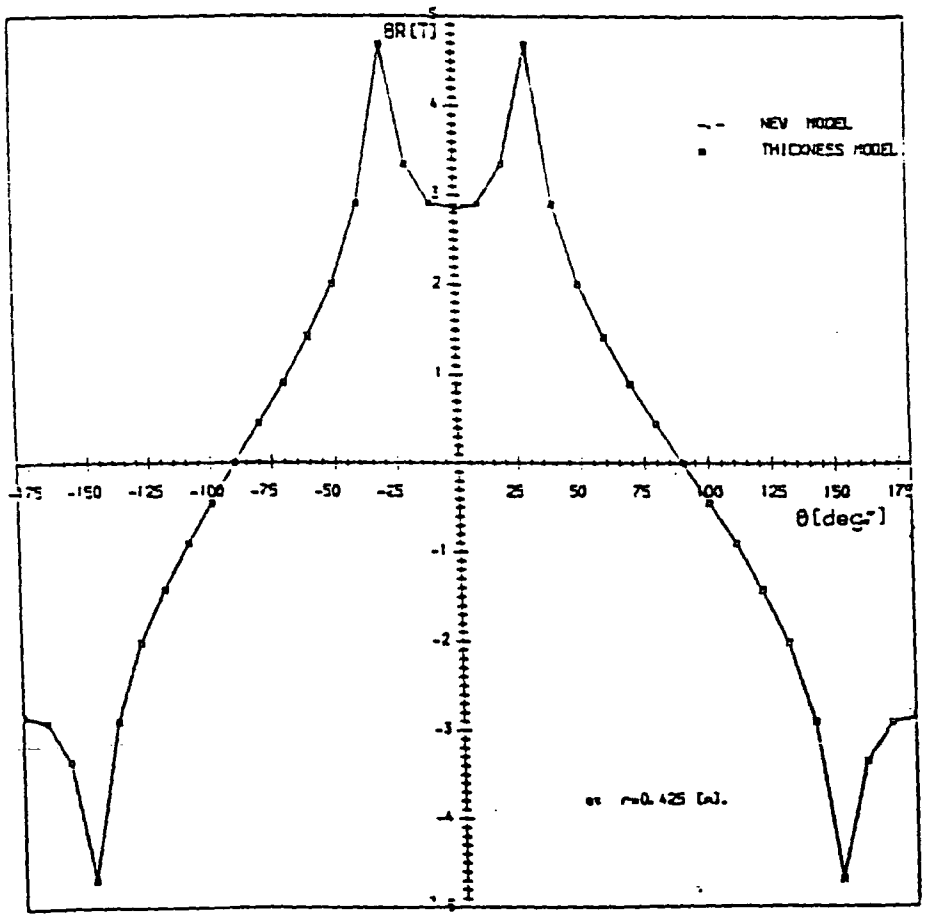

Fig. 2.6 Comparison of radial flux density between thickness and new models.

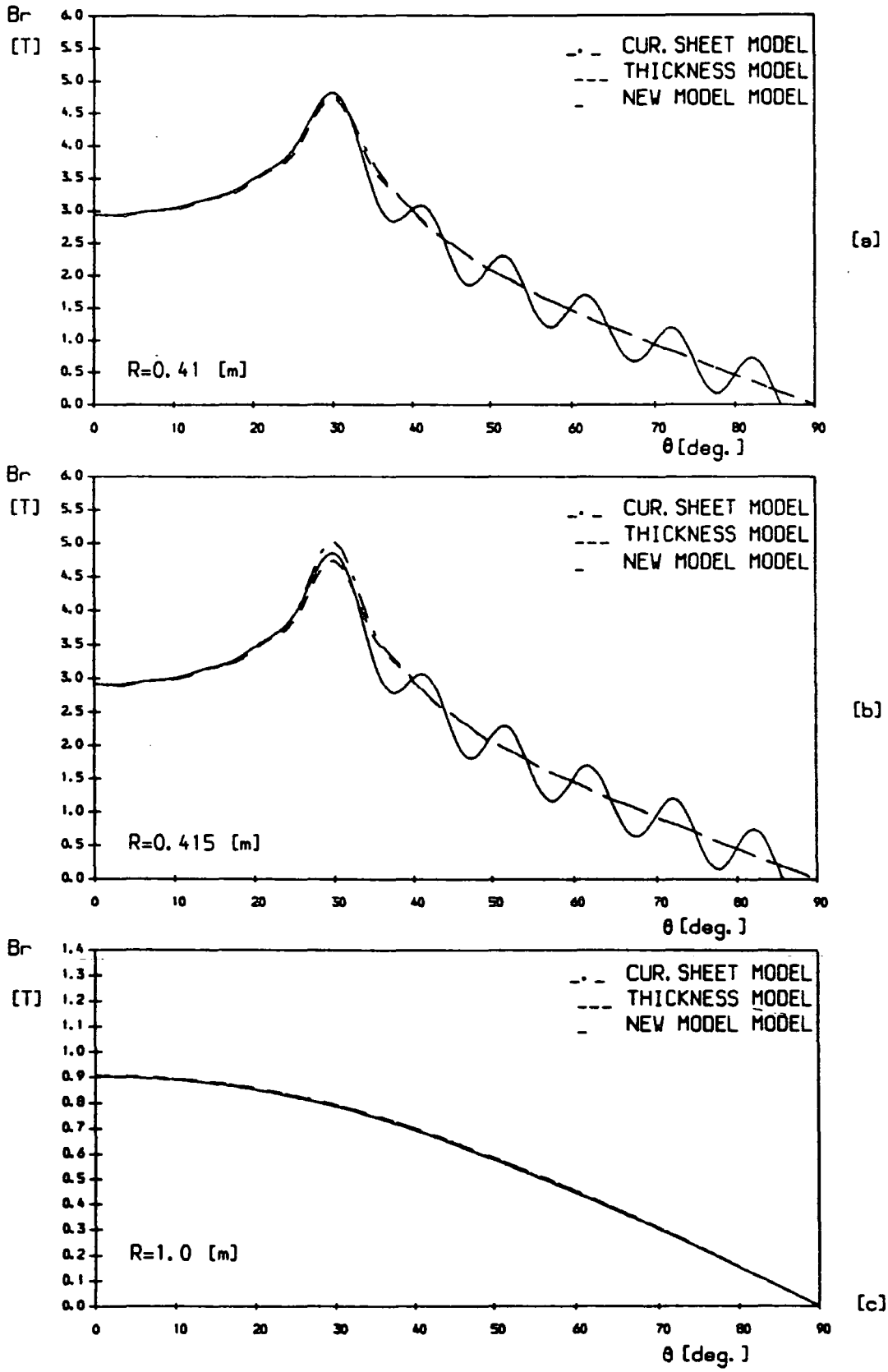

Fig. 2.7 Comparison of radial flux density as calculated by the new model and former models at different radius.

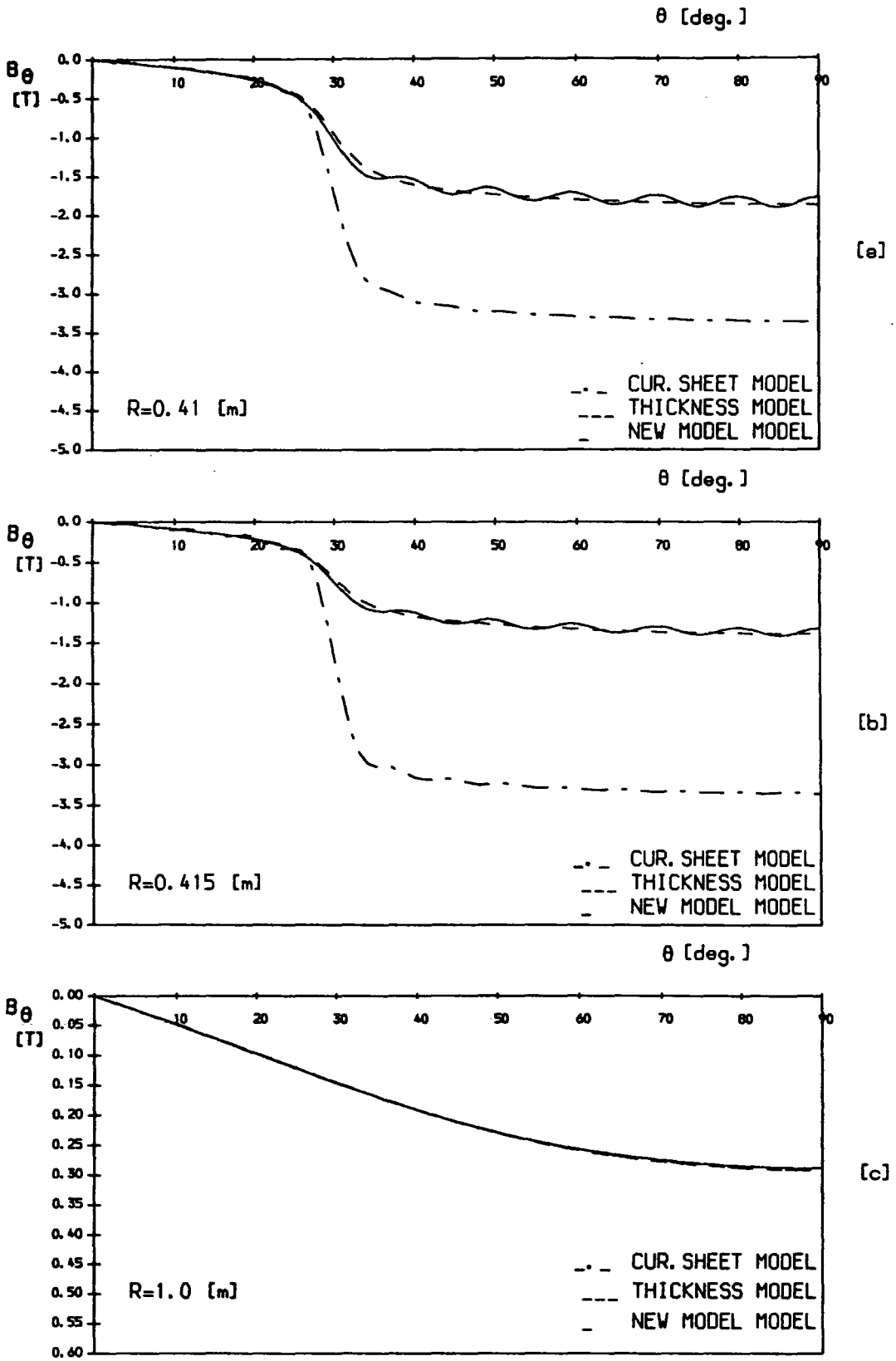

Fig. 2.8 Comparison of tangential flux density as calculated by the new model and former models at different radius.

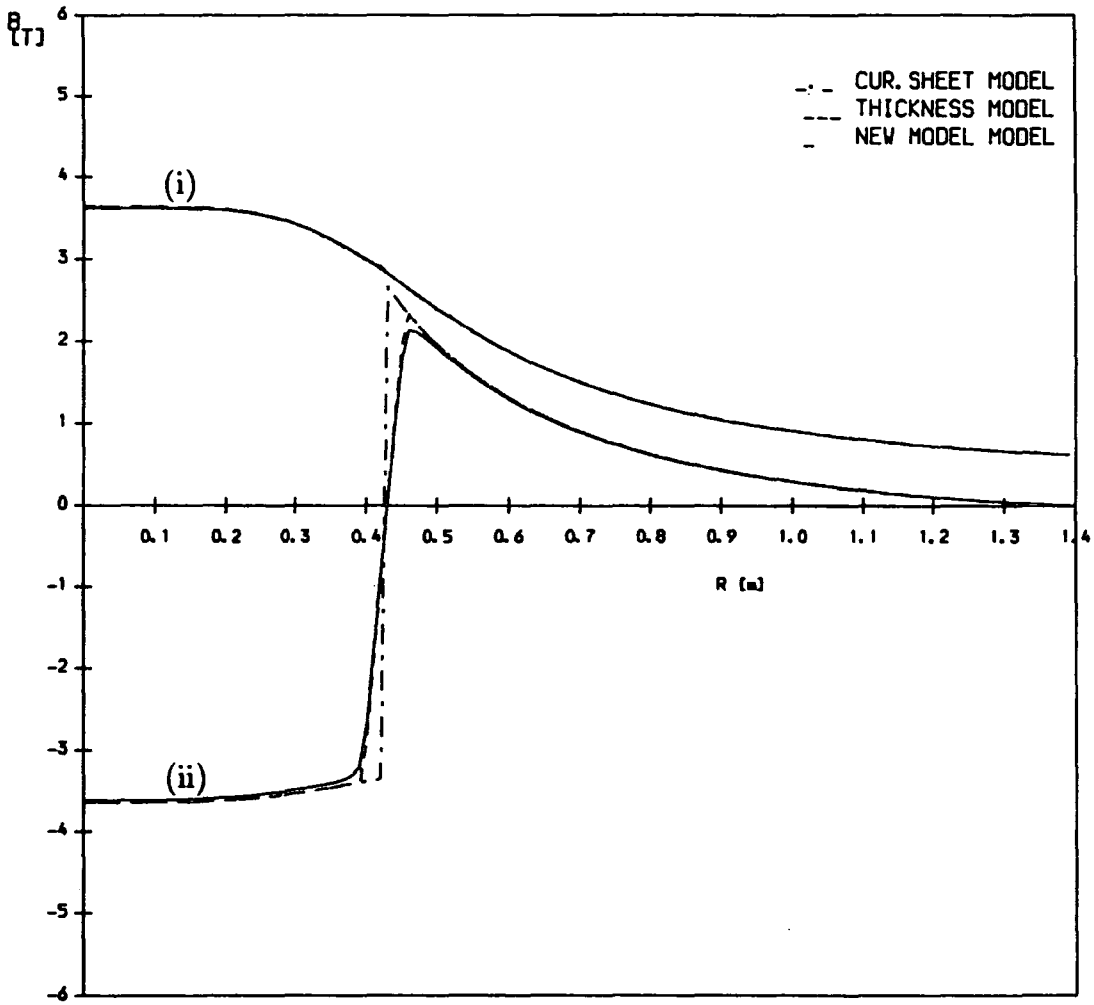

Fig. 2.9 Comparison of radial and tangential flux density as calculated by the new model and former models at no-load.

(i). B_r at 0°

(ii). B_θ at 90°

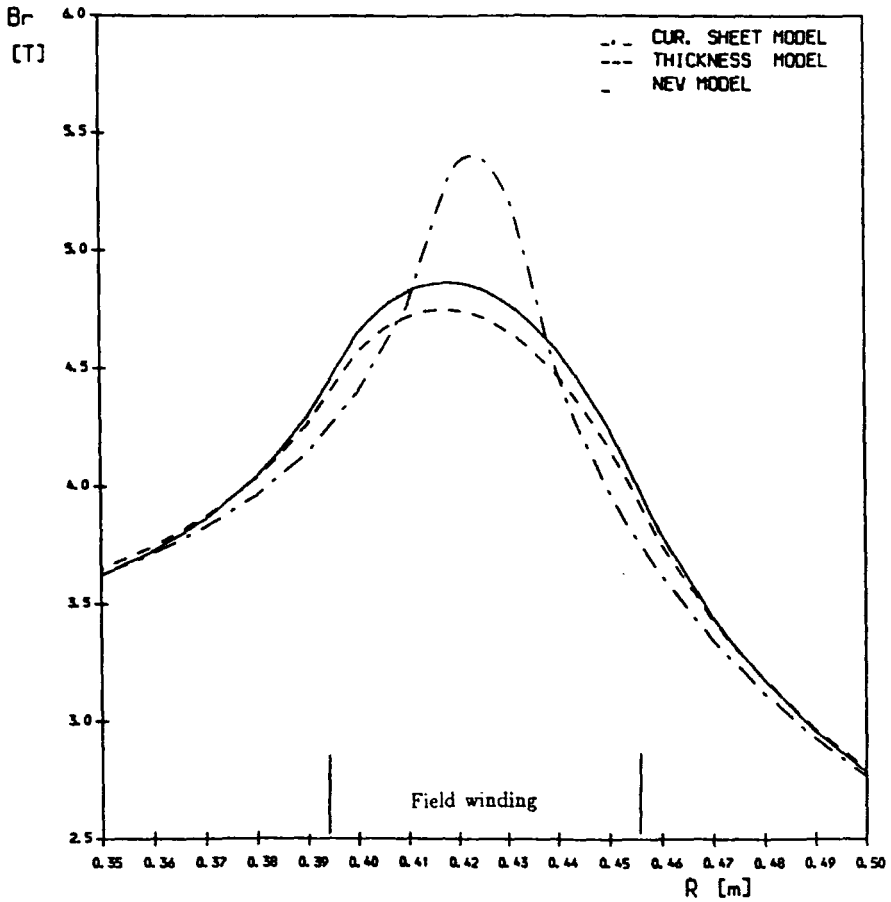

Fig. 2.10 Comparison of the radial flux density component calculated by the new and former models at the outermost slot on no-load.

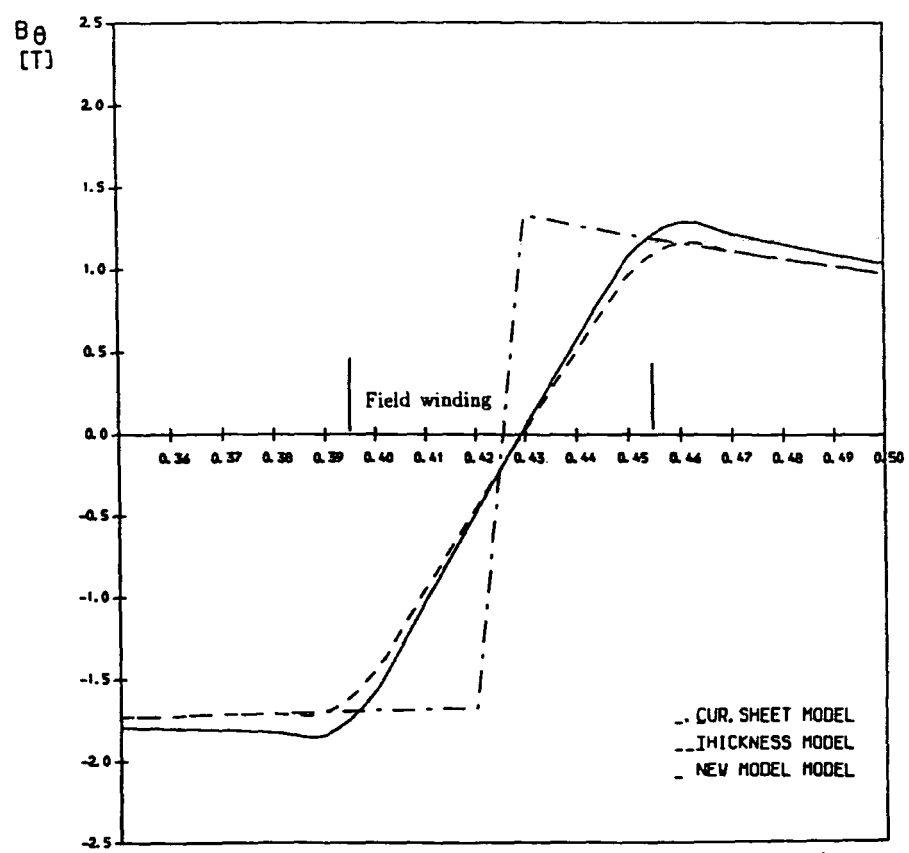

Fig. 2.11 Comparison of the tangential flux density component calculated by the new and former models at the outermost slot on no-load.

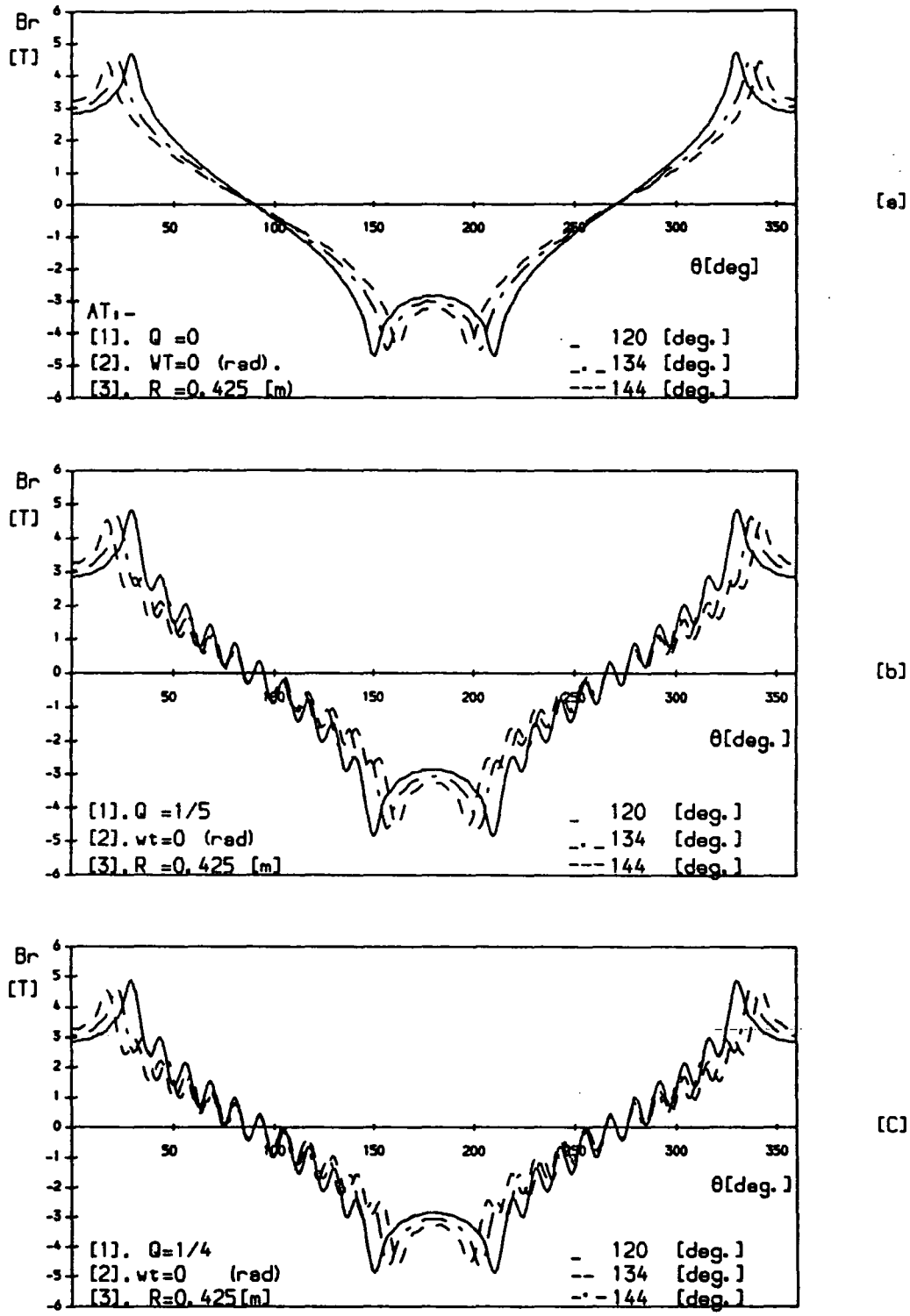

Fig. 2.12 Comparison of the radial flux density component produced by different winding configurations showing the effect of slot geometry

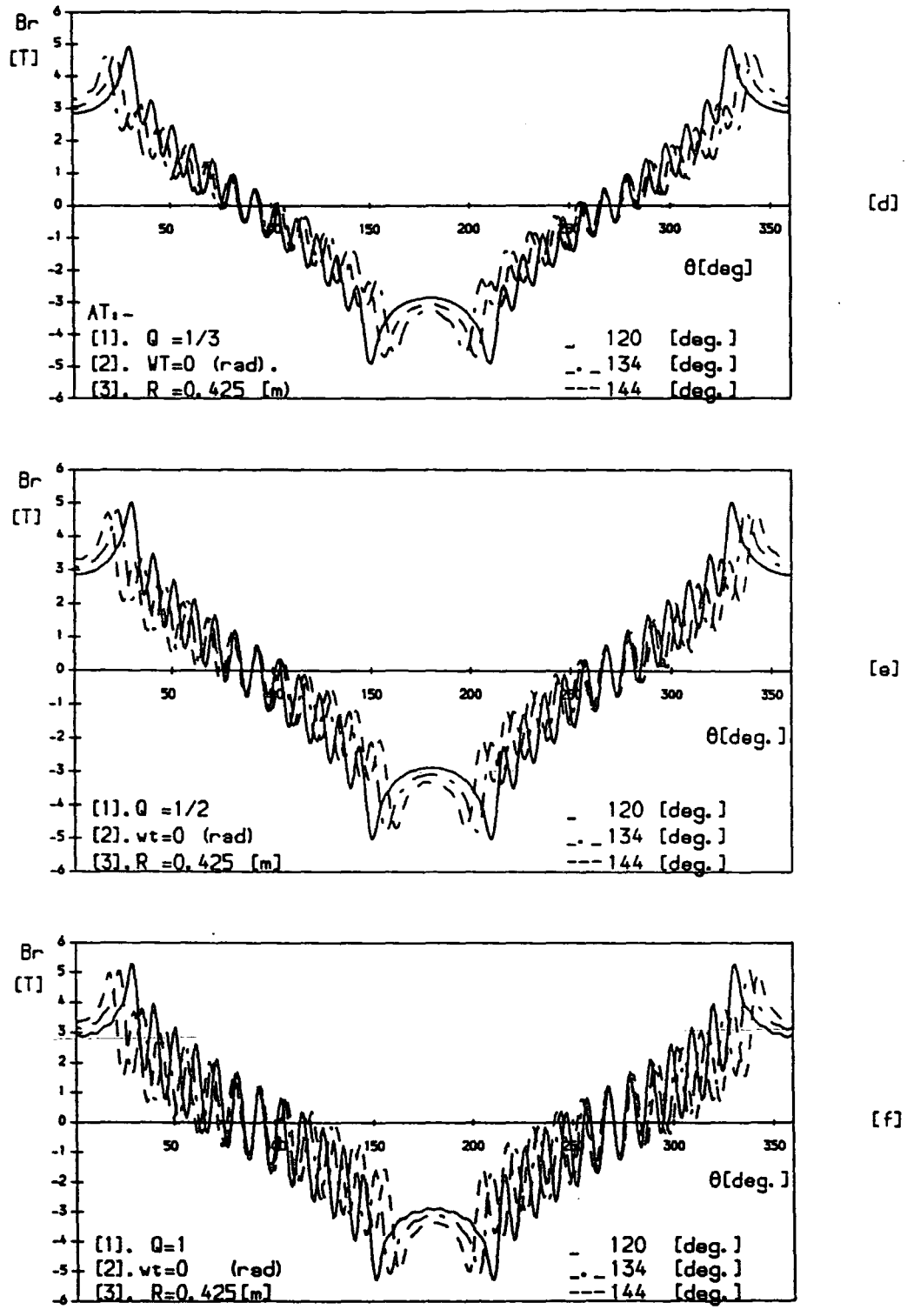

Fig. 2.12 Comparison of the radial flux density component produced by different winding configurations showing the effect of slot geometry

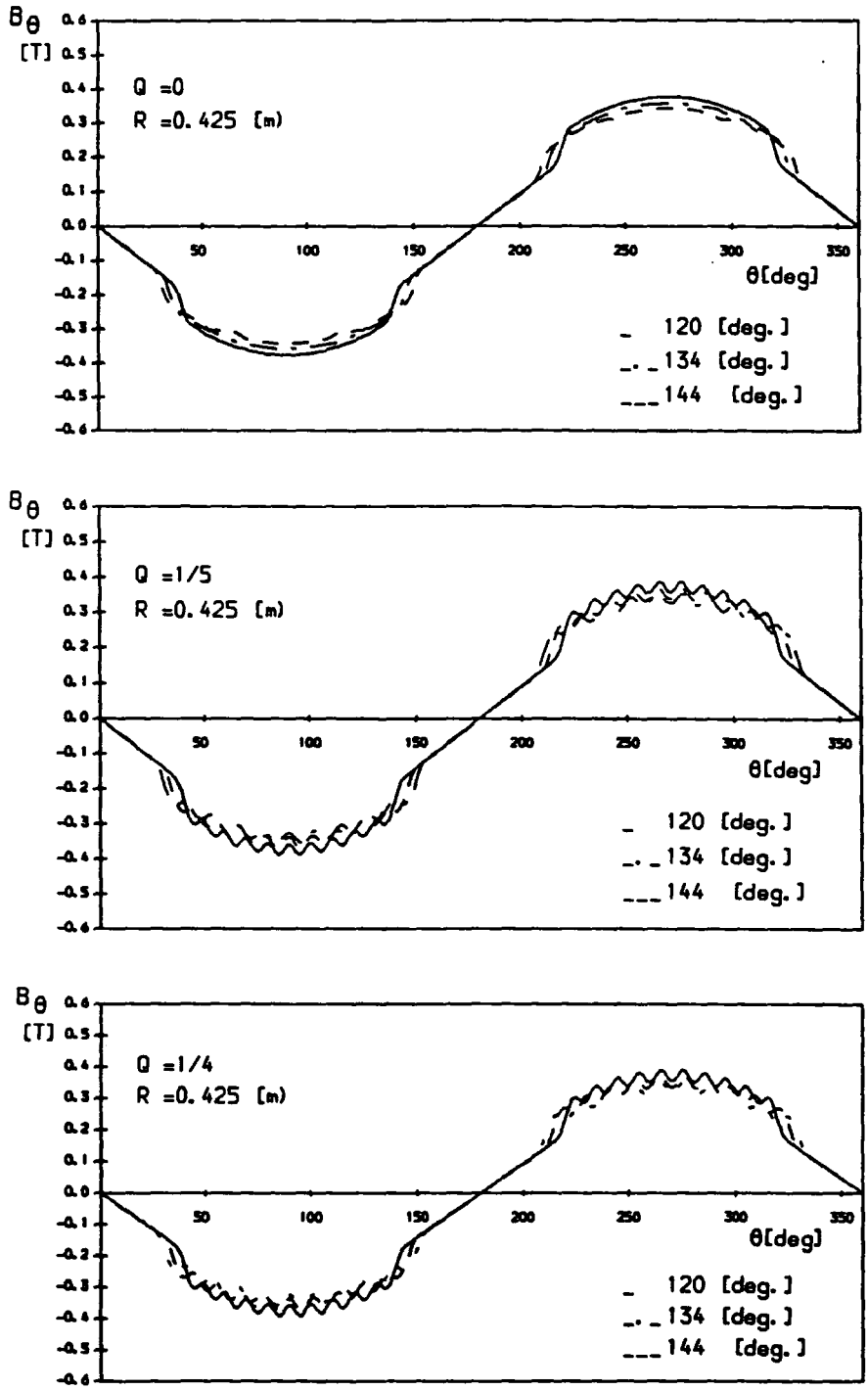

Fig. 2.13 Comparison of the tangential flux density component produced by different winding configurations showing the effect of slot geometry

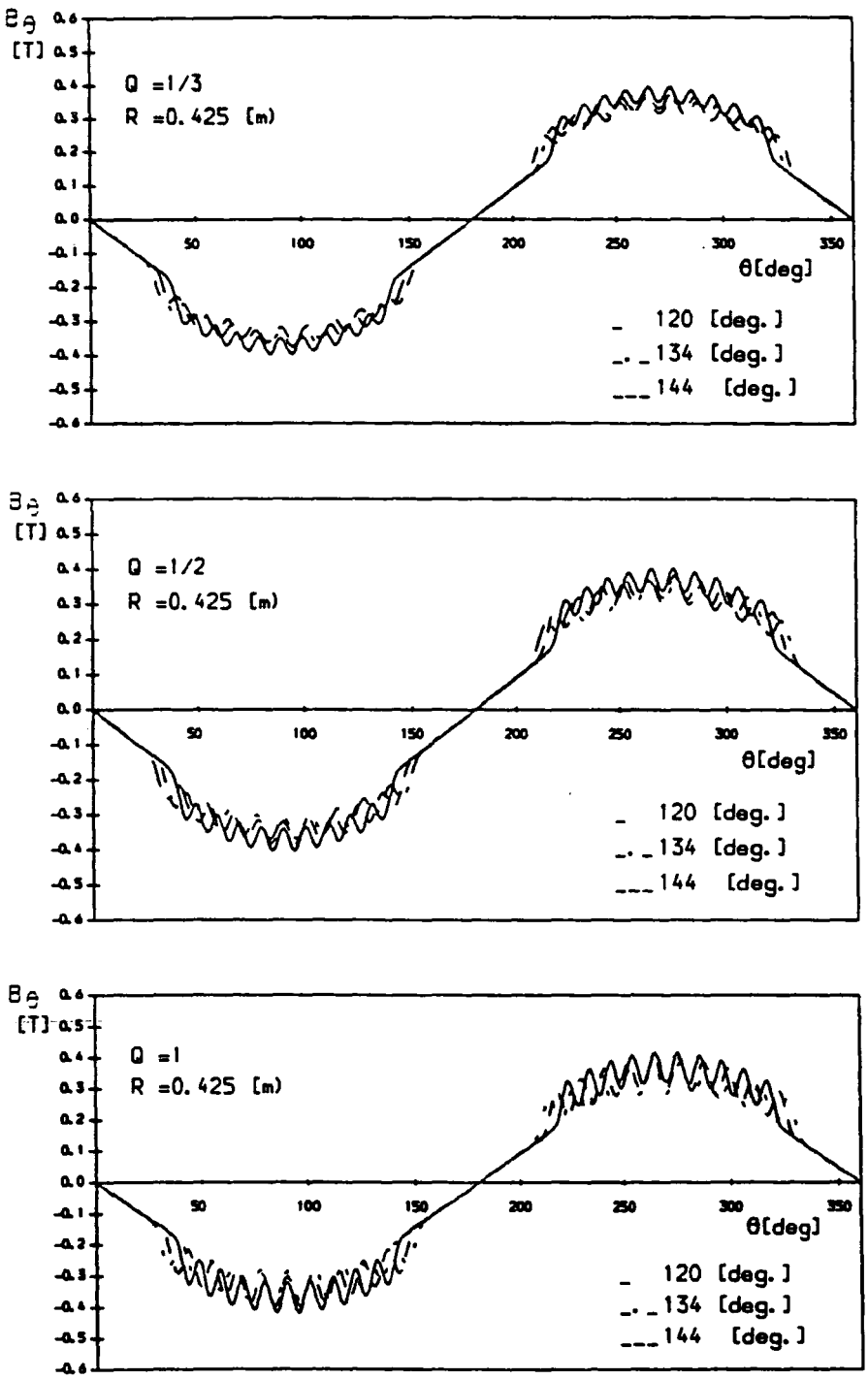

Fig. 2.13 Comparison of the tangential flux density component produced by different winding configurations showing the effect of slot geometry

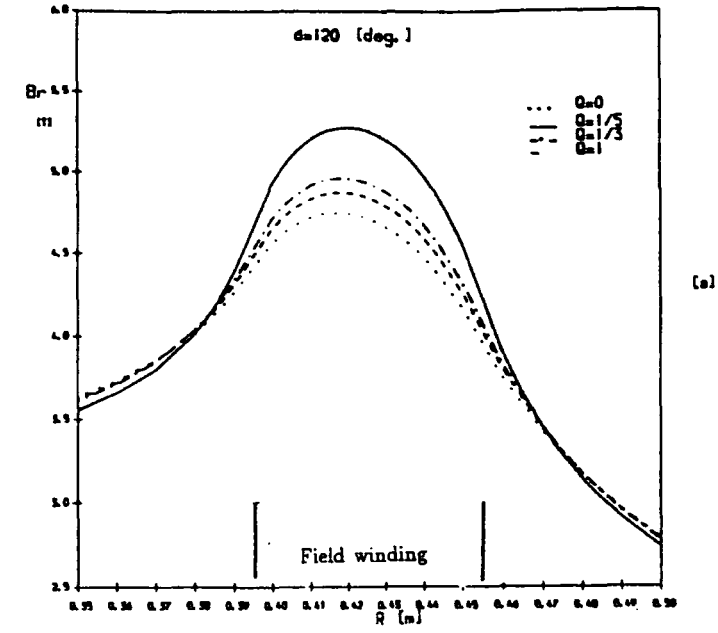

[a]

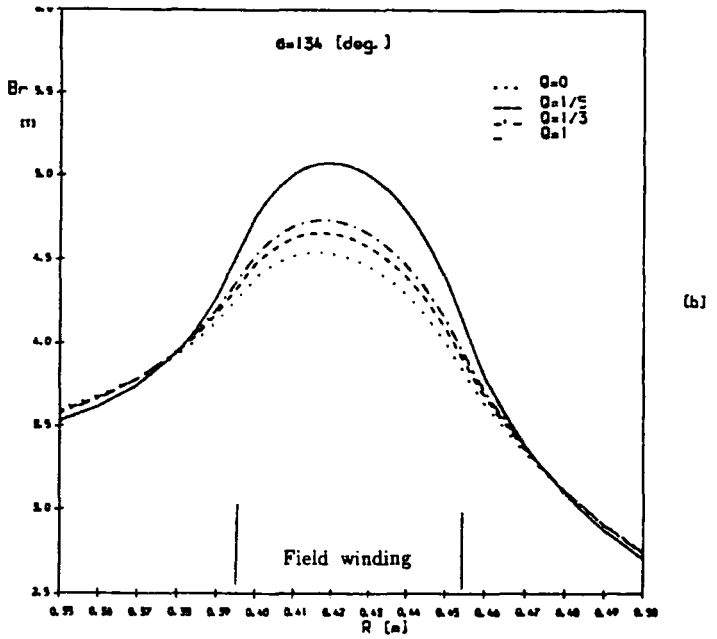

[b]

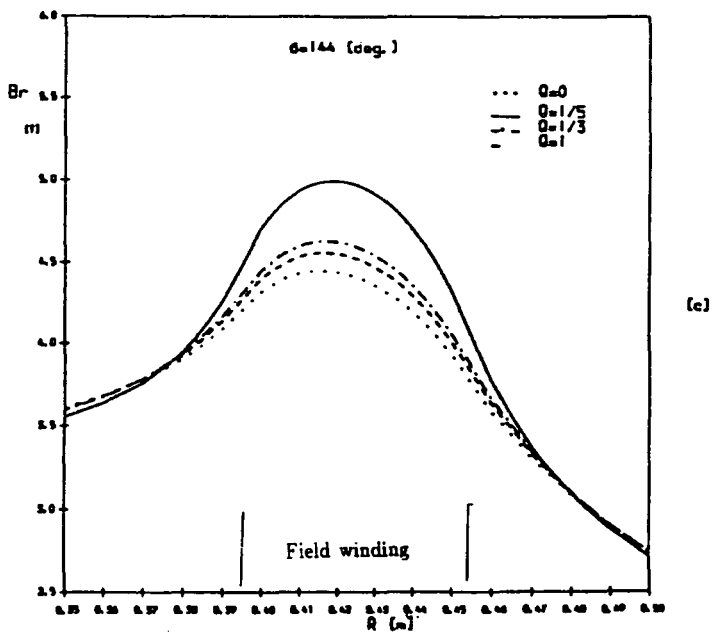

[c]

Fig. 2.14 Comparison of radial flux density component produced by different winding configrations at outermost slot at different values of Q factor.

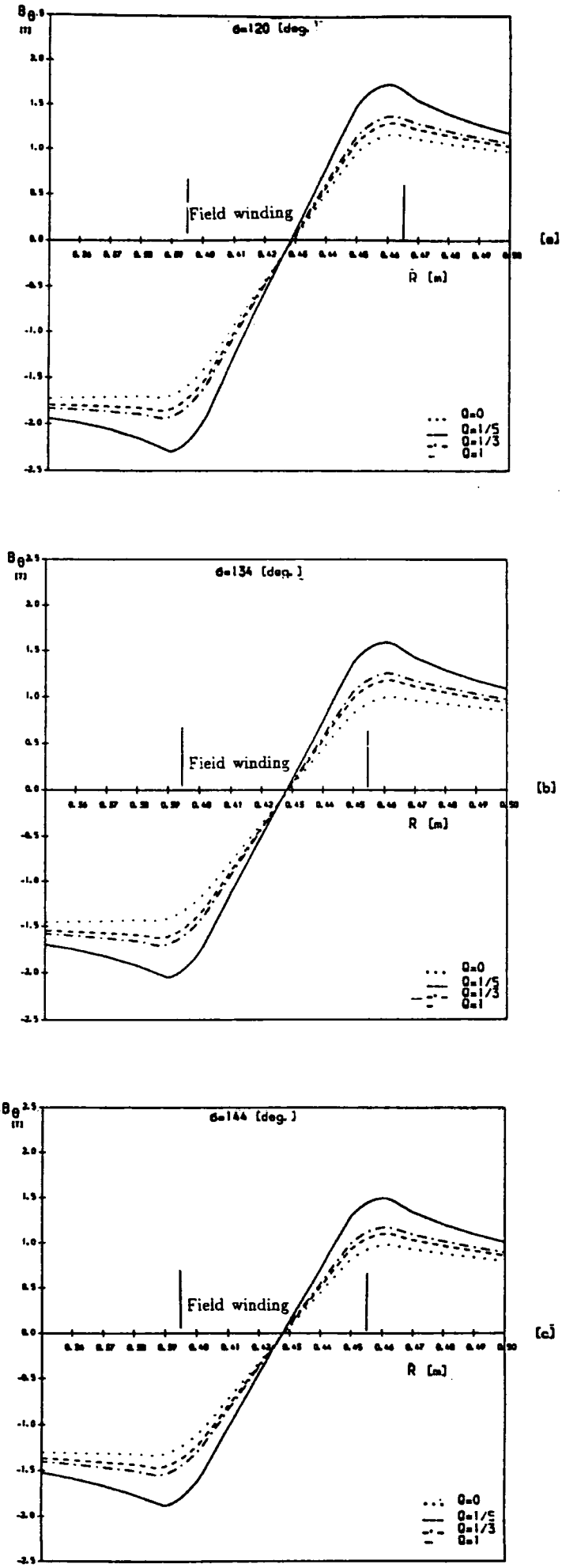

Fig. 2.15 Comparison of tangential flux density component produced by different winding configrations at outermost slot at different values of Q factor.

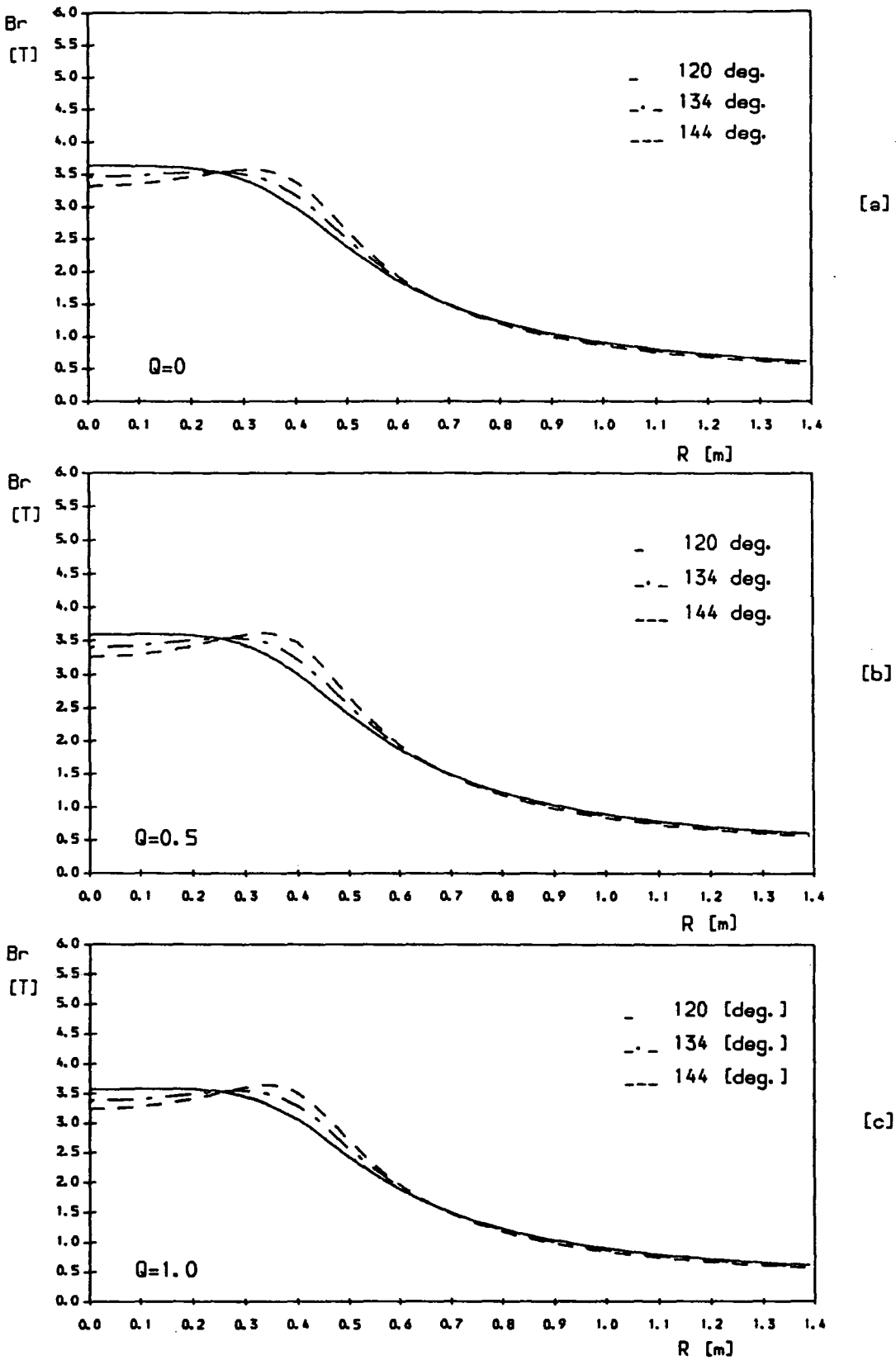

Fig. 2.16 The effect of winding spread angle and slot/tooth aspect ratio on the radial flux density calculated at $\theta = 0°$.

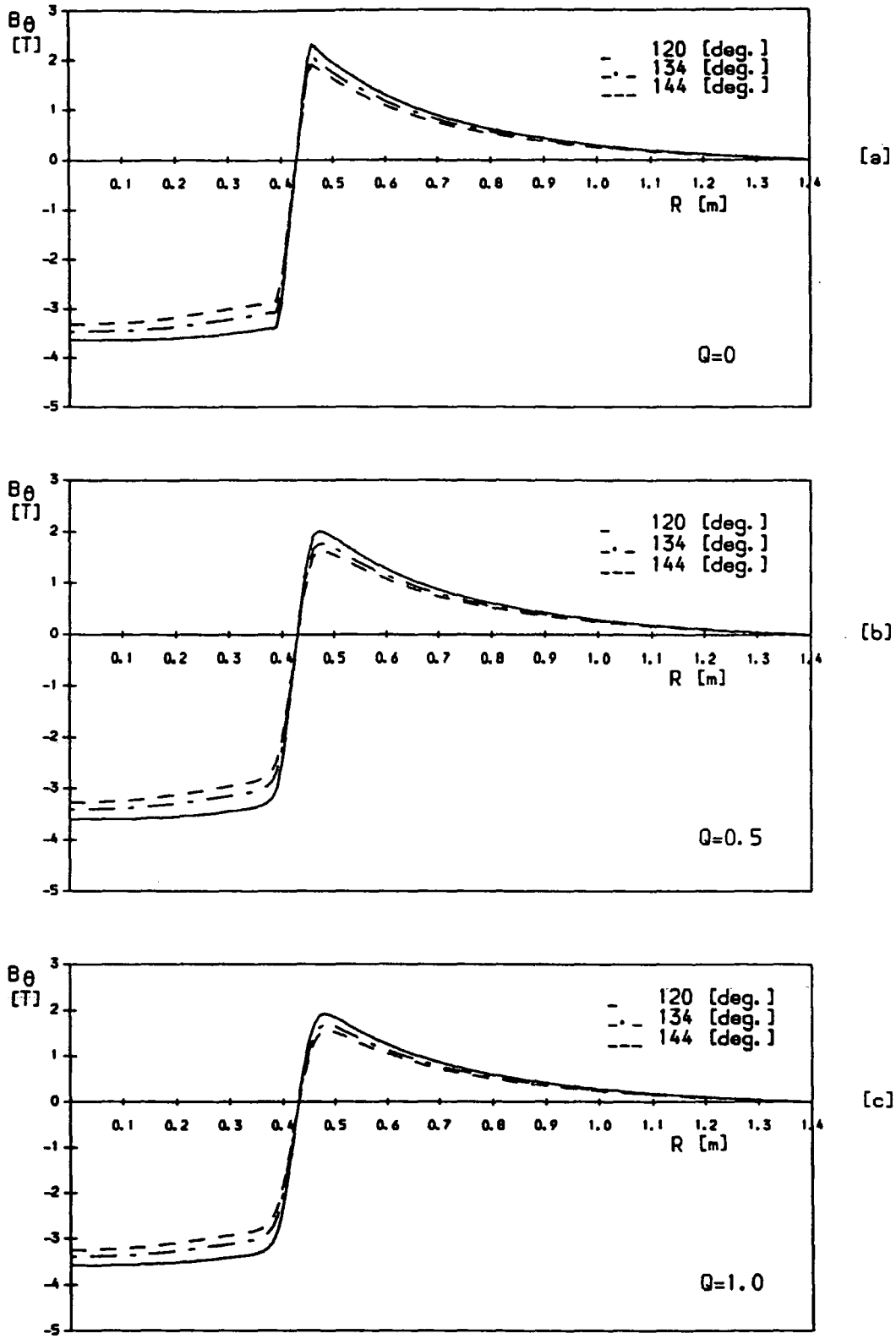

Fig. 2.17 The effect of winding spread angle and slot/tooth aspect ratio on the tangential flux density calculated at $\theta = 90°$.

CHAPTER 3

ELECTRICAL AND MECHANICAL DESIGN CONCEPTS FOR A SUPERCONDUCTING GENERATOR ROTOR

3.1 Introduction

The morphology involved in the machine design process can be resolved into fundamental components such as the recognition and definition of the design problem; this leads to the establishment of the specifications and requirements which the final design must satisfy. For an optimal machine design, it will be appropriate to assess the main factors which define the electrical and mechanical behaviour of the machine and the mandatory requirements for the machine components.

One of the most important elements in any superconducting generator design is the rotor; mechanical stress limits its physical size and hence places constraints on the excitation winding and the cross-sections of the magnetic circuit and cooling system. In choosing the rotor dimensions the mechanical properties of the rotor, which must withstand stress due to the maximum critical speed, are of prime importance. An analytical method has been developed to predict bursting speed by taking into account the geometry, the applied stresses and the material properties. Closely linked with the electrical and mechanical performance of the superconducting rotor design are the B/J limitations of the superconducting field winding material and the tip speed of the rotor components.

With these constraints in mind, the following sections describe calculation methods which relate these different effects. These behavioural constraints are then used in the design optimization procedure presented in chapter 5.

3.2 Overall design criteria

3.2.1 Design output equation

The apparent power output expression of the superconducting generator elegantly shows the effect the machine geometry and superconductor characteristics has on the design of the machine.

The output of a three phase machine may be written

$$S_r = 3 \times V \times I \qquad VA \tag{3.1}$$

Where V is r.m.s voltage per-phase and can be expressed as

$$V = \left(\frac{\sqrt{2}}{p}\right) \times k_{ws} \times N_a \times B_{r_s} \times r_s \times l \times w \qquad Volts \tag{3.2}$$

where $w = 2 \times \pi \times f \qquad rad./s$

Substituting equation 3.2 int 3.1, gives the apparent power

$$S_r = \left(\frac{3\sqrt{2}}{p}\right) \times k_{ws} \times N_a \times B_{r_s} \times r_s \times l \times w \times I \tag{3.3}$$

Proceeding further,

$$J_a = \frac{I}{A_c} \qquad A/m^2 \tag{3.4}$$

where A_c is the cross-section of one phase conductor

By substituting equation into 3.3, gives

$$S_r = \left(\frac{\sqrt{2}}{2 \times p}\right) \times k_{ws} \times B_{r_s} \times J_a \times r_s \times V_a \times w \tag{3.5}$$

where

$$V_a = 6 \times N_a \times A_c \times l \tag{3.6}$$

B_{rs} is the maximum value of the fundamental radial component of the flux density at stator winding.

In view of dependence of the inner rotor magnetic power (B_{rs}) on the geometrical dimensions and physical properties of the rotor, it is convenient to express the output of the machine in terms of these factors. From the two dimensional field analysis of a two pole machine, the radial flux density at the stator winding produced by the field winding is given by: (see chapter 2)

$$B_{r_s} = K_o \times J_f \tag{3.7}$$

where K_o is a factor that encompasses the geometric factors that determine the distribution of magnetic flux density in the (two dimensional) cross section of the machine.

Substituting equation 3.7 into 3.5, gives,

$$S_r = K \times K_o \times J_f \times J_a \times V_a \times \omega \tag{3.8}$$

where $K = (\frac{\sqrt{2}}{2 \times p} \times k_{ws})$ is a geometric factor.

3.2.2 Design strategy

The expression for apparent power S_r, (3.5), shows the potential advantage of using a superconducting field winding is to increase the power output of the generator by increasing the magnetic field produced by the superconducting field winding. Howerever, as will be shown in this study, the ability to use a higher flux density at the stator is limited by many conditions which determine the output power as related to the dimensions of the machine. Mechanical and electrical parameters affect the power output which is considerably influenced by the construction arrangement. To understand

the importance and significance of this result, it must be seen in terms of the design constraints on the inner rotor magnetic power. As shown in equation 3.6, the magnetic power of the inner rotor depends upon the dimensions and current density of the inner rotor. For optimal magnetic power (defined by $K_o J_f$), the achievable flux density is restricted by rotor dimensions and the current density. Consequentely, for a given number of poles and a given critical speed, the maximum practicable inner rotor outer radius is determined, in the first instance, by the centrifugal forces acting on the slotted inner rotor. This in turn depends for the most part on the dimensions of the slotted inner rotor. Other constraints on the design as related to J_f are imposed by the characteristic of the superconducting material. A further constraint is the saturation in stator core material. Increasing the inner rotor magnetic power is also constrained by the design of the support required between the cryogenic inner rotor and its room temperature external structure. Aside from design considerations, construction and superconductor costs can be expected to be a strong function of the inner rotor magnetic power. There are thus strong incentives for maximizing the inner rotor magnetic power.

3.3 Field winding design and support structure

From the viewpoint of generator cost, a superconducting field winding should be designed so that the ampere-turns (AT_s) of the field winding produce a flux density at the armature winding of about 1.0-1.5 T and a maximum flux density in the vicinity of the field winding of about 6.0 T [Maki, 1980].

It was noted in chapter 2 that the maximum flux density at the superconducting rotor winding depends on the winding geometry such that the maximum allowable current density of the superconducting winding is limited by localized flux concentrations which appear around the outermost

slot. Since flux concentration is caused by the field winding geometry this effect can largely be minimized by the use of a graded winding and different slot geometries (i.e. shortened outermost slot). This can be achieved by using the approach developed in the preceding chapter. This approach also provides a record of basic design information covering different slotted shapes of winding likely to be used in practice. The basic design has shown that a saddle shape winding is preferred with 120° and or 140° winding spread or with a limited amount of grading. However, for the same current density the fundamental component of radial flux density is larger when a 144° spread is used than when the winding spread is 120°. Further, the $3rd, 6th, 9th, \ldots$ harmonic components can be suppressed by using a star-connected armature winding and therefore the field winding angle of 144° is clearly more advantageous from the viewpoint of magnetic field utilisation.

Before making positive recommendations on the slotted, saddle shape, rotor design some other factors, particularly the effect of the helium system and mechanical aspects should be briefly emphasised.

It is generally more effective to use a slotted saddle shape design as the geometrical structure provides effective helium cooling of the field winding, both in the slotted straight part and in the end turns of the winding. Because this system is based on a combination of radial and axial passages, fed from a helium storage container, the helium flows in a large number of relatively short paths. Helium is circulated primarily by channels through radial ducts. This type of cooling system implies the minimum risk of losses under variable operating conditions which can lead to temperature rise and would therefore result in normalisation of the winding.

In such a slot design concept, the depth of the rotor slot is determined primarily by the choice of permissible maximum tangential stress at the rotor bore. Radial stresses in the rotor teeth determine the maximum width of

slot as well as the cross-section of the field windings and cooling ducts. The stresses are influenced by the shape and spacing of slots. Lower nominal stress levels are necessary in the tooth region than at the rotor bore in view of the higher stress concentration which exist at the tooth root and around the wedge dovetail.

In determining the maximum permissible design stress at the rotor bore, it is preferable to assume that boring the rotor may be necessary to permit internal inspections, and allow samples to be taken. The better physical properties of the rotor forging material, available for use in the superconducting generator, make it possible to use a winding slot of larger dimensions. For example, the slotted inner rotor of 1300 MVA generator, with radius 0.45 m, an austenitic steel is used because of its excellent properties at low temperature, despite the large outer radius, and still retain a good safety margin. With this material, a value of $300MP_a$ is obtained for a mahine rating 1300 MW.

To obtain maximum superconductor cross-section in the excitation winding, while conforming to acceptable radial stress level in the rotor teeth, it is necessary to employ a slotted saddle shape design which is wider near the rotor surface and which tapers to a narrower width at the tooth root. Such a structure more nearly equalizes the tooth stresses while allowing the slot to contain a significantly greater cross-section of superconductor for the same maximum stress. To ensure maximum reliability in the slot shape design the mechanical aspects of the design have been analysed in section 3.6 to determine the maximum stresses.

Considering the choice of superconductor, present opinion is generally in favour of the $Nb - Ti$ conductors and this alloy will be used for early commerical generators. This is because of the extensive experience that exists for it in terms of superconductor fabrication and utilization in the prototype

machines and in design studies for large machines. With these conductors, it possible to attain current density in slot of about $10^8 A/m^2$ when the continuous induction maintained is lower than $10T$ (the current density takes electric insulation, stabilisation, and refrigeration into account).

3.4 Field winding performance

As has been stated in the previous chapter, the major constraint on the design of the field winding is related to the superconductivity state. All superconductors exhibit a constraint on the current density, this maximum current density being a function of flux density at the winding. As consequence of this, the maximum permitted current density is limited because there is flux concentration around the open corner edge of the field winding. As shown in chapter 2, the radial flux density component at the open corner edge of the winding (i.e. at $\theta = 30°$) is typically 1.32 times the value of this component at $\theta = 0°$.

Additional factors can be introduced to account for environmental iron screen effect and the armature reaction effect at the superconductor, taking into account the fact that the superconductor is at 4 K. A typical fault is a three-phase short-circuit: the armature field is fully de-magnetised so the excitation field is a maximum when the iron screen is used. To obtain maximum reliability the field winding must be designed to cope with these effects and, hence, the following factors must be considered.

(i). Margin on B^f_{max} and J_f to accommodate variation during short-circuit operating conditions.

(ii). Reduction of B^f_{max} to allow for the effect of empirical factors such as flux concentration, armature reaction effects, and machine screen type.

According to the above statements, the maximum flux density at the field

winding has to be lower than the critical flux density corresponding to the existing current density. The criterion:

$$B^f_{max} \leq B^f_c(J) \qquad 3.9$$

is one of the main electrical constraints on the field winding design. Here B^f_{max} is a maximum flux density at the field winding, and will be described by (see chapter 2):

$$B^f_{max} = \mu_o \times k_c \times k_g \times J_f \qquad (3.10)$$

where concentration factor is $k_c \approx 1.32$ and k_g is a factor that encompasses the geometry factors that determines the maximum field in the vicinity of the field winding and is defined in chapter 2. By considering the curve B/J in figure 3.1, the critical flux density and current density can be related as follows:

$$B^f_c(J) = -qJ_f + p \qquad (3.11)$$

where p and q are the fitting constant which depend on the real characteristic of superconductor. Substituting equation 3.10 and 3.11 into equation 3.9, gives:

$$J_f \leq \frac{p}{\mu_o \times k_c \times k_g + q} \qquad (3.12)$$

This equation (3.12) gives an acceptable margin of safety to avoid normalization.

3.5 Environmental screen design

Any machine design incorporates either a laminated iron screen or solid copper or aluminum screen to screen the environment from magnetic fields produced inside the generator. According to the distribution of B_r and B_θ calculated in the previous chapter, the presence of an iron screen increases B_r and decreases B_θ. B_θ does not contribute to voltage generation. Since the copper or aluminum screen reduces the magnetic field for given field current, higher field currents may be necessary than if an iron screen were used.

The iron screen will have losses resulting from eddy current and hysteresis which may be calculated by

$$p_{sc} = \pi \times \left[\left(r_{xi} + t_x\right)^2 - r_{xi}^2\right] \times l_x \times \rho_x \times d_x \qquad Watts \qquad 3.14$$

Where

$l_x = l$

l_x is the length for calculating screen loss, m

t_x is the thickness of iron core, m

ρ_x is mass density of iron screen, kg/m^3

d_x is the loss per unit mass

Losses in the conducting screen are due to induced eddy currents and are given by

$$p_{co} = \frac{\pi \times B_{\theta_{xi}}^2 \times r_{xi} \times l_x}{\mu_o^2 \times \sigma \times \delta} \qquad Watts \qquad 3.15$$

Where

l_x is the length for conducting screen loss, m

δ is the skin depth screen material.

B_{θ_x} is the value of B_θ at $(r = r_{xi})$.

The radial dimensions of the iron core may be estimated by assuming the iron core material to remain in an unsaturated state. The required iron core thickness could be then determined by the maximum flux density at inner radius ($B_{r_{xi}}$) and the maximum flux density allowed in the core (i.e. flux saturation):

$$B_{(max)} \times t_x = \int_0^{\frac{\pi}{2}} B_{r_{xi}} dr d\theta \tag{3.16}$$

Where

$$t_x = \frac{4\mu_o J_{fs_i} sin\frac{n\sigma_{fi}}{2}}{\pi\left(2+np\right)B_{(max)}} r_{xi}^2 \left(\frac{r_{fo}}{r_{xi}}\right)^{2+np} \left[1 - \left(\frac{r_{fi}}{r_{fo}}\right)^{2+np}\right] \tag{3.17}$$

where

t_x is the minimum thickness of the core, m,

$B_{(max)}$ is the maximum flux density allowed in the core, T.

3.6 Mechanical analysis aspect of the inner rotor

3.6.1 Mechanical stress due to centrifugal force

It is the purpose of this section to develop an improved method from which the rotor configuration is determined in such a way that the allowable stresses are not exceeded.

Figure 3.2 shows the analytical model used for the analysis of the mechanical stresses and also a typical qualitative stresses distribution. The mechanical analysis of the superconducting inner rotor assumes the rotor is simply a rotating electromagnetic which is symmetrical with respect to its axis of rotation and the action of centrifugal loading. The model is divided into the following regions:

Region (1) $(r_{fo} \geq r \geq r_{fi})$

superconducting field winding with tensile strength (T_o)

Region (2) $(r_{fi} \geq r \geq r_c)$

core rotor body with tensile strength (T)

Region (3) $(r_c \geq r \geq 0)$

liquid helium container region

3.6.2 Analytical solution for stresses

The geometric configuration illustrated in figures 3.2-3.3 was analysed as an elastic problem consisting of a circular slotted region, a circular smooth core body, and a hole which contains a liquid having a free surface. The method is based on the replacement of the inner rotor by three regions with variable dimensions as well as material properties and satisfying the conditions at the boundary. Considering the three regions as shown in figure 3.3, the expressions for radial and tangential stresses at $r = r_c$ and r_{fi} will read, in normalized form as follows (see Appendix 2)

$$\sigma_{r_{(r=r_{fi})}} = -\rho_o \omega^2 r_{fi}^2 \Big[\frac{1-y^3}{3}\Big] \tag{3.18}$$

$$\sigma_{\theta_{(r=r_c)}} = \frac{1}{12(1-x^2)}\{12\big(1+x^2\big)p_i + 8\omega^2 r_{fi}^2 \rho_o \big(y^3-1\big) + 3\omega^2 r_{fi}^2 \rho \big(1-x^2\big)\big[\big(1-\nu\big)x^2 + \big(3+\nu\big)\big]\} \tag{3.19}$$

$$\sigma_{\theta_{(r=r_{fi})}} = \frac{1}{12(1-x^2)}\{24p_i x^2 + 4\omega^2 r_{fi}^2 \rho_o (y^3-1)(1+x^2) + 3\omega^2 r_{fi}^2 \rho (1-x^2)\big[(1-\nu) + (3+\nu)x^2\big]\} \tag{3.20}$$

By applying the Tresca yield criterion the above expressions may be written in the following form:

For slot/tooth (at $r = r_{fi}$)

$$\Omega \leq -\Big[\frac{3T_o}{\big(1-y^3\big)}\Big]^{1/2} \tag{3.21}$$

For core region (at $r = r_c$)

$$\Omega \leq \Big[\frac{12T\big(1-x^2\big) - 12\big(1+x^2\big)p_i}{8\rho_o\big(y^3-1\big) + 3\rho\big(1-x^2\big)\big[(1-\nu)x^2 + \big(3+\nu\big)\big]}\Big]^{1/2} \tag{3.22}$$

For core region (at $r = r_{fi}$)

$$\Omega \leq \Big[\frac{12T\big(1-x^2\big) - 24p_i x^2}{4\rho_o\big(1+x^2\big)\big(y^3-1\big) + 3\rho\big(1-x^2\big)\big[(1-\nu) + \big(3+\nu\big)x^2\big]}\Big]^{1/2} \tag{3.23}$$

where,

Ω is critical speed, $\Omega = \omega \times r_{fi}$

x is radii ratio, $x = \frac{r_c}{r_{fi}}$

y is radii ratio, $y = \frac{r_{fo}}{r_{fi}}$

ρ is rotor body density

ρ_o is slot wedge/tooth tip region average density

3.7 Rotor tip speed

An additional constraint on the structure of the rotor, is that of the tip speed. This is limited by the strength of the material from which the rotor is fabricated. The rotor usually runs above its second or third critical speed. The machine should not operate close to a critical speed for mechanical vibration reasons, and there is a distinct advantage to operate below the first critical speed. The inner rotor is designed so that yielding should not occur until the operating speed is at least 1.7× rated speed, and for the outer rotor 1.5× rated speed [Appleton, 1975]. In addition, for the inner rotor an austenic steel is selected. Stainless steel has a yield stress of 400 MN/m^2. For the outer rotor, non-magnetic stainless steel was proposed which has a maximum yield stress about 800 MN/m^2

Moreover, at some radius the safe stress is just sufficient to withstand the centrifugal force on the material itself. This critical radius is a characteristic of the material, it is given by:

For inner rotor:

$$r_{fo_c}^2 = \frac{\sigma_r}{f_{osf}^2 \times \omega^2 \times \rho_o} \qquad 3.24$$

For outer rotor:

$$r_{do_c}^2 = \frac{\sigma_d}{f_{osd}^2 \times \omega^2 \times \rho_d} \qquad 3.25$$

where

f_{osf} is the outer over-speed factor (inner rotor), $f_{osf} = \frac{n_{max}}{n}$ =1.7

f_{osd} is the outer over-speed factor (outer rotor), $f_{osf} = \frac{n_{max}}{n}$ =1.5

The feasiblity of these expressions depend again on the choice of the strength of the material, their density and burst speed.

3.8 Result and discussion of some mechanical factors and their influence on design

Befor considering design stresses computation by the analytical expressions derived in section 3.6, a few words of caution in using these expressions should be made. Firstly, it should be noted that the stress expressions are sufficient to define the value of the radial and the tangential stresses because of the choice of proper conditions in the procedure which have been used to derive the stresses (see appendix 2) and consequently have practical advantages, particularly in the pre-stressing operation. Secondly, the expressions define the lower limit of speed for bursting of a cylinder, i.e., it is assumed that, a cylinder could never burst at speed lower than that defined by these expressions.

The analytical expressions for stress components can now be manipulated to produce design information. An illustration of the use of these expressions has been used to calculate the critical speed of the inner rotor of a two pole 1300 MW generator. The main data for such design is given in table 3.1.

Comparisons of the critical speed expression with conventional formulae from the literature [Spooner, 1973]

$$\Omega \leq \left[\frac{3T\left(1-x\right)}{\rho_o\left(y^3-1\right)+\rho\left(1-x^3\right)}\right]^{1/2} \qquad 3.26$$

are given in figures 3.4-3.5. The result produced in figure 3.4 shows these two widely differing methods, this figure, however, shows that the value of the inner rotor critical speed is lower than that which would have been developed if Spooner's method is used. This should be expected as Spooner's procedure assummes that the effect of the radial stress is negligible where the new procedure takes into account these factors, thus giving a more accurate result for the stress distribution throughout the inner rotor. However, more features are given for the new method and are presented in figures 3.6 and 3.7 which, show in detail how to derive the critical speed for the inner rotor as function radius ratio r_c/r_{fo} and core radius. Figure 3.8 shows the radial stress being high at the bore radius (r_c) and then tapering off to a relatively low value at the outer radius of slots (r_{fo}). Further, the graphs in figure 3.8 are plotted to give directly the maximum radial stress in the core region and in the field winding as a function of the inner rotor radius and over speed factor(n_{max}/n); the overspeed factor being varied from 1.5 to 1.8 to cover the effect of this factor. Higher stresses in the inner rotor thickness are however associated with higher value of overspeed factor.

Computation results show that the overspeed factor and the rotor dimensions determine the ability of an inner rotor design to be satisfactory, i.e. the factor of safety at bursting depends on the inner, and outer radius, the ratio of the bore (i.e. r_c/r_{fo}), bursting speed factor, and the properties of the materials. Therefore, for safe design, the appropriate properties have to be known and factors of safety assigned that are consistent with these properties and the geometry of the inner rotor. It has also been noted from the results that the permissible stresses in the rotor body at over speed are set at a maximum of 60%-70% the yield stress of the material used and this ensures a sufficient design safety factor. The slotted rotors are of an austenitic stainless steel alloy 316 LN with a low carbon, $0.2\%N_2$ content.

This alloy possesses the required mechanical properties at low and ambient temperature.

For higher rating generators where weight is critical and maximum utilization of materials is desired, it is helpful to design for an optimum condition where failure, when it occurs, takes place in both parts of the inner rotor simultaneously and resulting best inner rotor geometry so that maximum mechanical performance may be expected with sufficient design factor.

3.9 Summary and conclusion

From this study it is concluded that the design of a superconducting generator is governed by conficiting mechanical and electrical requirements; both of which have to be taken into account when optimizing the rotor design. The major constraints which are placed on the generator rotor are the rotational centrifugal forces which should be known accurately since it is important in selecting the dimensions of the generator rotor to achieve various characteristics.

In this chapter, an analytical expression has been developed to determine the stresses distribution in the superconducting rotor components under rotating conditions. These expressions will be used to select the proper rotor dimensions.

The results of the analytical techniques developed in this chapter will be considered as the main imposed design constraints in the design optimization procedure presented in the following chapters.

Table 3.1
Data

Name	Symbol	Unit	Value
Dimensions			
Core radius	r_c	m	0.091
Field winding inner radius	r_{fi}	m	0.395
Field winding outer radius	r_{fo}	m	0.455
Mechanical data			
Field winding yield strength	T_o	MP_a	60
Inner rotor body yield strength	T	MP_a	400
Outer rotor strength	T	MP_a	400
Field winding average density	ρ_o	kg/m^3	7400
Rotor body density	ρ	kg/m^3	7950
Maximum speed	n_{max}	$r.p.m$	5100
Rated speed	n	$r.p.m$	3000
Passion ratio	ν		0.3

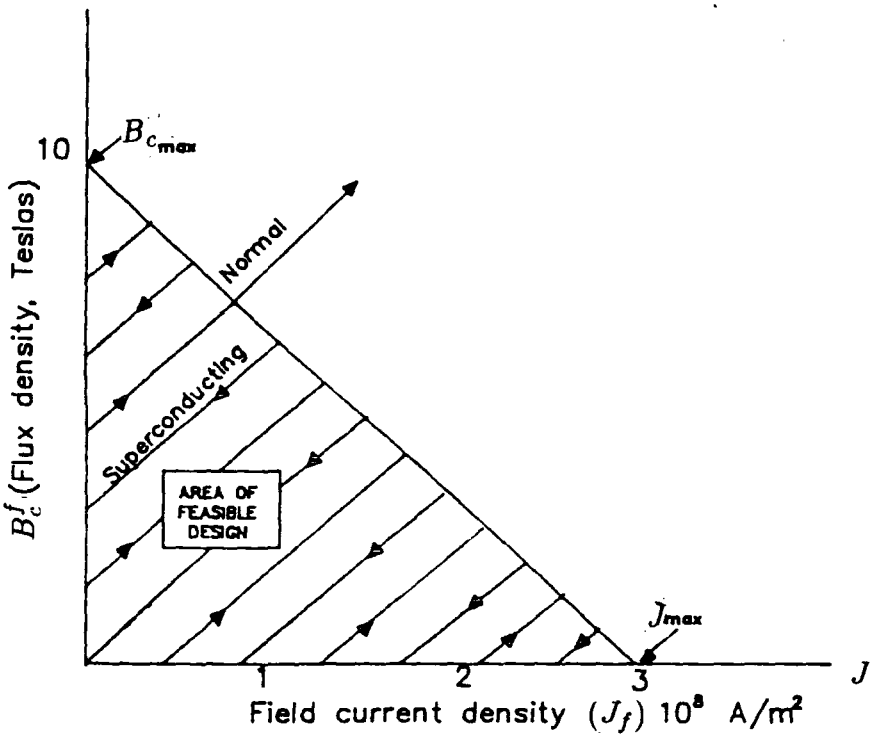

Figure 3.1 Calculated current density charateristic

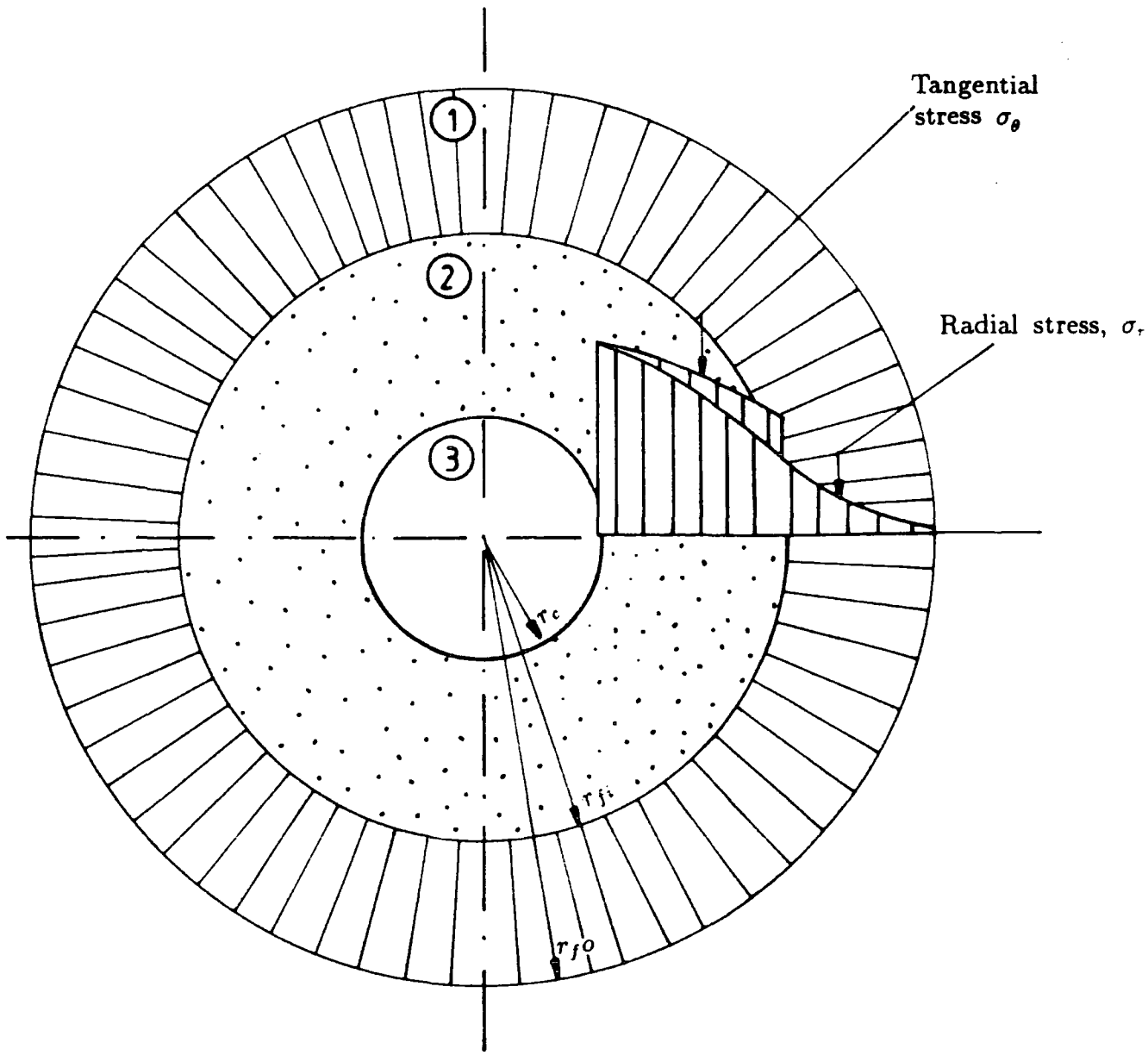

Fig 3.2 Analytical model for the analysis of inner rotor stress.

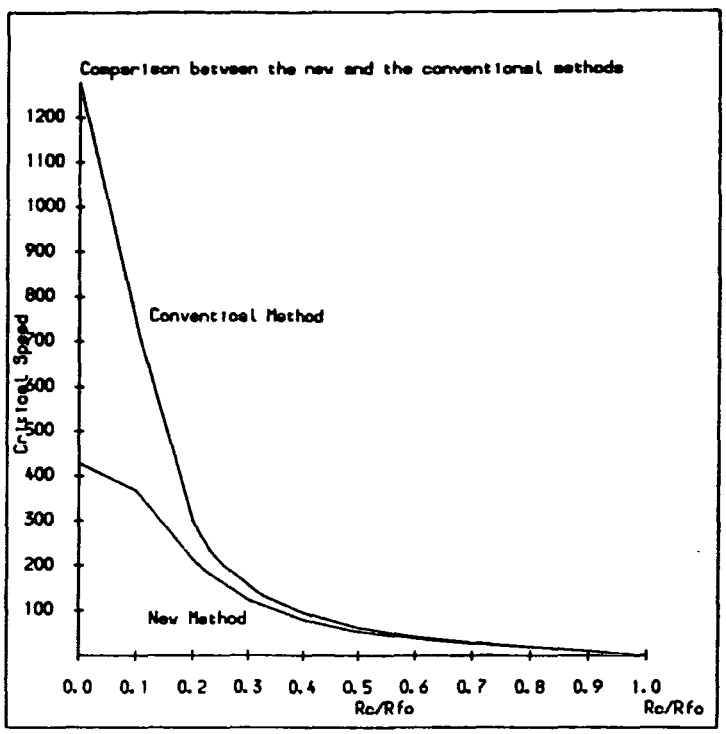

Fig. 3.4 Comparison of the inner rotor critical speed calculated by the conventional and new methods. Where $r_c = 0.2r_{fo}$

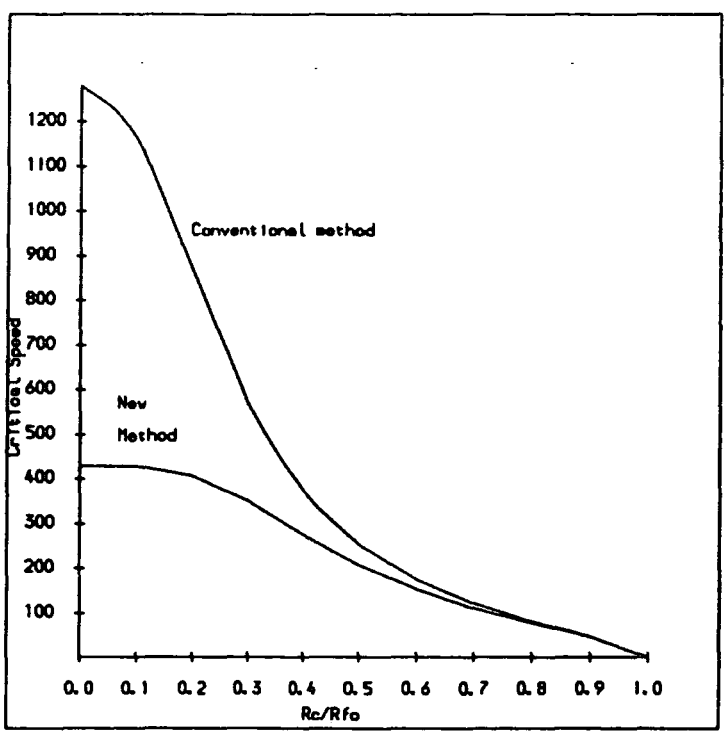

Fig. 3.5 Comparison of the inner rotor critical speed calculated by the conventional and new methods. Where $r_c = 0.8r_{fo}$

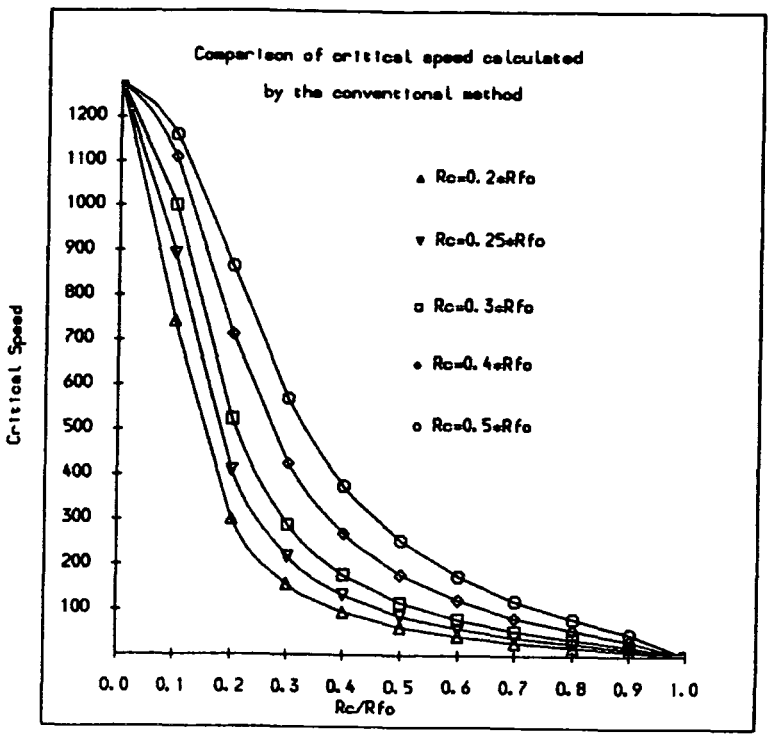

Fig. 3.6 Inner rotor critical speed calculated by the conventional method.

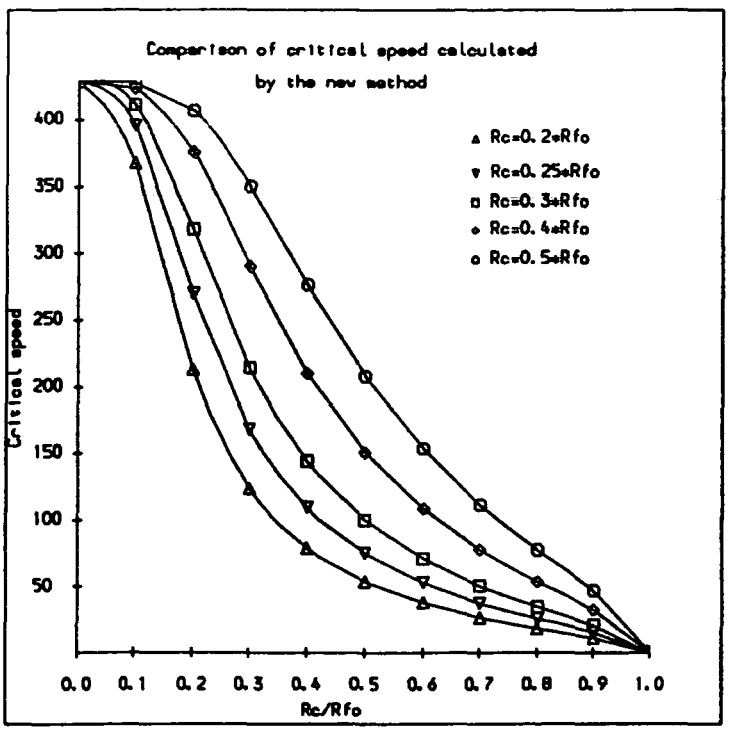

Fig. 3.7 Inner rotor critical speed calculated by the new method.

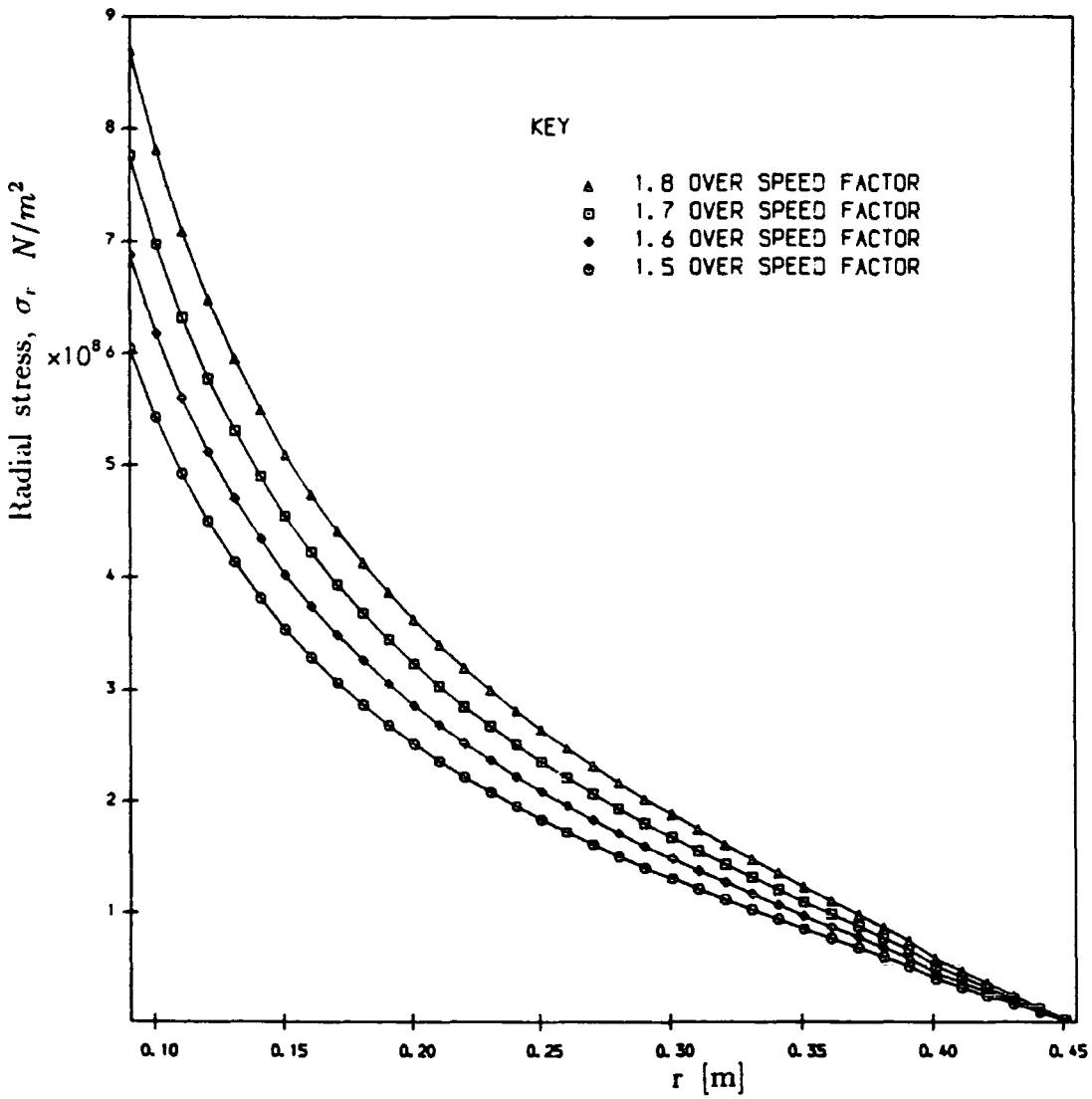

Figure 3.8 Radial stress distribution in inner rotor.

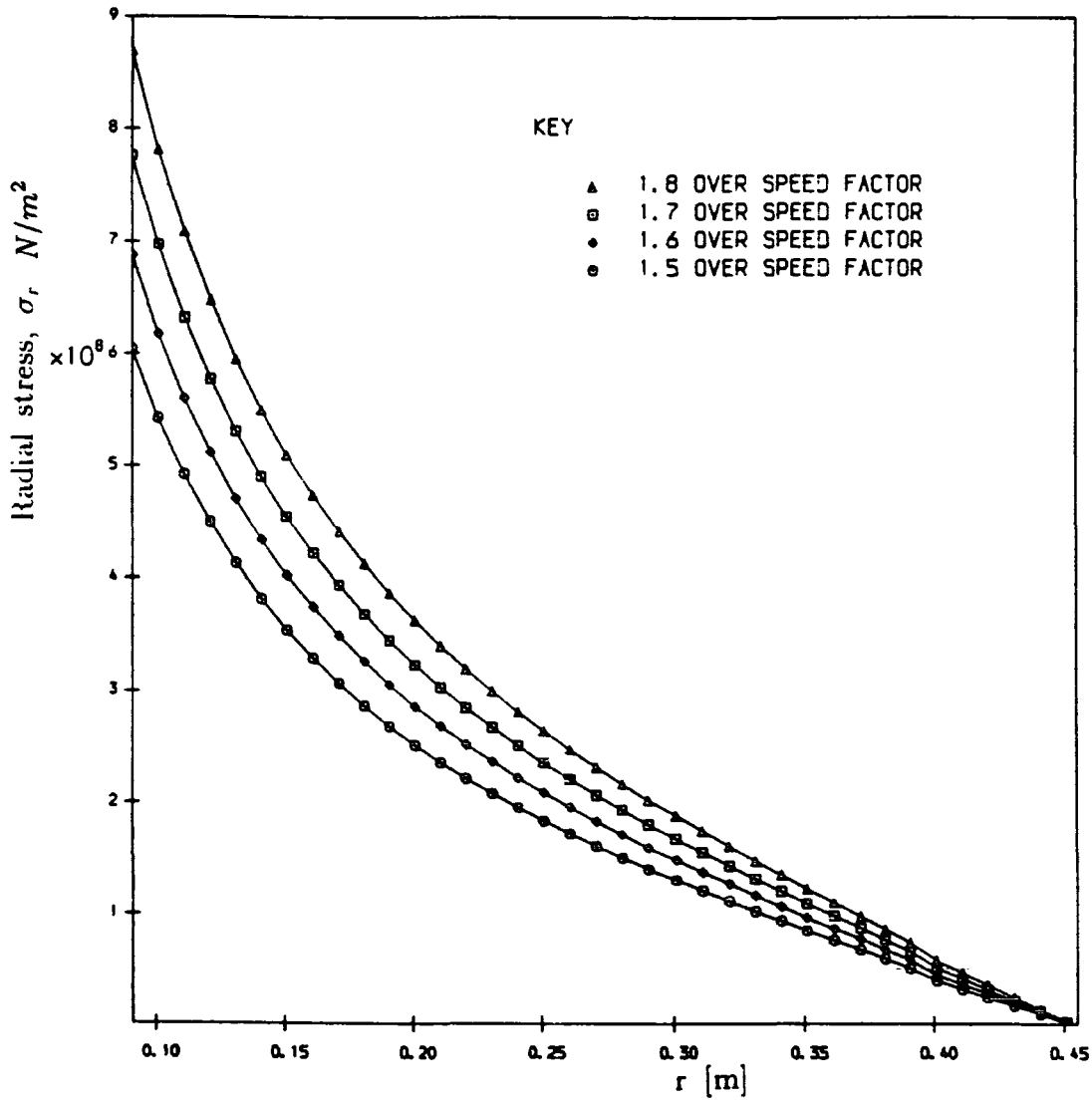

Figure 3.8 Radial stress distribution in inner rotor.

CHAPTER 4

SEARCH METHODS OF MINIMIZATION FOR MACHINE DESIGN

4.1 Introduction

A variety of methods, involving ordinary and variation calculus, mathematical programming, and a number of special techniques, are available to treat optimal design problems. Among these methods, the mathematical programming procedures appear to have the broadest range of application. As a consequence, these procedures have been found to be flexible, easy to adapt, and can offer an 'automatic' design computer solution [Chidambarab, et al, 1982], [Nagrial and Lawrenson, 1978], [Ammasai, et al, 1988]. The procedures solve, or attempt to solve, the design problem which can be stated as

$$\textit{find} \quad \textit{vector} \quad \bar{x} = \begin{Bmatrix} x_1 \\ x_2 \\ \vdots \\ x_n \end{Bmatrix} \textit{which} \quad \textit{maximizes the value of} \quad f(\bar{x}) \quad n = 1, 2, \ldots, N \tag{4.1}$$

subject to the M inequality constraints

$$g_m(\bar{x}) > 0, \qquad m = 1, 2, \ldots, M \tag{4.2}$$

and the I equality constraints

$$h_i(\bar{x}) = 0, \qquad i = 1, 2, \ldots, I \tag{4.3}$$

In addition 'limit' constraints of the form

$$\bar{x}^{(u)} > x_n > \bar{x}^{(l)} \tag{4.4}$$

In optimum machine design, $f(\bar{x})$ is the (scalar) property of the problem which has to be minimized. This could be magnetic power of the inner rotor, power output, volume, or any combination thereof. Minimizing a function is the same as maximizing the negative of the function so there is no loss of generality. The set, x_n, is a set of design parameters and could be, for example, dimensions, current density, and so on. On the other hand, $g_m(\bar{x})$ and $h_i(\bar{x})$ are a set of constraint functions which are used to control or define the behaviour of the design. The inequalities employed may be linear, or highly non-linear, functions for either superconductivity or mechanical stresses in a superconducting rotor. Inequality design constraints can also be used to control the values of the variables within certain limits (limit constraints) as presented in equation (4.4), where $\bar{x}^{(u)}$, $\bar{x}^{(l)}$ are the upper and lower limits (or bounds) on the variables. The problem stated above is non-linear if one of the function $g(x_n)$ or $f(x_n)$ is non-linear, otherwise it is linear programming problem (i.e. linear objective and constraints). For those problems where all the equations are linear, the highly effective linear programming methods can reliably, locate the global optimum in a finite number of steps. Most computer libraries include such methods and enjoy wide popularity and utilization. Unfortunately this situation does not exist in the case of general nonlinear problems. None of the many nonlinear methods proposed can guarantee a solution except in certain relatively restricted formulation [Wilde, 1964].

In this chapter, some formal non-linear programming procedures to search for minimum or maximum will be discussed in detail.

4.2 Selection of non-linear programming NLP as optimization model

Non-linear programming (NLP) methods are essentially optimal search strategies. They start from some arbitrarily selected point, usually in the feasible region, and then attempt to move toward the optimum on the basis of the local properties of the functions involved. The basic unconstrained non-linear problem is, by comparison with the general constrained linear problem, quite difficult. The difficulty is compounded when constraints are used. Equality constraints are particularly troublesome since they severely restrict the feasible region, thus substantially increasing search difficulty. Fortunately equality constraints can often be eliminated by using the equality to eliminate an independent variable thereby reducing the design problem dimensionality and difficulty, as will be seen in the next chapter. Thus, most non-linear optimization procedures used in design problems are essentially formulated to treat problems with inequality constraints.

Generally speaking, the majority of constrained non-linear optimization procedures that have been proposed in the literature to date are centered upon one of three basic concepts:

(1.) Extension of linear methodology to NLP problems by means of repeated linear approximation. Example: Kelly's cutting method.

(2.) Transformations of constrained NLP into a sequence of unconstrained problems through the use of a penalty function. Example: sequential unconstrained minimization method SUMT [Fiacco and McCormick, 1964].

(3.) Use of flexible tolerance to accommodate both feasible and non-feasible $\bar{x}$ vector. Example: the flexible tolerance method [Himmelblau, 1972].

Generally methods of type (1) are most attractive for problems in which

the constraints may be approximated closely by means of linearisation, while type (2) is of special interest when the objective function as well as the constraints are strongly non-linear. In the present optimization procedure, the penalty function methods are used. The basic idea of these methods is that a penalty parameter is selected and used to transform the constrained problem of equations (4.1-4.4) into the first of a sequence of "unconstrained" problems which converge to the solution of the original problem. A wide variety of alogrithms exist for the solution of such unconstrained problems. It is natural to distinguish between:

(1). Methods which use derivatives in optimization i.e. involve the calculation of gradients.

$$\Delta_f(x) = \frac{\partial f}{\partial x} \tag{4.5}$$

These methods are characterized also by each step of a best direction along which to move at each step and popular procedures such as steepest desent (or gradient), conjugate gradient or Newton are available.

(2). Methods which do not use derivatives of the objective function i.e. methods that do not involve the calculation of gradient.

The methods which belong to type (2) are commonly known as direct search methods [Hook and Jeeves, 1961], [Nelder and Mead, 1965]. With these methods, the solution is obtained in an iterative manner starting from some arbitrarily selected values and the improvement is achieved with successive iterations until the optimal solution has converged to the desired accuracy. However, these methods turn out to be preferable in the present work for following reasons:

(1). The selection of the direct search method is deter-

mined principly by the formulation difficulty. The selection of a minimization algorithm was determined primarly by the choice of minimization packages available in the computer centre. All available packages are based on gradient methods which are generally faster in computation time than direct search methods, but they need derivatives in order to solve the design problem. This is a practical disadvantage. Futhermore, the nature of the design problem under consideration rules out the possibility of formulating derivatives analytically and consequently direct search methods are mandatory. Furthermore, these gradient methods require relatively large amount of problem preparation by the user before the user introduces the design problem into algorithm, as compared with direct search methods.

(2). Direct search techniques are fully general as they do not require regularity restriction and continuity of the objective function and the existence of derivatives.

(3). In general, direct search methods are conceptually and mathematically simpler than other methods and are easier implemented in computer programming.

There has been a limited number of attempts to compare current methods of minimization and formulate a general conclusion. However, Box [Box, 1969] has compared direct search methods on a number of mathematical functions and from his results, it has been shown that the simplex method [Nelder and Mead, 1965] is the most efficient of the current sequential techniques. Kowalik [Kowalik and Osborne, 1963] confirms these results. Schnabel [Schnabel, 1966] also showed the simplex method as being a reasonable efficient technique. The direct search method of Hook and Jeeves [Hook and Jeeves, 1961] has already found useful application in the design of conventional ma-

chines involving a complicated design function and constraints. Ramaratham [Ramaratham et al, 1976] has given a comparison of some methods on the machine design problem and from the results, it is shown that the pattern search method [Hook and Jeeves, 1961] is as efficient as any other methods. At the same time, the pattern search of Hook and Jeeves has been successfully applied for predicting optimum design of induction motors [Chidambarab et al, 1982], [Menzies and Neal, 1975].

From the above discussion, it can be concluded that two direct search methods [Hook and Jeeves, 1961], [Nelder and Mead, 1965] have been found efficient on a number of design problems. These methods have not been used, as far as the author is aware, on superconducting machines. It is difficult to choose a generally suitable alogrithm because the comparative data is limited and superconducting machine design may include difficulties not treated in mathematical programming literature or conventional design problems. For this purpose, more than one search procedure is used to choose the suitable search method for the design problem at hand.

The direct search and random methods used in this procedure are compared on mathematical test functions used in earlier studies and the results are reported in this chapter. Two penalty function methods have been studied in conjunction with the direct search methods.

4.3 Description of search methods of minimization

4.3.1 General considerations

Methods which do not rely explicity on the evaluation or estimation of partial derivatives of objective function at any point are called direct search methods. Generally speaking, they rely on the sequential examination of trial solutions in which each solution is compared with the best obtained up to

that time, with a strategy generally based on past experience for deciding where the next trial solution should be located.

In the next section, the essential features of the direct search methods [Hook and Jeeves, 1961], [Nelder and Mead, 1965] are described while in section 4.4 a random and shrinkage method is outlined and compared with these direct search methods.

4.3.2 The pattern search of Hook and Jeeves

The pattern search of Hook and Jeeves [Hook and Jeeves, 1961] is designed to follow along fairly narrow valleys because it attempts to align a search direction along the valley. The alogrithm is as follows

(1). Starting at some arbitrary initial point an exploratory search is begun by changing one variable a predetemined small positive step length. If this improves the optimization function, it is used as the new reference value. If it does not, a negative step is taken. If both fail, no step is taken. The best value from the search of x_1 is used as the reference point for exploring x_2.

(2). The final result of a successful exploratory search is a new base point.

(3). A pattern move is now made by moving each independent variable from the latest base point an amount equal to the difference between the new and old base point values. This difference will commonly include a previous move.

(4). If the move fails to improve the optimization function, it is cancelled and a new search is made from the base point. If the move succeeds, it is followed by a new search.

(5). The process is repeated until the univariate search can

not locate a better point. Then the step length is reduced by some arbitrary fraction, and an exploratory search is continued. After each failure the step length is reduced until it reaches some predetermined minimum, when it is assumed the optimum has been reached. The method is illustrated for two dimensions in figure 4.1

Figure 4.2 shows an example of the pattern search strategy. The starting point $\bar{x}^1$ is first base point b^1. The first exploratory move from $\bar{x}^1$ begins by incremeting $\bar{x}^1$ and resulting in $\bar{x}^2$. Since $f^2 < f^1$, $\bar{x}^2$ is retained and exploration is continued by incrementing $\bar{x}^2$. $f^3 < f^2$ so $\bar{x}^3$ is retained in place of $\bar{x}^2$. The first set of exploratory moves being complete, $\bar{x}^3$ becomes the second base point b^2. A pattern move is now made to $\bar{x}^4 = 2b^2 - b^1$, i.e, in the direction $b^2 - b^1$, in the hope that the previous success will be repeated. The f^4 is not imediately compared with f^3. Instead, a set of exploratory moves are first made to try to improve on the pattern direction. The best point found in present example is $\bar{x}^5$ and, since $f^5 < f^3$, it becomes b^3, the third base point. The search continue a pattern move to $\bar{x}^8 = 2b^3 - b^2$.

When a pattern move and subsequent exploratory moves fail (as around $\bar{x}^{13}$), the strategy is to return the previous base point. If the exploratory moves about the base point fail (as at $\bar{x}^8$) the pattern is destroyed, the step length is reduced and the whole procedure restarted at that point. The search is terminated when the step length fall below prescribed levels. A flow chart illustrating the above procedure is given in figure 4.3.

4.3.3 Nelder-Mead flexible polyhedron search

This 'simplex' search of Nelder and Mead is an extension of the simplex method by Spendley [Spendley, et al, 1962]. Both methods utilize a regular geometric figure called simplex. This method accelerates the simplex method and makes it more general and has proved to be an effective strategy

easily implemented on digital computers. This procedure is based on the work by Nelder [Nelder and Mead, 1965]. The basic concepts of this procedure are given below.

(1). Intitialization

A 'simplex' in N-space is a set of $N + 1$ points (vertices) such that the N-vectors from one point to the other span the space (i.e are linearly independent). The initial simplex represents a certain mode of local exploration defined by the points l, s, and h and N-2 additional points in general N-dimensional problem. The points l, s, h are the lowest, second lowest and greatest function value (f). The point o is the centroid of all vertices except (h). The first simplex is conveniently chosen as regular (with equidistant vertices) in a suitably scaled parameter space and, hence, the co-ordinates of its vertices can be obtained by a simple general formula

$$\bar{x}_o = \frac{1}{N}\{\sum_{\substack{j=1 \\ j\neq h}}^{N+1} \bar{x}_j\} \tag{4.6}$$

when the location of its centroid and the vertex distance have been fixed.

(2). Generation of new simplex

The function is evaluated at each of the vertices, and the vertex which yields the highest function value is projected through the centroid of the remaining vertices into its systemetric image with respect to this centroid ('reflection'). This and other moves ('expansions', 'contraction', 'reduction') accompained by function evaluation and comparisons, lead to a new, not necessarily regular, simplex with better vertices (in particular, the vertex with the highest function value is always replaced by a point with lesser function value). Figures 4.4 gives a pictorial representation of this strategy while a discription of the alogrithm is given in figure 4.5. For all the

numerical experiments in this study, the available co-efficients for reflection (α), contraction (β) and expansion (γ) are given the value 1, 0.5, and 2 respectively, as recomended by Nelder [Nelder and Mead, 1965].

(3). Termination

As in other applications [Himmelblau, 1972], the criterion used to terminate the search is

$$\Big[\frac{1}{N}\sum_{j=1}^{N+1}\big(f(\bar{x}_j)-f(\bar{x}_o)\big)^2\Big]^{0.5} < \varepsilon \tag{4.7}$$

where ε is suitably chosen tolerance

Alogrithm

The alogrithmic procedure is as follow:

(1). Initialization. Set up the initial simplex of abitrary size and evaluate f_s, f_l, f_h

(2). Reflection. The first step is a reflection of $\bar{x}_h$ through the centroid to give a new vertex, $\bar{x}_r$

$$\bar{x}_r = \bar{x}_o + \alpha\big(\bar{x}_o - \bar{x}_h\big) \tag{4.8}$$

The point r should be better than h and probably better than s, unless it is in the vicinity of an optimum.

(3). If $f_s > f_r > f_l$, $\bar{x}_h$ is replaced by $\bar{x}_r$, and a new simplex is formed.

(4). Expansion. If $f_r < f_l$, the move is accelerated in r direction by the relation

$$\bar{x}_e = \bar{x}_o + \gamma\big(\bar{x}_r - \bar{x}_o\big) \tag{4.9}$$

(5). Contraction. If in step 2, $f_h > f_r > f_s$, then $\bar{x}_h$ is replaced by $\bar{x}_r$ and the simplex is contrcted by the expression

$$\bar{x}_c = \bar{x}_o + \beta\left(\bar{x}_h - \bar{x}_o\right) \tag{4.10}$$

This situation is indicated in the vicinty of the optimum in figure 4.5. $\bar{x}_h$ is replaced by $\bar{x}_c$ in a new simplex.

(6). If in step 2, $f_r > f_h$, the contraction has taken palce as in step 5 but without substituting $\bar{x}_r$ for $\bar{x}_h$.

(7). In step 5 or 6, the contraction is successful if $f_h > f_c$, and $\bar{x}_h$ is replaced by $\bar{x}_c$ in a new simplex.

(8). Reduction. Finally, if step 7 has failed (i.e a case of failure $f_h < f_c$), the last simplex is shrunk about the point of the lowest function value $\bar{x}_l$ by relation

$$\bar{x}_j = \bar{x}_l + 0.5 \times \left(\bar{x}_j - \bar{x}_l\right) \tag{4.11}$$

(9). The process is then restarted at step 1 by the new simplex generated in 4, 5, 6, 7, or 8.

(10). Termination. The stopping criterion used here to terminate the search (i.e. the search is presumed to be at optimum) is

$$\left[\frac{1}{N}\sum_{j=1}^{N+1}\left(f(x_j) - f(x_o)\right)^2\right]^{0.5} < \varepsilon \tag{4.12}$$

4.4 Random search with shrinkage methods

4.4.1 Random strategy

Random search methods do not require derivatives and rely only on direct function evaluation. They are based on generating a sequence of improved approximations to the minimum, each approximation being derived from the preceding one. Figure 4.6 shows a much simpler strategy. The direction of search at any point in such methods is selected at random. These methods are commonly called Monte-Carlo methods. In this strategy a certain number of points are selected at random over the operating space (i.e. the estimated range of all variables). The best result obtained is assumed to be an optimum point. The randomly selected values of x_n can be obtained from the relation:

$$x_n = l_n + r_n\left(u_n - l_n\right) \tag{4.13}$$

Where l_n and u_n are respectivily the lower and upper bounds on x_n and r_n a random number between zero and one. If one decides to evaluate the optimization function $f(\bar{x})$ for say 200 points one generates n random numbers r_n for each point and equation 4.13 defines the values of the independent variables x_n which are used to evaluate $f(\bar{x})$ for that point. A new random number is generated for each of 200 points.

4.4.2 Shrinkage or reduction strategy

Random search (Monto Carlo) methods may be improved by applying the process sequentially. Different strategies based on this method have been developed. One such method is the shrinkage strategy developed by Mcarther [Mcarther, 1960]. It starts off like the random strategy with a random set of points over the operating space. However, after running a certain number

of sets, the best point is selected and the operating space is reduced by some arbitrary amount based on intuition using as a centre point that point which gave the previous best value of $f(\bar{x})$. A new random set of values is calculated within this reduced operating space. The process is repeated until the space is shrunk to the desired amount. The shrink strategy consists of random search but in continually reduced operating space. The simple shrink strategy is shown in figure 4.6.

An alternative shrinkage strategy has been proposed by Brooks [Brooks, 1958]. In this method a normal distribution at each stage after the first instead of flat density function. The shrinking is done by progressively reducing the variance used. Use of a normal distribution has the advantage of tending to concentrate on the most likely vicinity of the optimum.

A third shrinkage method developed by Dickinson [Mcaurther, 1960] generates an automatic rather than an arbitrary shrinkage factor. The intuitive basis for the method can be appreciated by referring to the following example. For six variables, the search is begun by evaluating 40 random points by use of equation 4.13. From these the best 10 are picked and used as the basis for a new and shrunken range for each variable. Within this new space 40 new random points are evaluated. These plus the previous 10 best are, sorted to yield a new 10 best and new shrunken space. The process is repeated until the range of each variable is acceptably small.

4.5 Constrained minimization procedure

The general non-linear constrained optimization problem was defined in section 4.1. Direct search minimization methods defined in the section 4.3 were developed to solve unconstrained optimization problems but can be adapted to

the constrained problem by means of penalty functions [Spang, 1962], [Fiacco and McCormick, 1964]. The use of an appropriate penalty function allows a constrained non-linear programming problem to be transformed into a sequence of unconstrained minimization problems. Whenever there is a violation of a constraint a penalty may be put on the objective function so that during the course of iteration the constraints will eventually be satisfied (see figure 4.7). In this section, two methods of penalty function are discussed:

4.5.1 Exterior penalty function

A simple exterior penalty function has been developed by Spang [Spang, 1962] for the direct search method. The original objective function is replaced by a very large value whenever the inquality constraints are not satisfied so that the unconstrained optimization method is forced to search in the feasible region. This method is very simple and does not require an initial feasible slolution but it sometimes hangs on the ridged of the constraints. In this method the following transformation can be used

$$P(\bar{x}) = F(\bar{x}) + 10^{20} \sum_{m=1}^{M} |g_m(\bar{x})| \tag{4.14}$$

Where $P(\bar{x})$ is the unconstrained objective function used in the the search. $10^{20} \sum_{m=1}^{M} |g_m(\bar{x})|$ is regarded as a penalty factor attached to the objective function $F(\bar{x})$ to be minimized (or maximized).

4.5.2 The sequential unconstrained minimization technique (SUMT)

The sequential unconstrained minimization technique was adopted to solve the constrained optimization problem defined in section 4.1. This approach has been used extensively in recent years in application relating to conventional machine design [Nagrial, 1979], [Ramarathnam, 1973], [Bharadwaj, 1979], and some very encouraging results have been obtained. Sequential methods generate within the feasible region, a series of functions whose successive unconstrained optima converge to the optimum of the constrained problem. For the case of inequality constraint only, the resulting penalty function is:

$$P(\bar{x}, r_k) = F(\bar{x}) + \sum_{m=1}^{M} G[g_m(\bar{x})] \tag{4.15}$$

where:

$F(\bar{x})$ is the objective function to be maximized (or minimized).

M is total number of inequality constraints.

$G[g_m(\bar{x})]$ is the penalty function (based on constraints $g_m(\bar{x})$)

Various forms can be assigned to $G[g_m(\bar{x})]$, the one used in this work being

$$G[g_m(\bar{x})] = w_m r_k g_m^{-1}(\bar{x}) \qquad k = 1, 2, \ldots \tag{4.16}$$

Where

r_k is penalty parameter.

w_m are the postive weight given to the constraints.

This form was first given by Carrol [Carrol, 1961] and was subsequently

adopted by Fiacco and McCormick [Fiacco and McCormick, 1964]. When equation 4.16 is substituted into the general equation 4.15 it gives

$$P(\bar{x}, r_k) = F(\bar{x}) + r_k \sum_{m=1}^{M} \frac{w_m}{g_m(\bar{x})} \tag{4.17}$$

To use the technique an initial value for r_k, r_1, must be chosen along with the initial values of all the x_n and the weight w_m. The resulting unconstrained function is then minimized. The value of r_1 is then divided by a reduction factor (> 1.0) to give r_2, so that $P(\bar{x}, r_2)$ has reduced penalty which more closely resembles $F(\bar{x})$. This function is minimized using the optimum solution to the previous minimization as the new starting point as shown in figure 4.7. Further reduction of r_k and successive minimization create a series of optima that gradually tend to the optimum of objective function

$$min.P(\bar{x}, r_k) \rightarrow min.F(\bar{x}) \qquad when \qquad r_k \rightarrow 0 \tag{4.18}$$

In order to use the sequential penalty technique it is necessary to ensure that starting variables lie within the feasible region. This requirement poses no problems with the superconducting machine design problem. However, it may happen that an initial feasible point is not a variable so that it is necessary to adapt an auxiliary procedure to reach the feasible region from the infeasible region and is given by Fiacco [Fiacco and McCormick, 1968].

SUMT can only guarantee to locate the true minimum if the function $P(\bar{x}, r_k)$ is strictly convex. If not then the method can only be guaranted to locate a local minimum solution which may or may not concide with the true minimum solution. If the solution located is the true minimum then it is called the global optimum solution, otherwise it is a local optimum solution.

The required convexity condition will apply if the original objective function $F(\bar{x})$ is convex and the constraints are such that the feasible region is enclosed within a convex region. So far, the author has found that the rotor design problem does not meet the convexity requirement. As a result it is necessary to repeat the optimization several times with different starting point designs, and generate a number of approximiate local optimum the highest (or lowest) cost local optima must then be selected as the final solution.

4.5.3 Weighting factors

There are three weighting factors associated with the sequential penalty function, the value r_1, the values of w_i and the multiplying factor to use in reducing the value of r_k successive descents.

Box [Box et al,1969] found that the convergence of the sequential technique is more rapid when all the variables and constraints are scaled in order to be as far as possible of the same order of magnitude. However, Box further states that there is no analytical method or satifactory alogrithm avalible for calculating the optimum value of w_i. As a result the author has followed the suggestion of Fiacco and McCormick [Fiacco and McCormick, 1968] which involves taking all the w_m values as unity.

Fiacco and McCormick [Fiacco and McCormick, 1968] have mentioned that the rate at which r is reduced for successive minimization or penalty functions does not seriously affect the total efforts involved in finding the constrained maximum (or minimum). The larger the reduction factor, the fewer became the number of unconstrained minimizations required. Box [Box et al, 1969] found that the reduction in r_k by a multiplication factor of order 0.1 to give an extra decimal point at each minimization to be

advantageous. It is felt that this value is not particularly critical when solving the superconducting design problem. The value of the reduction factor of 0.05 is used in the author's computer program for all test problems used in this chapter. The selection of a suitable starting value of r_k, r_1, presents the greatest difficulty. The effect of choosing a suitable value for r_1 can be critical in determining the solution speed of minimization and can also effect the rate of convergence. If too small a value is used the penalty term contribution to the function value will be small and the function $P(\bar{x}, r_k)$ will approximate too closely to the true function $F(\bar{x})$ before the constrained minimum has been located. The effect of this can be to produce very slow convergence. Alternatively, termination of the process can occur at a point on the constraint boundary which does not correspond with optimum. If too large a value of r_1 is used, the minimum of the first few $P(\bar{x}, r_k)$ functions will be forced well into the interior of the feasible region and will be dominated by the penalty term.

The problem is to select a value for r_1 which gives optimal balance between the two conditions described above. The author's computer program uses the value of 1.0 suggested by Fiacco and McCormick [Fiacco and McCormick, 1968]. This value has been found to be a reasonable starting point value for most problems described in this chapter. For the design problem, described in the next chapter, an alternative procedure is used.

For more detailed mathematical treatment and proof of convergence of this method the pioneer work of Carrol [Carrol, 1961], Fiacco and McCormick [Fiacco and McCormick, 1964], [Fiacco and McCormick, 1968] may be referred to.

4.6 Numerical results for test minimization problems

This section summarizes the performance of the above minimization procedures on a number of unconstrained problems often used for comparing the minimization routines in the literature. Four test problems have been considered. These problems are quite typical ranging from simple quadratic functions to complicated ones with valleys and ridges. A brief description of the test functions are given below:

(1). Kuester and Mize

$$F(\bar{x}) = -3803.84 - 138.08x_1 - 232.92x_2 + 123.08{x_1}^2 + 203.64{x_2}^2 + 182.25x_1x_2 \tag{4.19}$$

This example is taken from [Kuester and Mize, 1973] and has been used for the comparison of minimization search procedure.

(2). Rosenbrock

$$F(\bar{x}) = 100({x_1}^2 - x_2)^2 + (1 - {x_1}^2) \tag{4.20}$$

The Rosenbrock function [Box, 1966] has been used as a test function for determining the efficiency of various types of search procedure. This function has several features which prove daunting to an inefficient search procedure. This is a well known function with a narrow valley.

(3). Powell

$$F(\bar{x}) = (x_1 + 10x_2)^2 + 5\left(x_3 - x_4\right)^2 + \left(x_2 - 2x_3\right)^2 + 10\left(x_1 - x_4\right)^4 \tag{4.21}$$

This function was proposed by Powell [Powell, 1962] and has been used extensively for comparison of minimization search procedures since then.

(4.) high dimensionality

$$F(\bar{x}) = \sum_{n=1}^{10} n x_n^2 \tag{4.22}$$

This test function has been chosen to study the effects of high dimensionality (maximum =10 variables).

The solution results of the test functions described above are summarized in table (4.1-4.4). The convergence value adopted for terminating all the optimization methods was $\epsilon = 10^{-5}$.

There is no universal basis for comparing minimization search procedures but the number of function evaluations and computer execution times have been recommended quite often in the literature. The author shares the view with others in recommending the number of function calls and time execution as a basis of comparison and this has been quoted in the tables. The number of function calls for each method on some test problems is also represented graphically in Figures (4.8-4.10).

In order to clarify the configuration of function evalution, equations 4.19-4.22 have been explored for this purpose. The evaluation of the minimum of Rosenborock's test function proves that pattern search which uses a certain degree of randomness and the results are considerably better than other search procedures used. Pattern search is particularly effective on narrow-ridge functions such as equation (4.20). Table (4.1-4.4) indicates that the number of function evaluations of the simplex method are significantly larger than the other methods, probably because 'contraction' and 'expansion' imply trials which involve function evaluations but do not necessarily generate directly

the new simplex, while reduction implies a number of function evaluations for new simplex. Further, the computation effort of the simplex procedure, measured in terms of the number of function evaluations, increases not much quicker than proportionally to the variable number (n), at least for small (n) [Himmelblau, 1972]. This is confirmed by tables 4.1-4.4. It can also be seen that the Hook and Jeeves method has used fewer function evaluations to reach certain minimum values for most of the test functions. This is due to its acceleration feature.

That the function complexity is a more critical consideration than dimensionality in non-linear programming, is revealed comparing execution times for examples 3 (equation 4.21) and 4 (equation 4.22). In addition, the result tables suggest that the direct methods are superior to the random and shrinkage method.

Finally, from the above computation experience, the method of Hook and Jeeves is seen to be a good choice. The minimization procedure can also be carried out using the simplex search of Nelder-Mead method, but this generally involves a greater computation effort and produces results with a greater accuracy than necessary. However, this conclusion is further strengthened when the above mentioned are compared on some complex constrained design problems.

4.7 Constrained optimization

4.7.1 Comparison on design problems

In this section, some design applications of the direct search methods are presented. These design problems are used to test both the direct search methods, to illustrate SUMT in machine design problems and to gain more

insight into the perfomance of the algorithms. Though it is possible to generate different objective functions, the result presented are restricted to one which can be regarded as quite complex among constrained types of problems, the problem is briefly stated below.

4.7.2 Rosen-Suzuki problem

This problem has been used in the literature [Himmelblau, 1972] to test various algorithms and although not related to any physical system is representative of the type of formulation required by a physical system. The problem is to minimize

$$F(x_1, x_2, x_3, x_4) = x_1^2 + x_2^2 + 2x_3^2 + x_4^2 - 5x_1 - 5x_2 - 21x_3 + 7x_4 \qquad (4.23)$$

subject to constraints

$$g_1(x_1, x_2, x_3, x_4) = x_1^2 + x_2^2 + x_3^2 + x_4^2 + x_1 - x_2 + x_3 - x_4 - 8 < 0 \qquad (4.24)$$

$$g_2(x_1, x_2, x_3, x_4) = x_1^2 + 2x_2^2 + x_3^2 + 2x_4^2 - x_1 - x_4 - 10 < 0 \qquad (4.25)$$

$$g_3(x_1, x_2, x_3, x_4) = 2x_1^2 + x_2^2 + x_3^2 + 2x_1 - x_2 - x_4 - 5 < 0 \qquad (4.26)$$

A starting design point is taken as (0, 0, 0, 0). Results from both direct search methods are summarized in table 4.5. For another starting point of (3, 3, 3, 3) the same optimum was obtained. For both optimum points, constraint g_3 is active at the optimum.

4.7.3 Superconducting design problem

The superconducting machine problem is that of the design of the generator rotor. The objective is to maximize the magnetic power of the inner rotor while meeting a number of design constraints. The objective function and constraints problem are given below and are fully described in the next chapter:

$$P(r_{fi}, r_{fo}, J_f, r_k) = F(r_{fi}, r_{fo}, J_f) + r_k \sum_{m=1}^{9} \frac{1}{g_m} \tag{4.27}$$

where

$$F(r_{fi}, r_{fo}, J_f) = inner \quad rotor \quad magnetic \quad power(B_{rs}) = C_o\left[r_{fo}^3 - r_{fi}^3\right] J_f \tag{4.28}$$

$$g_1 = r_{fi} - 0.2 > 0 \tag{4.29}$$

$$g_2 = 0.4 - r_{fi} > 0 \tag{4.30}$$

$$g_3 = r_{fo} - 0.4 > 0 \tag{4.31}$$

$$g_4 = 0.6 - r_{f0} > 0 \tag{4.32}$$

$$g_5 = r_{fi} - 2r_{fo} + 0.6 > 0 \tag{4.33}$$

$$g_6 = 10 - 9.14510^{-7} J_f[(r_{fo} - r_{fi}) + 0.25(r_{fo}^3 - r_{fi}^3)] - 3 \times 10^{-7} \times J_f > 0 \quad (4.34)$$

$$g_7 = r_{fi} > 0 \quad (4.35)$$

$$g_8 = r_{fo} > 0 \quad (4.36)$$

$$g_9 = J_f > 0 \quad (4.37)$$

This problem was tested using direct search minimization to establish the relative efficiency of the optimization methods. An optimization method was judged successful if it progressed towards the optimum and no constraint equation was violated by more than 10^{-6}. The result of the constrained optimization problems indicates that both the pattern search method (Hook and Jeeves) and simplex search method (Nelder and Mead) can be successfully employed for machine design. However, it was found that the simplex routine is more sensitive to the choice of prescribed accuracy. Tables 4.6 and 4.7 compare the number of function calls and time (CPU) during the minimization process for sequential pattern and simplex search using SUMT. The computional results show that the increase of convergence criterion accuracy of the simplex method causes a noticable increase in the number of evalution functions as can be observed from the result tables and also illustrated in figure 4.11. From computation results the pattern search method performed well in speed and accuracy. Despite the above comparison both methods show an agreement of results. From the limited computational results specified here, it appears that the sequential pattern search is preferable to the simplex

technique as it involves fewer function calls and has a faster solution speed. This is probably due to its greater ability to adjust the magnitude of the step move to minimize the objective function, despite the less sophisticated criteria for choosing move direction and acceleration in distance. However, this conclusion should be applied with caution as it is substantiated by limited experience and because any assessment of merit of this type is problem dependant. It is worth mentioning that, for substantially different and much larger size problems, different comparative conclusions will be achieved in the next chapter.

The computing time reported for calculation carried out on the Amdahl 58/6032 M bytes digital computer.

4.8 Conclusions

In this chapter, the application of non-linear programming methods to mathematical functions and design problems have shown encouraging results. These results show that the two direct search methods of minimization so far considered to be effective in the class of direct search. The optimization methods have been compared on mathematical functions and SUMT has been used for handling constraints.

The following conclusions can be drawn from the present investigation:

(1). Pattern search (Hook and Jeeves) and simplex (Nelder and Mead) have been found to be more efficient on most general mathematical test problems than the random and shrinkage method.

(2). In evaluating the minimum of a test problem it has been seen that function complexity is a more critical consideration than that of

dimensionalty in NLP programming.

(3). For all cases the simplex routine is more sensitive to the choice of parameters, such as prescribed accuracy and initial simplex.

(4). The pattern search method is much faster in finding the optimum solution compared to simplex.

(5). More than one direct search method for machine design optimization is perferred because of greater generality and ease of checking results.

Table 4.1
Results of the test problem for Kuester

Method	No. of variables	Min. funct.	Min. variables	No.of funct. call	CPU time (s)
HOOK and JEEVES	2	-3873.92	0.2056 0.4800	90	0.743
SIMPLEX	2	-3873.92	0.2056 0.4790	235	0.745
Random and shrinkage	2	-3873.92	0.2057 0.4800	126	0.613

Initial variables x_1=1.0, x_2=0.5

Table 4.2
Results of the test problem for Rosenbrock

Method	No. of variables	Min. funct.	Min. variables	No.of funct. call	CPU time (s)
HOOK and JEEVES	2	0.124×10^{-25}	1.0 1.0	85	0.753
SIMPLEX	2	0.495×10^{-5}	1.0018 1.0022	147	0.725
Random and shrinkage	2	0.774	1.0139 0.9025	206	0.621

Initial variables x_1=-1.2, x_2=1.0

Table 4.3
Results of the test problem for Powell

Method	No. of variables	Min. funct.	Min. variables	No.of funct. call	CPU time (s)
HOOK and JEEVES	4	5.953×10^{-6}	7.937×10^{-5} -0.8326×10^{-6} 2.1875×10^{-2} 2.1875×10^{-2}	294	0.766
SIMPLEX	4	3.77×10^{-6}	-2.522×10^{-3} 3.9815×10^{-3} 6.8766×10^{-3} 6.3189×10^{-3}	932	0.725
Random and shrinkage	4	p	-	-	-

p: Did not slove the problem.
Initial variables x_1=3.0, x_2=-1.0, x_3=0.0, x_4=1.0

Table 4.4
Results of the test problem for High dimensionality

Method	No. of variables	Min. funct.	Min. variables	No.of funct. call	CPU time (s)
HOOK and JEEVES	10	1.73×10^{-30}	all 10 values of order10^{-15}	248	0.753
SIMPLEX	10	4.785×10^{-6}	all 10 values of order 10^{-3}	2901	0.716
Random and shrinkage	10	1.977×10^{-3}	p	2425	p

p: Did not slove the problem.
Initial value for all 10 variables =1.0

Table 4.5
Results of Rose-Suzuki problem

Method	No. of variables	Min. funct.	Min. variables	No.of funct. call	CPU time (s)
HOOK and JEEVES	4	42.830	0.2500 1.0500 1.8500 -0.9000	243	0.706
SIMPLEX	4	43.595	0.0361 0.7970 2.0440 -0.9016	2344	0.774

Initial variables $x_1=x_2=x_3=x_4=0.0$

Table 4.6
Results of the machine design problem

Method	No. of variables	Min. funct.	Min. variables	No.of funct. call	CPU time (s)
HOOK and JEEVES	3	0.518979	0.38519 0.49202 0.240125×10^8	572	0.738
SIMPLEX	3	0.518974	0.38571 0.47859 0.23265×10^8	4663	0.806

Initial variables $r_{fi}=0.395$, $r_{fo}=0.455$, $J_f = 1.05 \times 10^8$. Accuracy=0.00001

Table 4.7
Results of the machine design problem

Method	No. of variables	Min. funct.	Min. variables	No.of funct. call	CPU time (s)
HOOK and JEEVES	3	0.518914	0.38515 0.49202 0.240125×10^8	523	0.735
SIMPLEX	3	0.4940352	0.30709 0.45341 0.22050×10^8	1616	0.812

Initial variables $r_{fi}=0.395$, $r_{fo}=0.455$, $J_f = 1.05 \times 10^8$. Accuracy=0.001

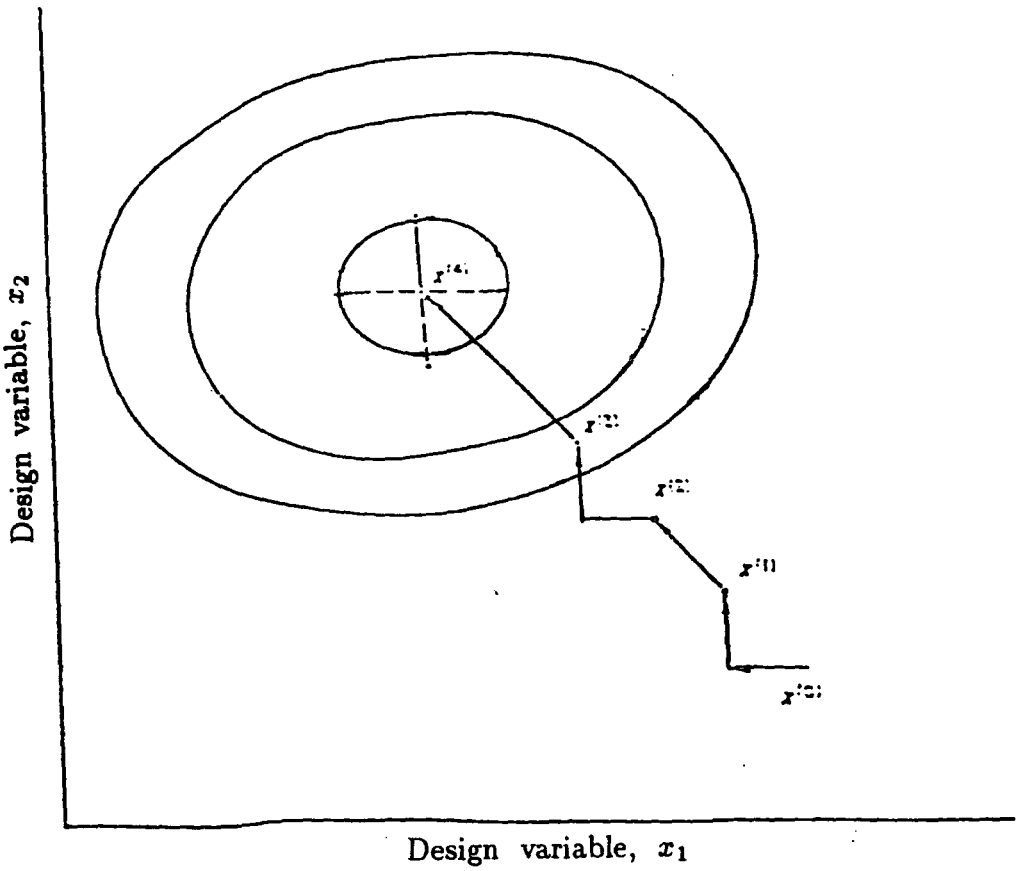

Figure 4.1 Search of pattern search of Hook and Jeeves

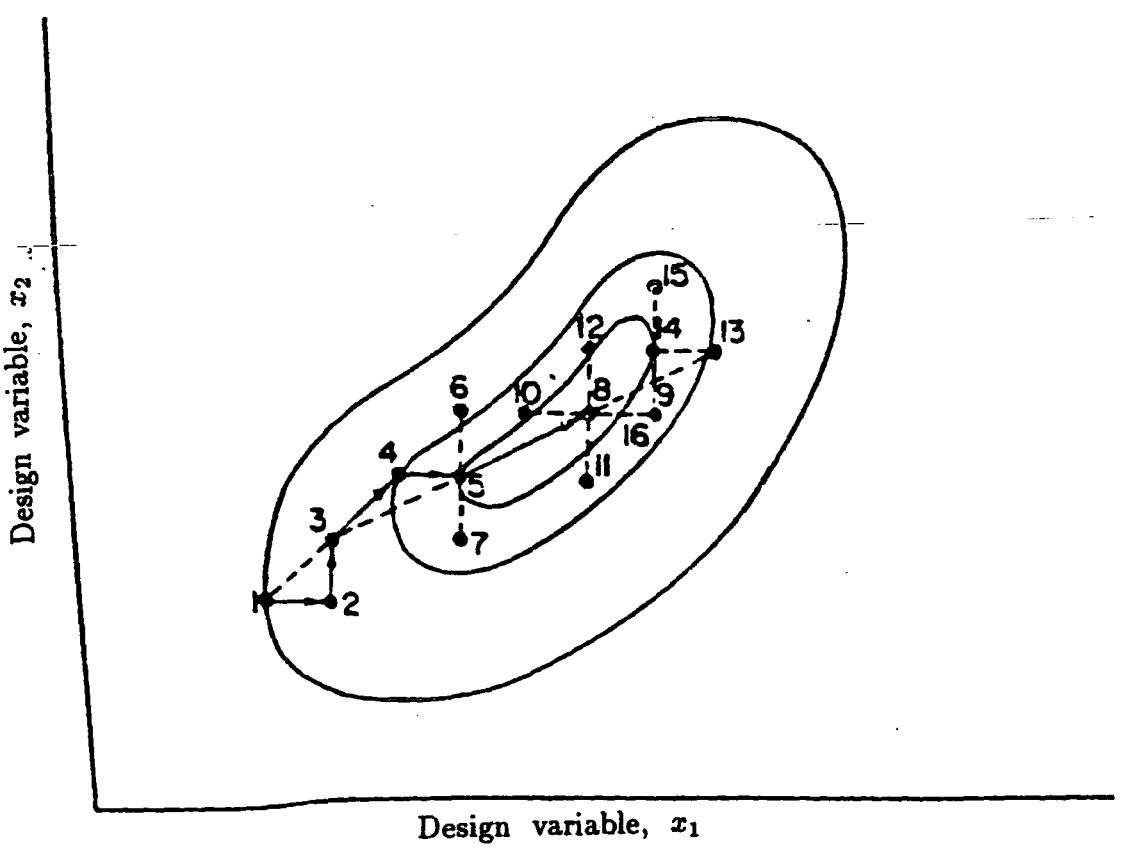

Figure 4.2 Following a valley by pattern search

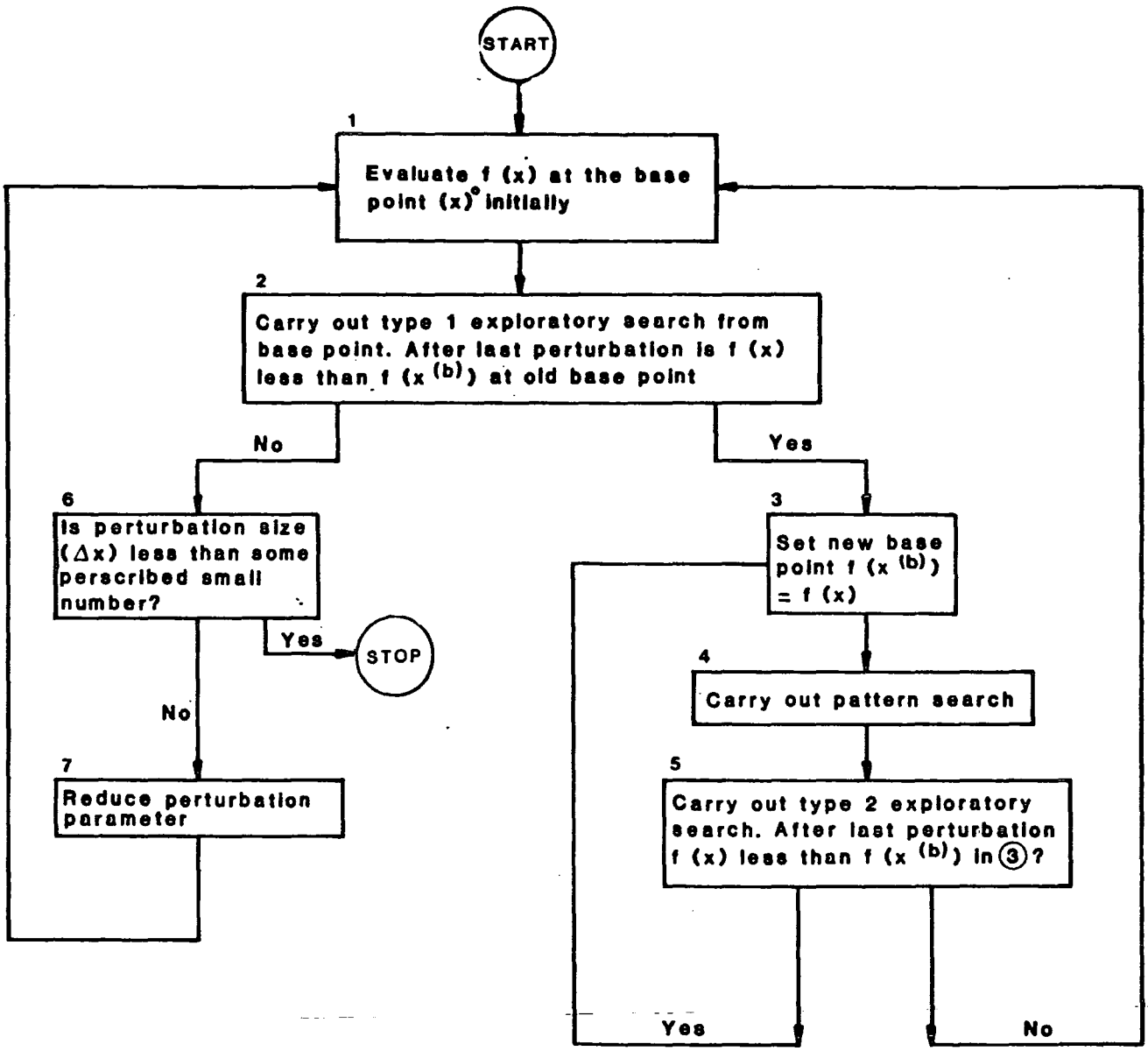

Figure 4.3 Flow chart for pattern search of Hook and Jeeves.

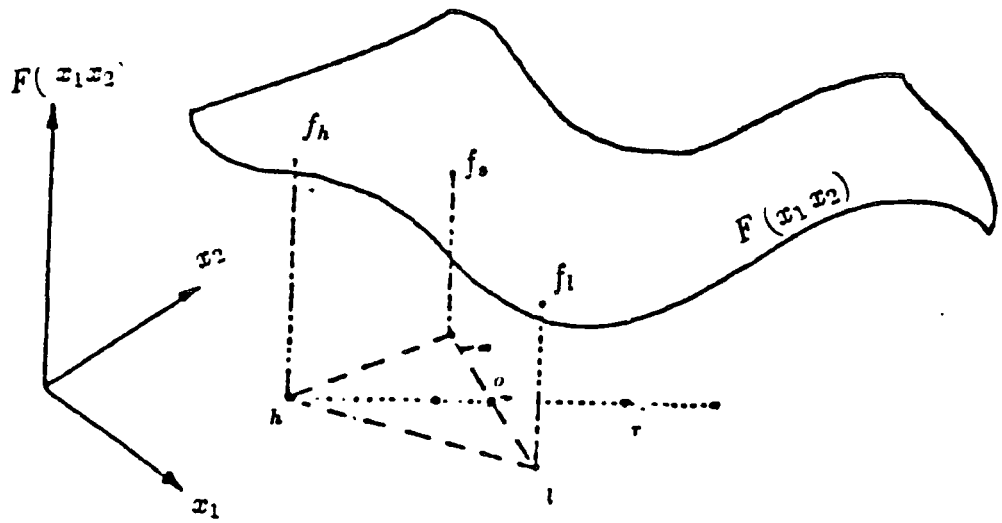

4

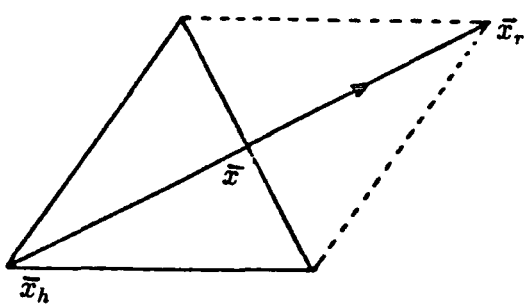

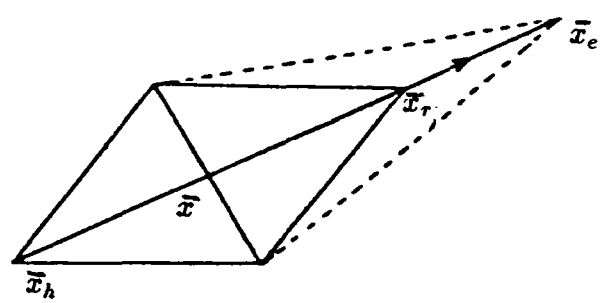

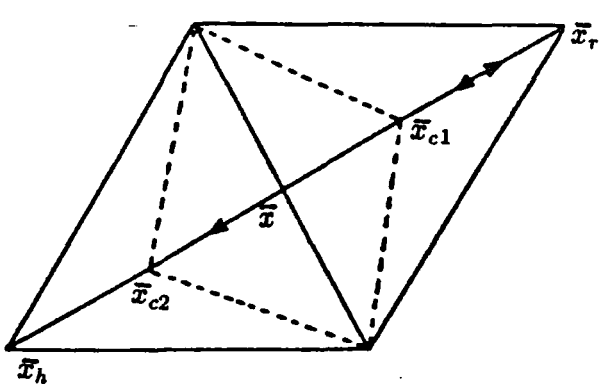

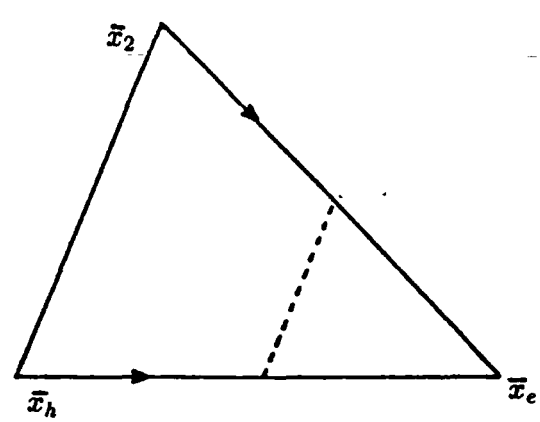

Figure 4.4 Search of simplex method [Nelder and Mead]

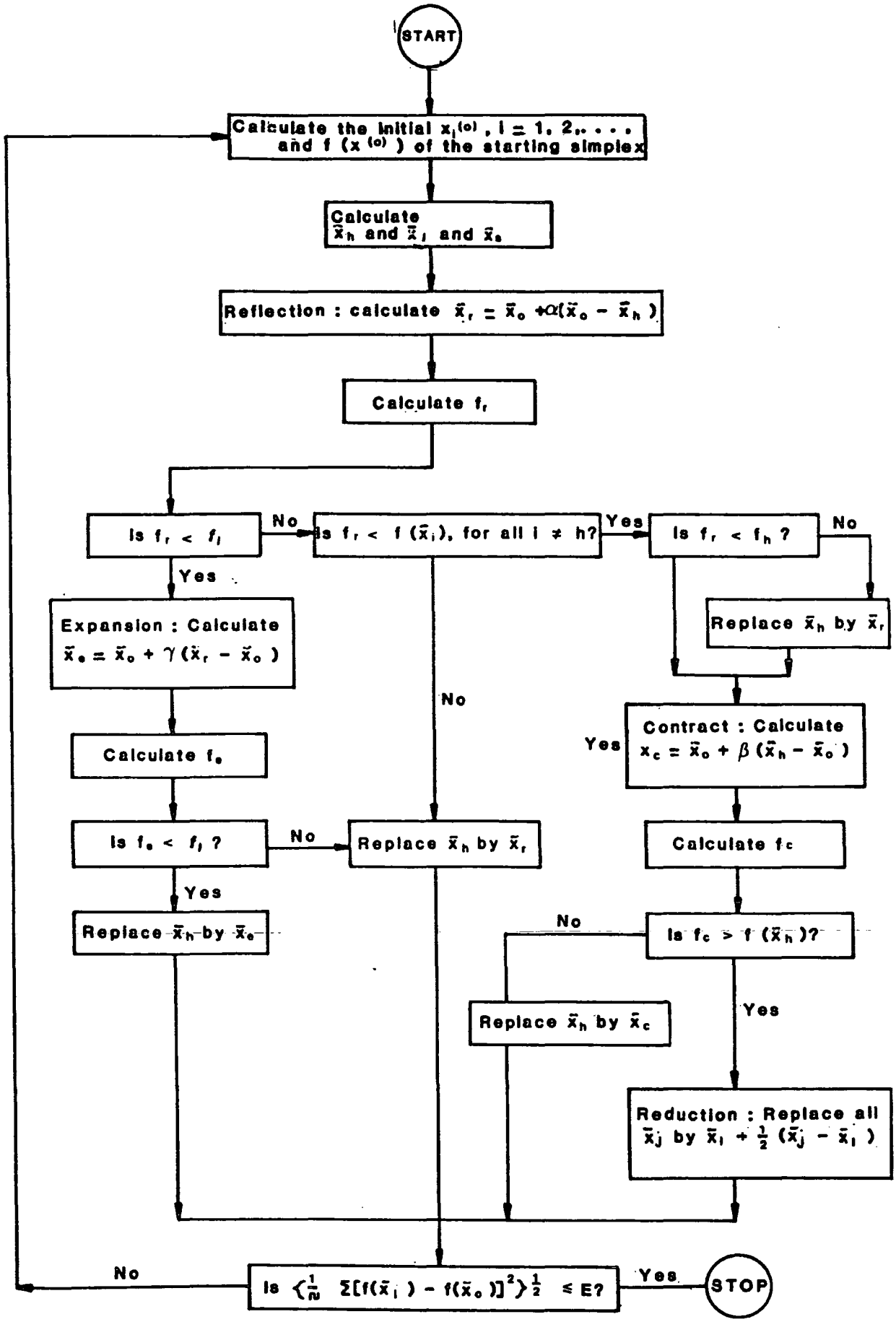

Figure 4.5 Flow chart of simplex search [Nelder and Mead]

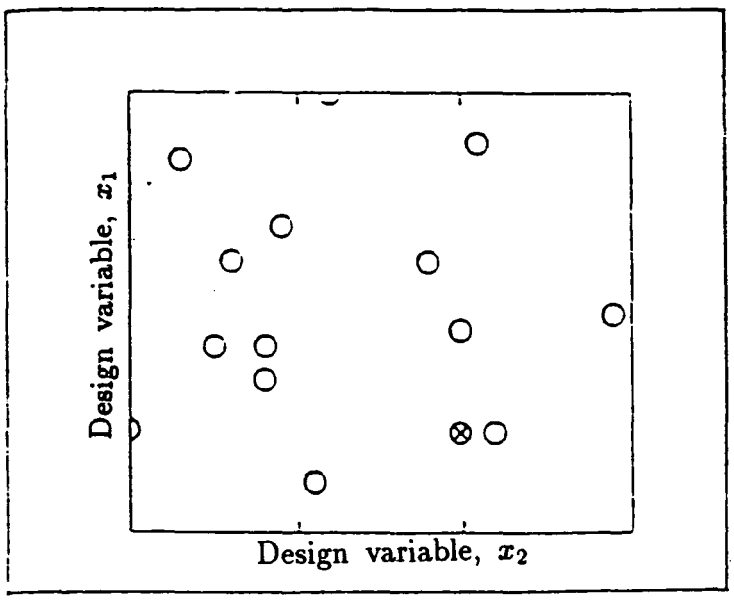

RANDOM SEARCH.

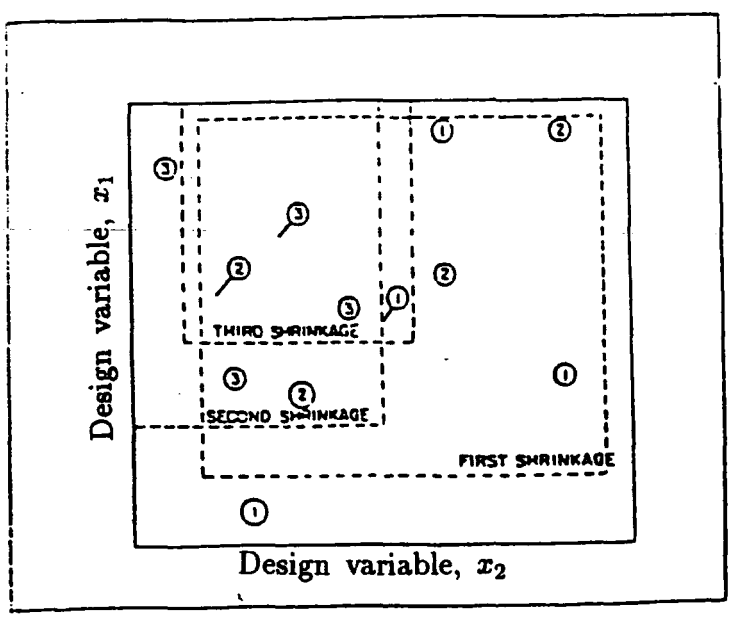

SHRINKAGE SEARCH.

Fig. (4.6) Random and Shrinkage search.

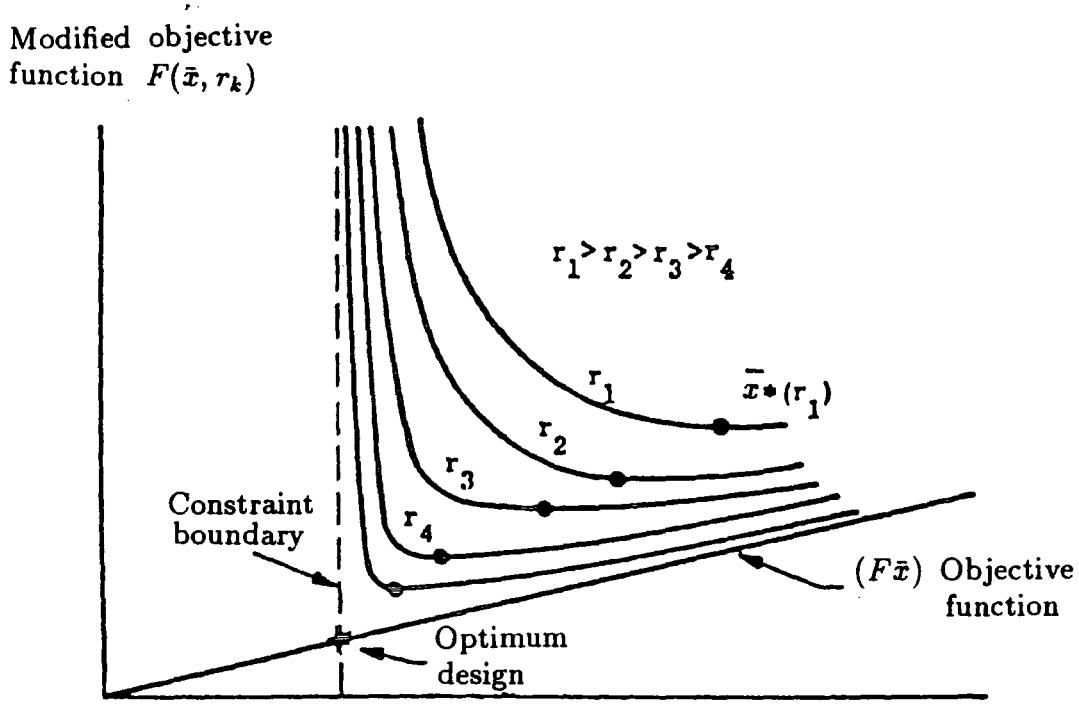

Figure 4.7 A Family of response surfaces for the modified objective function

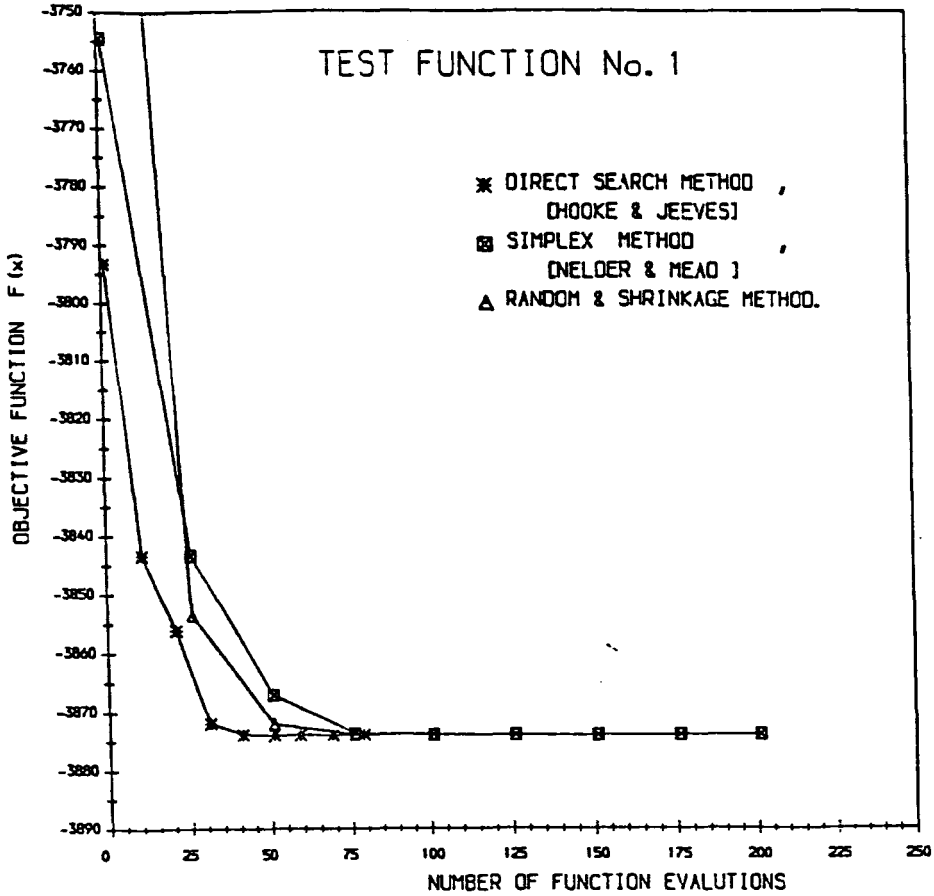

Fig. 4.8 Comparison of direct search and random methods.

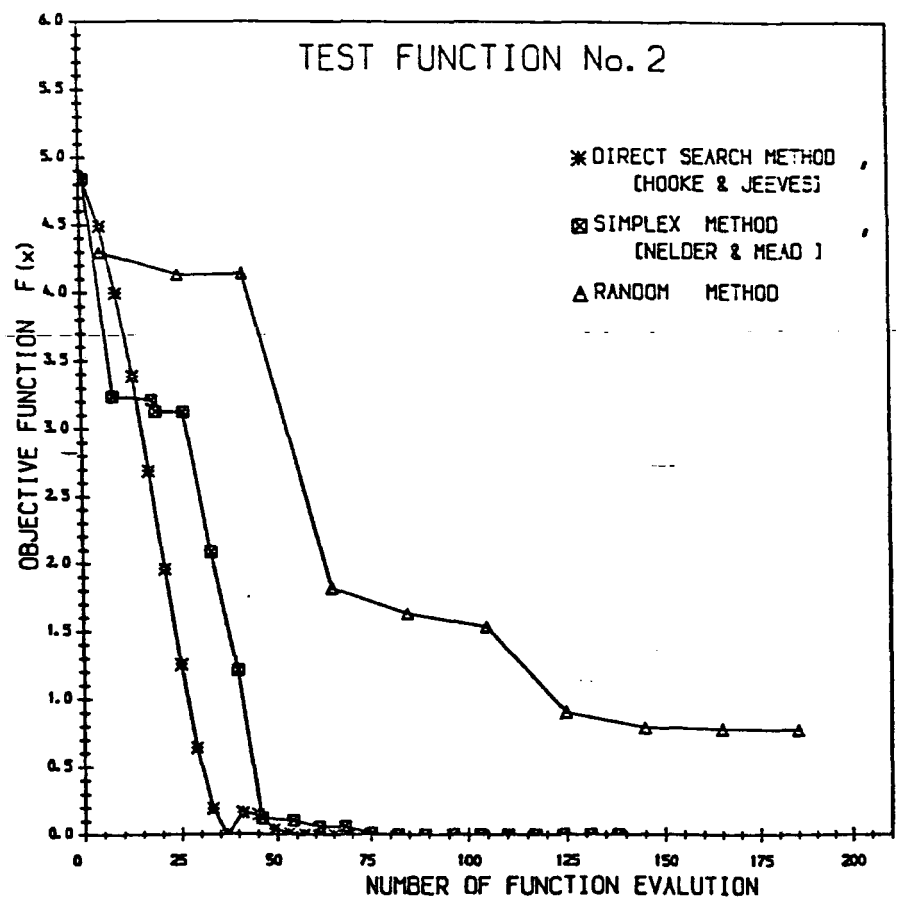

Fig. 4.9 Comparison of direct search and random methods.

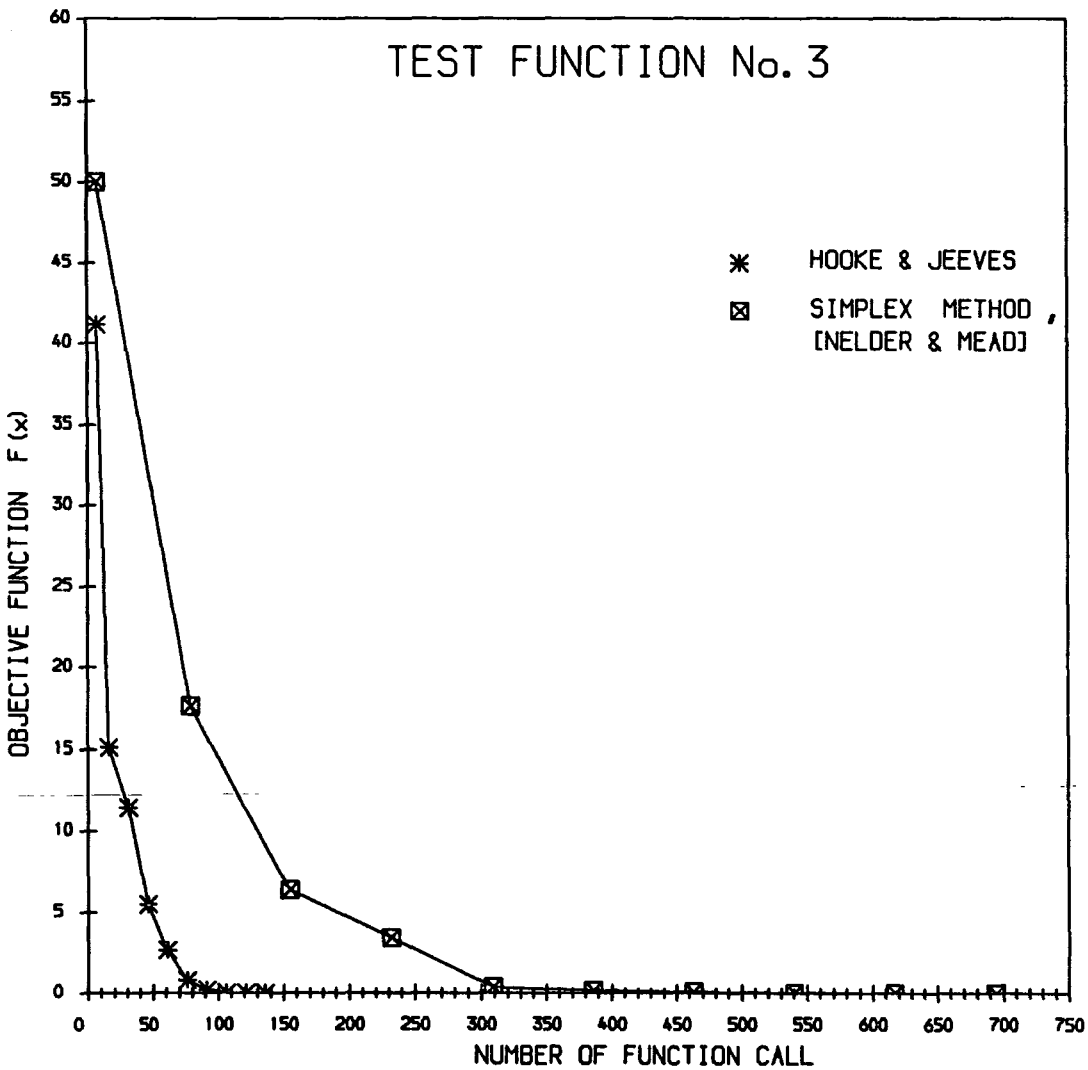

Fig. 4.10 COMPARSION OF DIRECT SEARCH METHOD

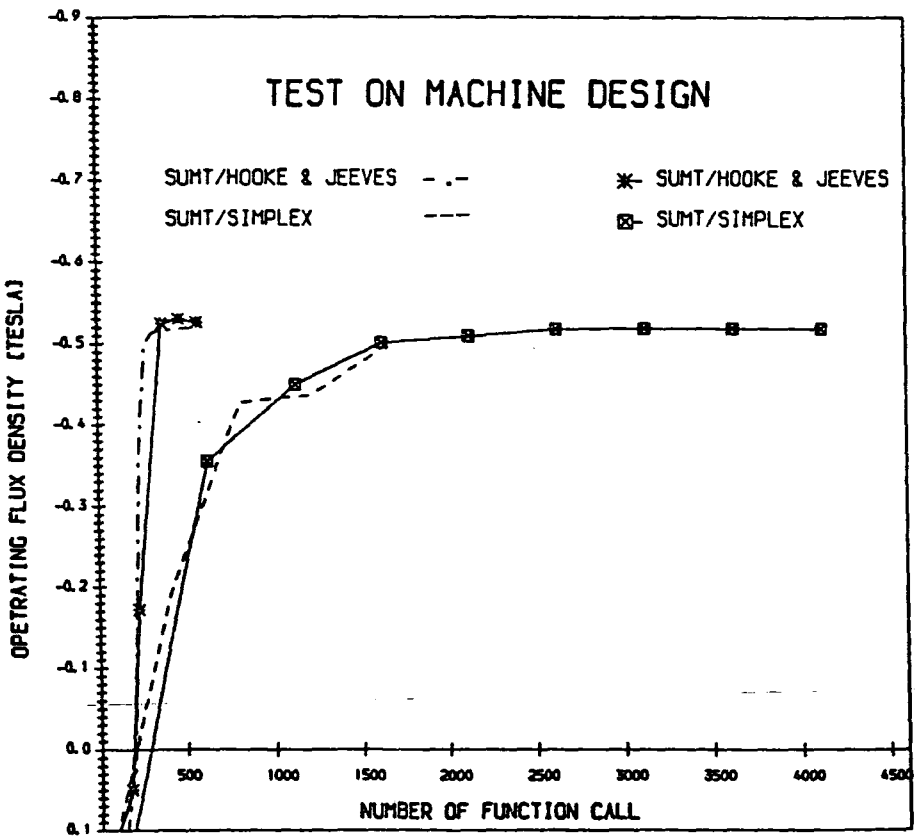

Fig. 4.11 Comparison of direct search methods. for two different values of convergence accuracy 0.001 and 0.00001

CHAPTER 5

USE OF DIRECT SEARCH METHOD IN OPTIMAL DESIGN OF A SUPERCONDUCTING GENERATOR ROTOR

5.1 General

An "optimum" design can be defined as a search for a "best" solution using mathematical methods. For present purposes, the term "optimized design" means the highest flux density obtainable with the permissible range of the variables that meet all of the design criteria.

The use of mathematical optimization methods on superconducting design problems has not yet been applied. However, optimum design of conventional machines have been predicted using these mathematical techniques [Erlicki and Appelbaum, 1965], [Ramarathnam et al, 1973], [Bharadwaji et al, 1979]. This chapter reports on the design optimization of a superconducting rotor. The behavioural requirements, discussed in chapter 3, are exploited in the optimization procedure as superconductivity, and mechanical constraints to ensure a secure and reliable design. The design procedure uses the direct search optimization techniques for minimization [Hook and Jeeves, 1961], [Nelder and Mead, 1965]. SUMT method [Fiacco and McCormick, 1968] is used for handling constraints for reasons discussed in chapter 4. This procedure has resulted in a general purpose optimization system which can be applied to a variety of design optimization problems having the generic structure of a non-linear objective function which is to be a maximum or minimum yet subject to a set of linear and non-linear design constraints. In comparing the relative merits of the optimization system, emphasis is placed on the insight gained from answers. An analysis routine is linked to the optimization procedure to achieve such a purpose. The present study was

performed on a 1300 MW superconducting a.c. generator.

5.2 Definition of design problem and choice of method of solution

As noted in chapter 3, the superconducting generator has a very favourable power output compared with existing machine design by maximum the inner rotor magnetic power. Thus, the optimum design is to realise such a rotor whose magnetic flux output attains as high value as possible while satisfying all the given design requirements in order to maintain a practical design. This requires that before any consideration can be given to design optimization the factors influencing the magnetic field distribution must first be defined. The main factors to be considered may be summarized as;

(a). The inner rotor geometric dimensions, (r_c, r_{fi}, r_{fo}).

(b). The field winding current density, (J_f).

(c). The environmental screen factor, (k_r).

(d). The characteristics curve of the superconductor.

(e). Mechanical performance requirement.

(f). Stator core flux capability.

In the design procedure of the inner rotor and excitation winding, the basic parameters associated with geometry and physical properties contribute to both the inner rotor performance and its mechanical and electrical behaviour. For instance, the simplest way to obtain greater inner rotor magnetic power consists of increasing the main dimensions of the rotor component. An increase in the inner rotor dimensions are particularly effective because the capability varies with the outer radius of the inner rotor. This possibility is limited by the physical properties of the inner rotor components which must safely withstand the centrifugal stresses that occur during maximum overspeed at the bore and on the conductors.

On the other hand, the current capacity of the conductor depends on the magnitude of magnetic field in which it is located. The larger the magnetic field, the smaller will be the current carrying capacity of the superconducting conductor. As the magnetic field strength is a function of the winding geometrical parameters. So the allowed current density of a superconducting field winding is also a function of its geometrical parameters. Thus, the current density is a coherent parameter in its optimum design. As a result, in view of the restriction imposed with regard to the current density, it is necessary to introduce the effect of the critical characteristic superconductor to the field current density.

The inner rotor magnetic power is also affected by the type of environmental screen employed. The iron screen tends to increase the flux density by $\left[1+\left(r_s/r_{xi}\right)^2\right]$, while the conducting screen reduces the flux density by $\left[1-\left(r_s/r_{xi}\right)^2\right]$. The environmental iron screen looks the most promising from a magnetic flux density point of view. The dimensions of this screen are themself constrained by the maximum screen weight. Any attempt to operate the superconductor at higher fields results in a thicker stator core because of the magnetic saturation characteristic of the iron core. The optimization may be extended to include the geometric dimensions of the environmental iron screen. The dimensions can be chosen by considering the maximum flux density at the screen inner radius and the magnetic saturation of the core material.

The need to optimise the inner rotor on the basis of its magnetic power is a consequence of the above factors. Besides, suboptimization of separate generator components, such a inner rotor, may be a practical and effective design approach [Appleton, et al, 1975].

By considering the above factors, the optimum design can proceed in the following manner

(1). Choose r_{fi}, r_{fo} consistent with mechanical considerations. The limiting parameter is mechanical stress due to the maximum critical speed in different parts of the inner rotor as well as allowing adequate room for the outer rotor and the radiation screen.

(2). Choose the current density (J_f) consistent with the superconductivity constraint, i.e. the current density of the field winding must be kept below a critical current density to maintain superconductivity.

(3). Select the inner radius (r_{xi}) and thickness (t_x) of the environmental screen. These values are determined by the maximum flux density at the core and saturation flux density of the material.

(4). Design the inner rotor and field excitation to maximize the magnetic power of the inner rotor.

(5). Find r_{fi}, r_{fo}, J_f, r_{xi}, and t_x to achieve an optimum.

(6). Evaluate and repeat (1) through to (5) as required.

While a maximum magnetic power of the inner rotor is always desirable, several restrictions on the rotor performance have to be recognized. Appleton [Appleton, et al, 1975] has discussed the use of a design approach in which the inner rotor magnetic power is maximized subject to constraint parameters imposed by the properties of material (centrifugal forces) and the critical characteristics of the superconductor. In this classical way of design there is, obviously, a wide variation in preparation time, cost, and accuracy of the results. Moreover, this method only allows the study of a small selection of design parameter influences. Furthemore, in this procedure, parametric studies are restricted to two-or three dimensions to establish a refined conceptual design. When suitable mathematical optimization methods are used, however,

this way of designing will generally be more efficient and conclusive. The optimization methods described in the following section provide economical, multidimensional designs that are a substantial improvement in both time and cost. As discussed in previous chapter, these methods should provide the capability to determine the combination of design prameters that produce the best design for the machine magnetic circuit. It should be able to identify an optimum design within conflicting requirements.

5.3 Formulation of the optimum design problem

5.3.1 Introduction

Any optimization problem involves the identification of design variables, constraints, and objective function. However, this section describes the implementation of the design problem formaulation.

5.3.2 Design variables

As discussed in the previous section, it is desirable to select as variables only these which have a significant effect on the performance and magnetic power of the inner rotor. In the present investigation, the following design variables ($\bar{x}$) are considered for formulation of the design problem:

(i). Inner rotor core radius, r_c

(ii). Field winding inner radius, r_{fi}

(iii). Field winding outer radius, r_{fo}

(iv). Field winding current density, J_f

(v). Stator core inner radius, r_{xi}

(vi). Stator core thickness, t_x.

Some of variables, such as the spread angle of the field winding (σ_f), and mean radius of the stator winding (r_s) are assumed to be "fixed" for a particular case.

5.3.3 Design constraints

The values assigned to the design variables are usually restricted by a number of constraints imposed on the superconducting rotor as dictated by the actual design problem. Those presented in the following section thought to represent the variety of possible inquality constraints as well as being important in themselves.

A desirable design would restrict the dimensions of the field winding so as the rotor can withstand the centrifugal stresses that occur during maximum over speed. With regard to this, two mechanical inequality constraints can be established from the mechanical analysis (see chapter 3). Although the stresses (σ_r,σ_θ) vary throughout the inner rotor radius, only their maximum values have been included in the present analysis. According to the mechanical analysis, maximum stresses induced in the inner rotor are determined by centrifugal force and are required to be less than a specified yield strength of the materials. This requirement leads to a constraint relation for the stress in the slot/tooth region (at $r = r_c$) of the form:

$$g_{(\bar{x})} = T_o + \omega^2 r_{fi}^2 \rho_o \frac{\left[1 - y^3\right]}{3} \geq 0 \tag{5.1}$$

togther with the hoop stress of the core region (at $r = r_{fi}$):

$$g_{(\bar{x})} = T - \left(\frac{1}{12(1-x^2)}\right)\left\{8\omega^2 r_{fi}^2 \rho_o \left(y^3-1\right) + 3\omega^2 r_{fi}^2 \rho \left(1-x^2\right)\left[\left(1-\nu\right)x^2 + \left(3+\nu\right)\right]\right\} \geq 0 \tag{5.2}$$

This equation assumes that the internal pressure, p_i, is zero. In equation 5.1 and 5.2 T_o is the effective field winding/tooth region material to resist bursting, and T is the tensile strength of the bore material. The specified maximum tensile strength for both the effective field winding and bore material

are 60 MP_a and 400 Mp_a respectively. Other parameters in equations 5.1-5.2 are taken as fixed and are given in table 5.1.

Another important constraint which must be considered in the optimization procedure is the limitation on the current density as a result of the characteristic curve of the superconductor. This limitation is essentially of the same form as discussed in chapter 3:

$$g_{(\bar{x})} = 10.0 - J_f \times \left[\mu_o \times k_c \times k_g - 3.010^{-7}\right] \geq 0 \tag{5.3}$$

Since the environmental screen geometry is to be selected by considering the maximum flux density and saturation flux density for the screen material, this defines another inequality constraint: (see chapter 3)

$$g_{(\bar{x})} = B_{(max)} - \{\frac{4 \times J_f \times sin\frac{\sigma_f}{2}}{3\pi \times t_x}\left(\frac{1}{r_{xi}}\right)\left[r_{fo}^3 - r_{fi}^3\right]\} \geq 0 \tag{5.4}$$

In order to avoid undesirable shapes, ensure compatibility of the design, and to hold the design between fixed limits, extra geometry, or side, constraints are introduced using the inequality type:

$$\bar{x}_{min} \leq \bar{x} \leq \bar{x}_{max} \tag{5.5}$$

which is equivalent to two constraint relationships, namely

$$g_{(\bar{x})} = \bar{x} - \bar{x}_{min} \geq 0 \tag{5.6}$$

and

$$g_{(\bar{x})} = \bar{x}_{max} - \bar{x} \geq 0 \tag{5.7}$$

Side constraints must be set on design variables to stop them from attaining zero or negative values. This requires design variables to be positive:

$$g_{(\bar{x})} = \bar{x} \geq 0 \tag{5.8}$$

Design variable constraints can be introduced into the study using equality constraints, for example, the core radius must be 0.2 times the outer radius of the field winding, hence, the equality constraint [Appleton, et al, 1975]:

$$\frac{r_c}{r_{fo}} = 0.2 \tag{5.9}$$

or in the standard form,

$$h(\bar{x}) = r_c - 0.2r_{fo} = 0 \tag{5.10}$$

Equality design constraints often offer the opportunity to reduce the dimensionality of the problem. Such constraints represent functional relationships among the variables often allowing some variables to be expressed in terms of others. The design problem presented here can be formulated with the outer radius of the rotor as the only variable, thereby eliminating one variable and one constraint simultaneously, namely the variable r_c and the constraint of equation 5.9. This is done by substituting equation 5.9 into equation 5.2.

Finally, the rotor stress limits (T, T_o), the characteristic superconductor curve $J_c(B)$ and stator core flux saturation ($B_{(max)}$) are all dependent on the design variables ($\bar{x}$) and hence, the constraint equations 5.1-5.4 denote the behaviour constraints. Equations 5.5-5.8 represent the geometrical or side constraints which impose limits on the size of design variables.

5.3.4 Design objective function

A design problem usually has several solutions which may satisfy the specified functional requirements adequately. The objective function in a general optimization problem represents a basis for the choice between alternate acceptable designs. It was noted in the previous section that one of the primary causes of increasing the power output of the machine is to achieve maximum inner rotor magnetic power. Thus, the magnetic power of the inner rotor is chosen as the objective function. The expression for objective function is given by equation 3.7 (chapter 3) and will be denoted by $F(\bar{x})$.

5.4 Results and discussion

5.4.1 Systematic optimization

The synthesis of the design problem may now be formulated as a mathematical programming problem of standard form:

Find $\bar{x}$ such that $F(\bar{x}) \rightarrow max.$ (5.11)

subject to a set of design constraints $g_m(\bar{x}) \geq 0$ (5.12)

As before (chapter 4), this inequality constrainted maximization problem is transformed into a sequence of constrained maximization by applying the Fiacco-McCormick penalty function method. In this case, the objective function $P(\bar{x}, r_k)$ is defined

$$P(\bar{x}, r_k) = F(\bar{x}) + r_k \sum_{m=1}^{11} \frac{1}{g_m(\bar{x})} \tag{5.13}$$

To determine the successive maxima of the modified objective function $(P(x, r_k))$, two direct search methods [pattern search of Hook and Jeeves and simplex search of Nelder and Mead] are used, for reasons discussed in chapter 4.

To implement the systematic optimization approach a computer program package has been developed for this purpose and will be discussed in the following section. A series of results for this program are shown in figure 5.1. For convenient reference, the results are also briefly summarised in table 5.2.

Table 5.2a illustrates the five dimensional design space (r_{fi}, r_{fo}, J_f, r_{xi}, t_x) with an initial design point (0.2, 0.275, 0.88×10^8, 0.8, 0.5) chosen to lie within the feasible region. The first value of the penalty parameter r_k is selected so that the penalty term of $P(\bar{x}, r_1)$ is approximately equal to the flux density of the initial design, $F(\bar{x})$ (in this case $r_k = 0.035$). Subsequent maximization of sequences are performed dividing by 5. This design is systematically optimized by a sequence of maximization, using simplex search [Nelder and Mead, 1962] is shown in the figure 5.1 and table 5.2.

It is seen that the penalty term acts as a "constraints repulsion" during the initial design synthesis, since the design point is forced away from the behaviour constraints. The optimization process then continue until an approximate maximum is found (after 11 evaluation). The first maximum point (0.2983, 0.3732, 0.4573×10^8, 1.1075, 0.4819) is then used as the starting point for the next maximization in the sequence. For the second maximization the penalty is reduced to $\frac{1}{5}$. This systematic optimization by maximization was terminated at a point design of (0.3337, 0.3854, 1.040×10^8, 0.9000, 0.6437). Table 5.2 shows the complete sequence of unconstrained maximization leading to an optimum design flux density. Here, the optimum flux density increase of about 12.5% has been obtained, as compared with the flux density which is obtained in the conventional way.

The sequence of maximization is indicated in table 5.2b. It is seen that the constraint repulsion quality of the modified objective function $P(\bar{x}, r_k)$ is felt only during the initial maximization. As the gain of the penalty

function (the penalty parameter r_k) is gradually reduced, the maximum point apporoaches the constraint boundaries of stator core flux saturation. As table 5.2a illustrates the strength of the penalty function (indicated by ratio $(P(\bar{x}, r_k)/F(\bar{x}))$ gradually increase until for small r_k the modified function is essentially equal to the objective function.

5.4.2 Discussion of optimized design

Result of the optimum design corresponding to the two main alogrithms namely the simplex search method and pattern search (which are implemented in the computer program) are given in table 5.3.

It can be seen from the result table that both methods do optimize the design problem but with the slight difference observed being due to the different converge criteria imposed in both methods.

The result of the design problem presented here indicate that direct search methods, namely simplex search and pattern search can be successfully employed for machine design problems.

An interesting point should be made on the result in general, that simplex method is more sensitive to the choice of prescribed accuracy. Experience shows that the increase of convergence criteria of simplex method causes a noticable increase in the number of function evaluation. A value of *convergence criteria* $= 1.0 \times 10^{-4}$ was chosen. This is somewhat stringent, but if the method converges at all it has no difficulty satisfying this criteria.

5.4.3 Computational considerations

Some points in the basic SUMT alogrithm deserve further discussion. First of all, experience using SUMT has shown that the starting point (initial design point) is not very critical if the response factor (r_1) is chosen large. If a good initial design is known, many extra computation can, however, be

saved by the application of a smaller value of r_1. When a large value of r_1 is used, the penalty term will dominate the search procedure for the first response surface and the first maximum tends to be pushed away from the constraint surfaces. For a small value of r_1 the starting point will be much more important. The influence of the penalty term will be rather small. Thus, for non-convex feasible region it is likely that the search will converge to the closest local optimum.

The problem is then to select a value for r_1 which gives optimal balance between the two conditions described above. The simplest approach involves choosing the first value of r_k, so that the penalty term of $(P(x, r_k))$ is approximately equal to the initial original design objective function. This approach was successful in improving the optimal result.

A second consideration is the choice of the rate at which r is reduced for successive maximization. The choice of this factor does not seriously affect the total computational requirements of the optimization method. If the value of this factor is chosen too large, the fewer are the number of unconstrained maximizations needed, but the longer each of these maximizations takes. The author found a reduction of the order 0.2 on this factor to be a reasonable value for the systematic optimization procedure used in the previous section.

In practical calculations, the convexity of the function to be maximized or minimized is difficult to check. Experience has shown that more than one solution may exist, and that each solution will yield a different value of the design function.

Although multiple solutions exist, there is no way to determine how many there are. A new solution might be found by trying a new starting point, i.e. initial values of design variables. However, there is no way to determine beforehand whether or not the solution found is the best.

A local maxima that has already been found may be eliminated from

the feasible region by imposing an additional limit constraint. This may be useful in cases where it is known that several local minima or maxima exist.

5.4.4 The effect of design constraints on the optimal solution

It would be interesting to know how the design constraints influence the optimal solution. In this section a preliminary study has been carried out to assess the influence of the design constraints, namely the centrifugal stress, superconductor characteristic and stator core maximum flux density on the optimal design.

To investigate the effect on the optimal solution of different allowable stress in the rotor body material, the design problem was run with different stress levels. Here, the tensile strength of slot/tooth material is the same value as in previous section (i.e.$T_o = 60MP_a$), except that the tensile strength of the inner rotor body material has been increased from 300 to 400 MP_a.

A very interesting phenomenon occured when the problem was run under this condition. The results in table 5.4 and figure 5.2 serve merely as a quantitative measure of the effect the inner rotor material strength has on the optimal solution. The maximization sequence traced by the optimization process using the simplex search method leads to an optimum design as shown in table 5.4a. Its nearness to the behavioural constraint boundaries of the feasible design space is indicated in table 5.4b. As expected an increase in the tensile strength of the inner body material allows the radial dimensions of the inner rotor to be increased. This in turn leads to an increase in the environmental iron screen radius. This is an interesting observation, but it should also noted from the constraints indicated in table 5.4b, further increase in the magnitude of dimension of the machine components now depend sensitively on maximum flux density allowed in the stator core. Therefore, it was concluded that the optimal magnetic power of the inner rotor is governed

mostly by the allowable stress level in the inner rotor materials and saturation in the stator core, rather than the superconductor capability. For convenient references, the results for simplex search and pattern methods are also briefly summarized in table 5.5.

5.5 Computer program package for design optimization of superconducting machine problems

5.5.1 Program implementation

As discussed in chapter 4, there is no single maximization or minimization routine that has yet been shown to be completely general. It is therefore necessary to try more than one direct search method because the method may work well on a given class of design problem, but fail to produce acceptable results on others.

Since it would be very expensive to construct an individual optimization procedure for each design problem, it has been the aim of the research to develop a general purpose optimization package whose methods and strategy can be applied to superconducting machine problems for which the analysis module is available. A simplified flow chart for the computer program package is shown in figure 5.3. The design optimization package is best explained in the following steps

(a). To provide an effective tool to aid in the design of superconducting machines (it is also commonly applicable to the design problem of any machine).

(b). To provide a general structure in order to permit other optimization methods to be easily introduced into the package and to permit further revisions without major re-design.

(c). It is designed to handle inequality and equality design problem constraints.

(d). It is easy to choose the non-linear optimization method which

is most suitable for the design problem.

(e). Display of optimized design by tabulation of the results.

5.5.2 Optimization methods

The program possesses the following optimization strategies:

(i). Pattern search of Hook and Jeeves

(ii). Simplex search of Nelder and Mead

For these methods the sequential penalty method is used to handle the design problem constraints.

5.5.3 Analysis module

The results of the optimization process have to pass through the analysis module in order to predict the behaviour of the design with the optimized parameters.

The way in which the optimization and analysis modules are interfaced depends on the form in which the analysis module is implemented. In the optimization package the analysis module is formed as a subroutine. This is a rather simple approach to work with. The design variables are determined by the optimizer, these parameters have to be converted to input parameters of analysis subroutine as shown in figure 5.4. In this way, it is easily observed if the optimal design matches its requirements. If it does not, the areas of weakness are noted and the design changed within the specified constraints to improve the design.

5.5.4 Computer program structure

The optimization program consist of the main program and nine subroutines. A general flow chart of the computer program package structure

is shown in figure 5.5.

This package is designed so that all input operation is handled in the main program. The package input is straightforward and the user is prompted by messages displayed on the screen. Safeguards are provided such that it is virtually impossible to break the package flow because of mistyped input value. Checks on the input values are made in an attempt to minimize input errors. A brief description of each subroutine is now given

Subroutine SIMPLEX: This is optimization subroutine using simplex method.

Subroutine PATTERN: This is the main routine for pattern search method.

Subroutine SEARCH: The purpose of this routine to realize the pattern method.

Subroutine OBJECT: This subroutine is used to calculate the value of the original objective function for a given set of design variables.

Subroutine PENALTY: This subroutine is used to evaluate the modified objective function using the Fiacco and McCormick penalty fuction method.

Subroutine CONST.: This subroutine evaluates the value of all inequality constraints of the design problem.

Subroutine EQUL.: This subroutine is used to evaluate all the equality constraints of the design problem.

Subroutine ANSWER: The subroutine is used to print out the optimal results and detailed behaviour of the optimum design.

Subroutine ANALYSIS: This subroutine is used to check the performance of the design problem.

Finally, the package has been programmed to handle up to 20 variables and uses double precision arithmetic.

5.6 Summary and Conclusions

The results of this chapter have demonstrated the feasibility of applying direct search methods of optimization to the complex rotor structure of a superconducting a.c. generator. During the course of this investigation a new design tool has been presented which permits the optimization of a superconducting generator to take place.

Although this chapter discussed the special case of optimizing the magnetic field by selecting the magnetic parameters of the inner rotor, any property of the machine design, such as volume (or weight), or cost, can be optimized by using the optimzation package. The application demonstrated in this chapter is believed to be the first effort in this direction.

Table 5.1
Constant data for optimum design problem

Name	Symbol	Unit	Value
No. of pole pairs	p	-	1
Field winding spread angle	σ_f	degree	120
Armature mean radius	r_s	m	1
Max. flux density allowed the stator core	$B_{(max)}$	T	1.4
Field winding yield strength	T_o	MP_a	60
Inner rotor body yield strength	T	MP_a	400
Field winding average density	ρ_o	kg/m^3	7400
Rotor body density	ρ	kg/m^3	7950
Maximum speed	n_{max}	$r.p.m$	5100
Rated speed	n	$r.p.m$	3000
Passion ratio	ν		0.3

Table 5.3
Initial and optimum design variables for inner rotor magnetic circuit

				Optimal design variables			
				First starting point		Second starting point	
Methods	Design Variables	Bounds Lower	Bounds Upper	initial point	optimum point	initial point	optimum point
Hook & Jeeves	Core radius, r_c	-	-	-	0.764	-	0.076
	Field winding inner radius, r_{fi}	0.00	0.670	0.200	0.322	0.300	0.320
	Field winding outer radius, r_{fo}	0.00	0.685	0.275	0.382	0.375	0.382
	Field winding current density, J_f	0.000	4.4×10^8	0.88×10^8	1.031×10^8	1.0×10^8	1.039×10^8
	Environmental screen inner radius, r_{xi}	0.000	1.600	0.800	0.800	0.985	0.825
	Enviromental screen thickness, t_x	0.000	0.800	0.600	0.649	0.600	0.649
Nelder & Mead	Core radius, r_c	-	-	-	0.764	-	0.076
	Field winding inner radius, r_{fi}	0.000	0.670	0.200	0.333	0.300	0.385
	Field winding outer radius, r_{fo}	0.000	0.685	0.275	0.385	0.375	0.375
	Field winding current density, J_f	0.000	4.4×10^8	0.88×10^8	1.040×10^8	1.0×10^8	1.034×10^8
	Environmental screen inner radius, r_{xi}	0.000	1.600	0.800	0.900	0.825	1.034
	Enviromental screen thickness, t_x	0.000	0.800	0.600	0.643	0.600	0.620

Note: This optimal results for design problem, where $T = 300MP_a$ and $T_o = 60MP_a$

Table 5.5
Initial and optimum design variables for inner rotor magnetic circuit

				Optimal design variables			
				First starting point		Second starting point	
Methods	Design Variables	Bounds Lower	Bounds Upper	initial point	optimum point	initial point	optimum point
Hook & Jeeves	Core radius, r_c	-	-	-	0.090	-	0.0902
	Field winding inner radius, r_{fi}	0.000	0.670	0.200	0.407	0.300	0.410
	Field winding outer radius, r_{fo}	0.000	0.685	0.275	0.450	0.375	0.451
	Field winding current density, J_f	0.000	4.4×10^8	0.88×10^8	1.303×10^8	1.0×10^8	1.347×10^8
	Environmental screen inner radius, r_{zi}	0.000	1.600	0.800	1.303	0.885	0.986
	Enviromental screen thickness, t_z	0.000	0.800	0.600	0.649	0.600	0.649
Nelder & Mead	Core radius, r_c	-	-	-	0.090	-	0.088
	Field winding inner radius, r_{fi}	0.00	0.670	0.200	0.407	0.300	0.379
	Field winding outer radius, r_{fo}	0.000	0.685	0.275	0.450	0.375	0.442
	Field winding current density, J_f	0.000	4.4×10^8	0.880×10^8	1.303×10^8	1.0×10^8	1.047×10^8
	Environmental screen inner radius, r_{zi}	0.00	1.600	0.800	1.303	0.825	1.510
	Enviromental screen thickness, t_z	0.000	0.800	0.600	0.649	0.600	0.623

Note: This optimal results for design problem, where $T = 400MP_a$

```
**********************************************************************
                        OPTIMIZATION PACKAGE
              ENGINEERING DEPARTMENT OF DURHAM UNVERSITY
             ********************************************
---GIVE COMMON DATA FOR THE PACKAGE
         COMMON DATA FOR THE PACKAGE
         NUMBER OF DESIGN VARIABLES                        5
         NUMBER OF INEQUALITY CONSTRAINTS                 11
         NUMBER OF EQUALITY CONSTRAINTS                    0
         INTERMEDIATE OUTPUT EVERY INPUT CYCLE             0
         INTERMEDIATE OUTPUT                               1
          ESTIMATED UPPER BOUNDS ON X(I)
             0.670000E+00     0.685000E+00     0.440000E+09
             0.160000E+01     0.800000E+00
         ESTIMATED LOWER BOUNDS ON X(I)
             0.000000E+00     0.000000E+00     0.000000E+00
             0.000000E+00     0.000000E+00
---GIVE STARTING VALUES OF X(I)
        STARTING VALUES OF X(I)
             0.200000E+00     0.275000E+00     0.880000E+08
             0.800000E+00     0.500000E+00
---SELECT FUNCTION MINIMIZATION METHOD
----------------------------------------------------------------------
         YOU HAVE CHOSEN SIMPLEX METHOD (NELDER & MEAD)
---GIVE DATA FOR METHOD
         DATA FOR THE METHOD
         DESIRED CONVERGENCE                          0.10000E-03
         SIZE OF INITIAL POLYHEDRON                   0.10000E+00
         PENALTY PARAMETER USED IN SUMT               0.35000E-01
         REDUCTION FACTOR FOR (R) AFTER EACH CYCLE    0.20000E+00
         MAXIMUM NUMBER OF MOVES PERMITTED           2000
         NUMBER OF SIMPLEX POINT GENERATED            6
----------------------------------------------------------------------
```

(a) OPTIMIZATION USING NELDER & MEAD METHDOD

OPTIMIZATION SEQUENCE FOR A DESIGN PROBLEM

SEQUE. MEMBER k	PENALTY PARAMETER r	MODIFIED OBJ. P(x,r)	ORIG. OBJ. F(x)	FUNCT. RATIO P/F	DESIGN VARIABLES rfi	rfo	Jf	rxi	tx
1	0.35000E-01	0.50265	-0.48778	-1.03048	0.2983	0.3732	0.4573E+08	1.1075	0.4819
2	0.70000E-02	-0.30850	-0.53161	0.58032	0.2983	0.3732	0.4587E+08	1.0143	0.5093
3	0.14000E-02	-0.76812	-0.85313	0.90036	0.3063	0.3809	0.8554E+08	0.9821	0.5634
4	0.28000E-03	-1.00367	-1.04757	0.95810	0.3309	0.3839	0.1090E+09	0.9783	0.6373
5	0.56000E-04	-1.04661	-1.06175	0.98574	0.3332	0.3840	0.1075E+09	0.9221	0.6393
6	0.11200E-04	-1.06146	-1.06707	0.99475	0.3339	0.3841	0.1072E+09	0.9076	0.6396
7	0.22400E-05	-1.07313	-1.07539	0.99790	0.3337	0.3854	0.1041E+09	0.9026	0.6436
8	0.44800E-06	-1.07562	1.07665	0.99905	0.3338	0.3854	0.1041E+09	0.9010	0.6437
9	0.89600E-07	-1.07670	-1.07716	0.99958	0.3338	0.3854	0.1041E+09	0.9005	0.6437
10	0.17920E-07	-1.07716	-1.07745	0.99973	0.3338	0.3854	0.1041E+09	0.9003	0.6437
11	0.35840E-08	1.07735	-1.07738	0.99997	0.3338	0.3854	0.1040E+09	0.9003	0.6437

(b) BEHAVIOUR CONSTRAINTS FOR A DESIGN PROBLEM

SEQUE. MEMBER k	PENALTY PARAMETER r	STRENGTH CONSTRAINT g1	STRENGTH CONSTRAINT g2	SUPERCONDUCTOR CONSTRAINT g3	STATOR CORE CONSTRAINT g4
1	0.35000E-01	0.18966E+05	0.31187E+07	0.51016E+01	0.59986E+00
2	0.70000E-02	0.12029E+05	0.34692E+07	0.50030E+01	0.55547E+00
3	0.14000E-02	0.20185E+07	0.30028E+07	0.21279E+00	0.13898E+00
4	0.28000E-03	0.16553E+08	0.28177E+07	0.41622E+00	0.19747E-01
5	0.56000E-04	0.18610E+08	0.25542E+07	0.71594E+00	0.89137E-02
6	0.11200E-04	0.18893E+08	0.26456E+07	0.75492E+00	0.39952E-02
7	0.22400E-05	0.17688E+08	0.31966E+05	0.86812E+00	0.25777E-02
8	0.44800E-06	0.17716E+08	0.55215E+05	0.87162E+00	0.11114E-02
9	0.89600E-07	0.17706E+08	0.33334E+05	0.87180E+00	0.59808E-03
10	0.17920E-07	0.17712E+08	0.52462E+05	0.87086E+00	0.17109E-03
11	0.35840E-08	0.17700E+08	0.15431E+05	0.87267E+00	0.20031E-03

* OPTIMUM FUNCTION VALUE = 1.07738

* OPTIMUM DESIGN VARIABLES

0.33376 0.38542 0.10404867E+09 0.90027 0.64375

RESULTS OF OPTIMIZATION ON THE DESIGN PROCESSES

****

TABLE DESCRIBING THE DESIGN PROBLEM SPECIFICATION

****

NUMBER OF ROTOR POLES ---------	P	= 2
ROTOR POLE ARCE----------	SIGMA	= 120 deg.
STATOR CORE SATURATION---------	Bmax	= 1.500 T
ROTOR SPEED----------	Ns	= 3000 rpm
MAX. YIELD STRENGTH OF SLOT REGION	To	= 60.00 MPa
MAX. YIELD STRENGTH OF ROTOR BODY	T	= 300.00 MPa
AVER. MASS DENSITY OF FIELD WINDIN	Po	=7400.00 kg/m
MASS DENSITY OF ROTOR BODY-----	P	=7950.00 kg/m
LIMIT VALUE OF CORE RADIUS-----	rc	=0.2rfo m

****

```
**********************************************************
        TABLE OF INITIAL FEASIBLE DESIGN PROBLEM
**********************************************************

       CORE RADIUS-------------------- rc   =  0.0550 m
       FIELD WINDING INNER RADIUS----- rfi  =  0.2000 m
       FIELD WINDING OUTER RADIUS----- rfo  =  0.2750 m
       FIELD WINDING MEAN RADIUS------ rf   =  0.2375 m
       FIELD WINDING THICKNESS-------- t    =  0.0750 m
       FIELD WINDING CURRENT DENSITY-- Jf   = 0.880E+08
       STATOR CORE INNER RADIUS------- rxi  =  0.8000 m
       STATOR CORE THICKNESS---------- tx   =  0.5000 m

**********************************************************


**********************************************************
     CHARACTERSTIC AND PARAMETERS OF OPTIMIZED DESIGN
**********************************************************

 RESULT OF GEOMETRIC CONFIGURATION
 ---------------------------------
          CORE  RADIUS------------- rc  =  0.0771 m
    FIELD WINDING INNER RADIUS----- rfi =  0.3338 m
    FIELD WINDING OUTER RADIUS----- rfo =  0.3854 m
    FIELD WINDING MEAN RADIUS------ rf  =  0.3596 m
    FIELD WINDING THICKNESS-------- tf  =  0.0517 m
    STATOR CORE INNER RADIUS------- rxi =  0.9003 m
    STATOR CORE INNER RADIUS------- rxo =  1.5440 m
    STATOR CORE THICKNESS---------- tx  =  0.6437 m

 RESULT OF ELECTRICAL QUANTITIES
 -------------------------------
    FIELD WINDIN MAX. FLUX DENSITY- Bo  =  5.6933 T
    RADIAL FLUX DENSITY AT STATOR-- Bs  =  1.0775 T
    STATOR CORE FLUX SATURATION---- Bmax=  1.4999 T
    FIELD WINDING CURRENT DENSITY-- J(B)= 0.460E+09
    FIELD WINDING CURRENT DENSITY-- Jf  = 0.104E+09
    APPARENT POWER----------------- Pr  = 1193.0564 MW

 RESULT OF MECHANICAL QUANTITIES
 -------------------------------

    CENTRIFUGAL HOOP STRESS-------  T =299.995586 MPa

**********************************************************
---DO YOU WANT TO SELECT ANOTHER OPTIMIZATION METHOD
---DO YOU WANT TO GIVE NEW STARTING VALUES OF X(I)
---DO YOU WANT TO CONTINUE CALCULATIONS
---END OF JOB,THANK YOU---
```

Figure 5.1 Printout of results for T=300 MP_a anda $T_o = 60$ MP_a for the design problem using simplex search of Nelder and Mead.

```
**************************************************************************
                    OPTIMIZATION PACKAGE
            ENGINEERING DEPARTMENT OF DURHAM UNVERSITY
           ***********************************************
---GIVE COMMON DATA FOR THE PACKAGE
        COMMON DATA FOR THE PACKAGE
        NUMBER OF DESIGN VARIABLES                      5
        NUMBER OF INEQUALITY CONSTRAINTS               11
        NUMBER OF EQUALITY CONSTRAINTS                  0
        INTERMEDIATE OUTPUT EVERY INPUT CYCLE           0
        INTERMEDIATE OUTPUT                             1
         ESTIMATED UPPER BOUNDS ON X(I)
            0.670000E+00    0.685000E+00    0.440000E+09
            0.160000E+01    0.800000E+00
        ESTIMATED LOWER BOUNDS ON X(I)
            0.000000E+00    0.000000E+00    0.000000E+00
            0.000000E+00    0.000000E+00
---GIVE STARTING VALUES OF X(I)
       STARTING VALUES OF X(I)
            0.200000E+00    0.275000E+00    0.880000E+08
            0.800000E+00    0.500000E+00
---SELECT FUNCTION MINIMIZATION METHOD
--------------------------------------------------------------------------
        YOU HAVE CHOSEN SIMPLEX METHOD (NELDER & MEAD)
---GIVE DATA FOR METHOD
        DATA FOR THE METHOD
        DESIRED CONVERGENCE                        0.10000E-03
        SIZE OF INITIAL POLYHEDRON                 0.10000E+00
        PENALTY PARAMETER USED IN SUMT             0.35000E-01
        REDUCTION FACTOR FOR (R) AFTER EACH CYCLE  0.20000E+00
        MAXIMUM NUMBER OF MOVES PERMITTED         2000
        NUMBER OF SIMPLEX POINT GENERATED            6
--------------------------------------------------------------------------

            OPTIMIZATION USING NELDER & MEAD METHDOD
```

(a) OPTIMIZATION SEQUENCE FOR A DESIGN PROBLEM

SEQUE. MEMBER k	PENALTY PARAMETER r	MODIFIED OBJ. P(x,r)	ORIG. OBJ. F(x)	FUNCT. RATIO P/F	DESIGN VARIABLES rfi	rfo	Jf	rxi	tx
1	0.35000E-01	0.50265	-0.48778	-1.03048	0.2983	0.3732	0.4573E+08	1.1075	0.4819
2	0.70000E-02	-0.30850	-0.53161	0.58032	0.2983	0.3732	0.4587E+08	1.0143	0.5093
3	0.14000E-02	-0.76812	-0.85313	0.90036	0.2463	0.3279	0.8554E+08	0.9421	0.5634
4	0.28000E-03	-1.03177	-1.07365	0.96099	0.4160	0.4524	0.1376E+09	1.2487	0.6369
5	0.56000E-04	-1.07726	-1.08859	0.98959	0.4136	0.4518	0.1391E+09	1.3136	0.6349
6	0.11200E-04	-1.10360	-1.11083	0.99349	0.4100	0.4511	0.1318E+09	1.2954	0.6474
7	0.22400E-05	-1.11063	-1.11337	0.99753	0.4097	0.4510	0.1311E+09	1.2906	0.6485
8	0.44800E-06	-1.12077	-1.12156	0.99930	0.4081	0.4507	0.1316E+09	1.3287	0.6478
9	0.89600E-07	-1.12146	-1.12175	0.99974	0.4081	0.4507	0.1316E+09	1.3284	0.6479
10	0.17920E-07	-1.12184	-1.12200	0.99986	0.4081	0.4506	0.1316E+09	1.3280	0.6479
11	0.35840E-08	-1.12324	-1.12339	0.99986	0.4077	0.4505	0.1304E+09	1.3186	0.6499
12	0.71680E-09	-1.12384	-1.12396	0.99989	0.4076	0.4505	0.1303E+09	1.3204	0.6499

(b) BEHAVIOUR CONSTRAINTS FOR A DESIGN PROBLEM

SEQUE. MEMBER k	PENALTY PARAMETER r	STRENGTH CONSTRAINT g1	STRENGTH CONSTRAINT g2	SUPERCONDUCTOR CONSTRAINT g3	STATOR CORE CONSTRAINT g4
1	0.35000E-01	0.18966E+05	0.10312E+09	0.51016E+01	0.59986E+00
2	0.70000E-02	0.12029E+05	0.10347E+09	0.50030E+01	0.55547E+00
3	0.14000E-02	0.20185E+07	0.16003E+09	0.21279E+00	0.13898E+00
4	0.28000E-03	0.25220E+08	0.30422E+06	0.34307E+00	0.18644E-01
5	0.56000E-04	0.23549E+08	0.18244E+06	0.41047E-01	0.10144E-01
6	0.11200E-04	0.20753E+08	0.27948E+05	0.15775E+00	0.51878E-02
7	0.22400E-05	0.20570E+08	0.31333E+05	0.17361E+00	0.21337E-02
8	0.44800E-06	0.19399E+08	0.19344E+05	0.37679E-02	0.86332E-03
9	0.89600E-07	0.19400E+08	0.65059E+04	0.41598E-02	0.83342E-03
10	0.17920E-07	0.19398E+08	0.88032E+04	0.44706E-02	0.33037E-03
11	0.35840E-08	0.19146E+08	0.85165E+05	0.49426E-01	0.14973E-03
12	0.71680E-09	0.19060E+08	0.16036E+05	0.48202E-01	0.75610E-04
13	0.14336E-09	0.19058E+08	0.76348E+04	0.47050E-01	0.51121E-04

* OPTIMUM FUNCTION VALUE = 1.12396

* OPTIMUM DESIGN VARIABLES
0.40761 0.45054 0.13031975E+09 1.32035 0.64994

RESULTS OF OPTIMIZATION ON THE DESIGN PROCESSES

****
TABLE DESCRIBING THE DESIGN PROBLEM SPECIFICATION
****

NUMBER OF ROTOR POLES ---------	P	= 2
ROTOR POLE ARCE----------	SIGMA	= 120 deg.
STATOR CORE SATURATION---------	Bmax	= 1.500 T
ROTOR SPEED----------	Ns	= 3000 rpm
MAX. YIELD STRENGTH OF SLOT REGION	To	= 60.00 MPa
MAX. YIELD STRENGTH OF ROTOR BODY	T	= 400.00 MPa
AVER. MASS DENSITY OF FIELD WINDIN	Po	=7400.00 kg/m
MASS DENSITY OF ROTOR BODY-----	P	=7950.00 kg/m
LIMIT VALUE OF CORE RADIUS-----	rc	=0.2rfo m

****

```
**********************************************************
        TABLE OF INITIAL FEASIBLE DESIGN PROBLEM
**********************************************************

      CORE RADIUS-------------------- rc   =  0.0550 m
      FIELD WINDING INNER RADIUS----- rfi  =  0.2000 m
      FIELD WINDING OUTER RADIUS----- rfo  =  0.2750 m
      FIELD WINDING MEAN RADIUS------ rf   =  0.2375 m
      FIELD WINDING THICKNESS-------- t    =  0.0750 m
      FIELD WINDING CURRENT DENSITY-- Jf   = 0.880E+08
      STATOR CORE INNER RADIUS------- rxi  =  0.8000 m
      STATOR CORE THICKNESS---------- tx   =  0.5000 m

**********************************************************


**********************************************************
     CHARACTERSTIC AND PARAMETERS OF OPTIMIZED DESIGN
**********************************************************

 RESULT OF GEOMETRIC CONFIGURATION
 ---------------------------------
         CORE  RADIUS------------- rc  =  0.0901 m
    FIELD WINDING INNER RADIUS----- rfi =  0.4076 m
    FIELD WINDING OUTER RADIUS----- rfo =  0.4505 m
    FIELD WINDING MEAN RADIUS------ rf  =  0.4291 m
    FIELD WINDING THICKNESS-------- tf  =  0.0429 m
    STATOR CORE INNER RADIUS------- rxi =  1.3204 m
    STATOR CORE INNER RADIUS------- rxo =  1.9703 m
    STATOR CORE THICKNESS---------- tx  =  0.6499 m

 RESULT OF ELECTRICAL QUANTITIES
 -------------------------------
    FIELD WINDIN MAX. FLUX DENSITY- Bo  =  5.6522 T
    RADIAL FLUX DENSITY AT STATOR-- Bs  =  1.1240 T
    STATOR CORE FLUX SATURATION---- Bmax=  1.5000 T
    FIELD WINDING CURRENT DENSITY-- J(B)= 0.964E+09
    FIELD WINDING CURRENT DENSITY-- Jf  = 0.130E+09
    APPARENT POWER----------------- Pr  = 1244.5226 MW

 RESULT OF MECHANICAL QUANTITIES
 -------------------------------
    CENTRIFUGAL HOOP STRESS-------  T =399.999208 MPa

**********************************************************
---DO YOU WANT TO SELECT ANOTHER OPTIMIZATION METHOD
---DO YOU WANT TO GIVE NEW STARTING VALUES OF X(I)
---DO YOU WANT TO CONTINUE CALCULATIONS
---END OF JOB,THANK YOU---
```

Figure 5.2 Printout of results for T=400 MP_a anda $T_o = 60$ MP_a for the design problem, using simplex search of Nelder and Mead.

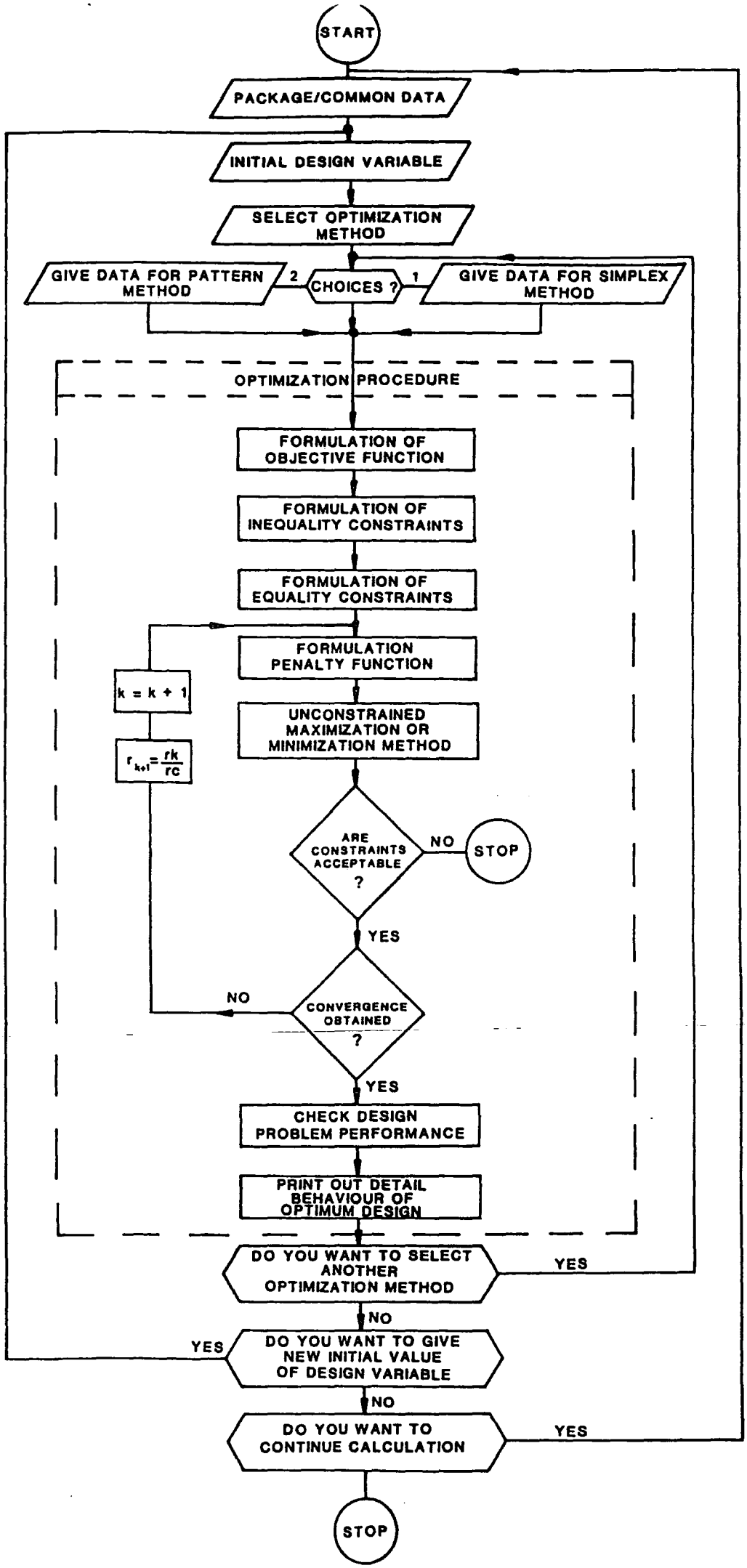

Figure 5.3 Simplified flow chart for optimization package.

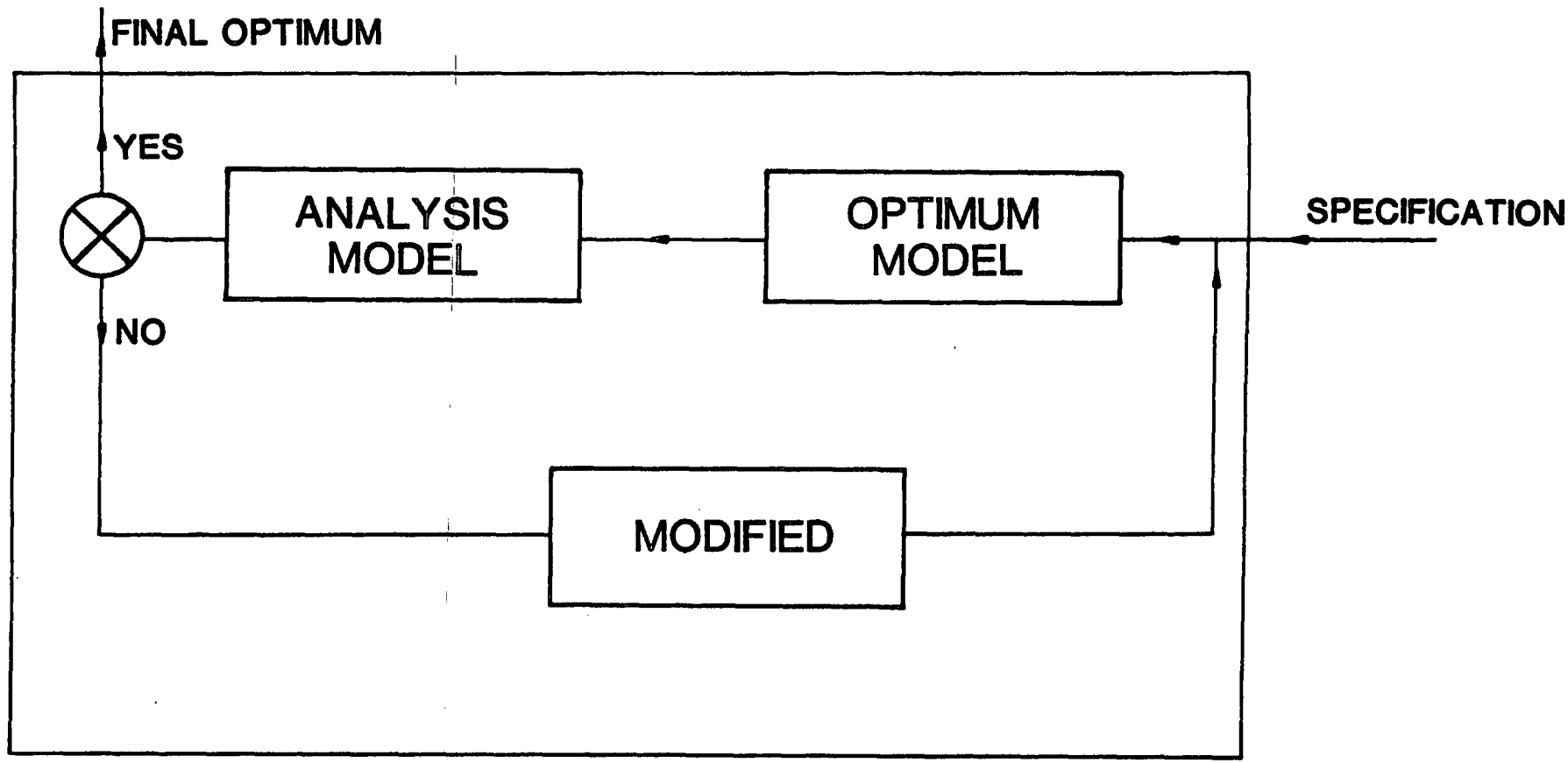

Figure 5.4 Block diagram of synthesis process.

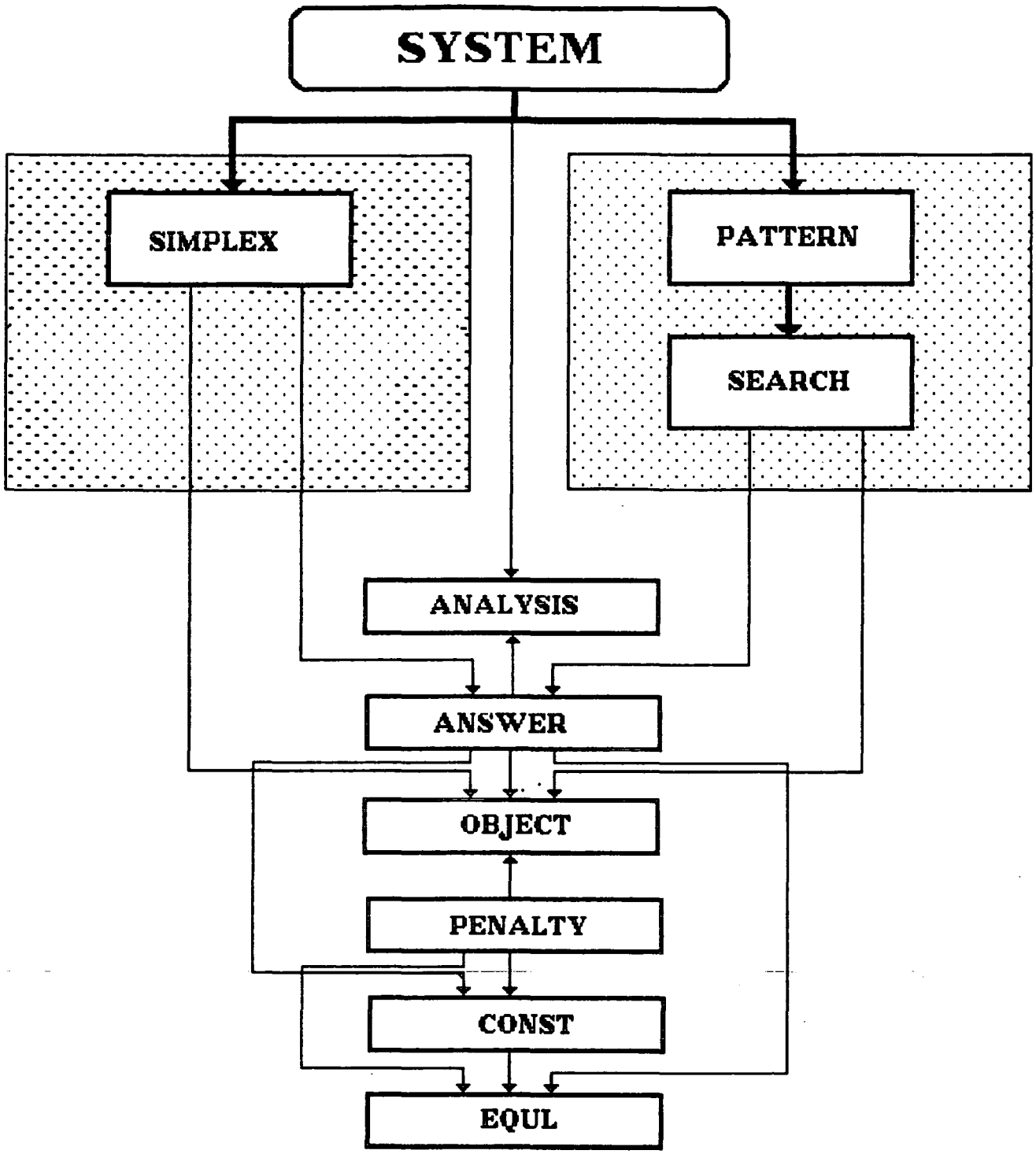

Figure 5.5 . Structure of the computer program

CHAPTER 6

SUMMARY, GENERAL CONCLUSIONS, AND SUGGESTIONS FOR FURTHER WORK

6.1 Summary and General Conclusions

The work presented in this thesis has been concerned with the development of a general design strategy for the superconducting generator rotor. In chapter 1 an overall description of the design and construction of individual components of the generator was presented along with a review of the general concept of the superconducting generator. This type of machine was compared with the present day copper-iron machine and the potential advantages of this new concept, both technical and economic, outlined.

As shown in chapter 1, the use of a superconducting field winding in a.c. generators holds bright prospects of increasing the unit power ratings. Such machines also exhibit unique theoretical and practical design problems which still remain to be solved. The optimal selection of the principle design parameters of the superconducting generator constitute a problem of relevant interest. The work in this thesis is a contribution to this and has proposed the use of mathematical optimization techniques to allow an optimal solution to the machine design problem.

Along with developing an understanding of the concept of the electromagnetic interaction and the limitations that this configuration imposes on the magnetic field design, the specifications demand the development of an accurate method for magnetic field calculation, in order to predict the performance charateristics of the machine. Chapter 2 presents a new method for calculating the magnetic field inside the machine in which the theoretical field

distribution is modified to take into account the slot geometry of the machine. The new method of calculation was applied to a generator as an example, and the results obtained were compared with former methods which are based on the current sheet and winding thickness models. An interesting outcome of the computation results is the conclusion that the new method has better accuracy than former methods. Further, the results indicate that the effect of certain odd harmonic (localised flux concentration) around the outermost slot has very adverse influence on the machine performance. As it is the $J_c - B_c$ characteristic of the superconducting conductor which determines the relationship between current density and magnetic field in the superconductor, the maximum permitted current density in the superconducting field winding is limited by the localised flux concentration. Therefore, the magnitude and location of maximum magnetic field within the field winding can now be predicted more accurately by using the new method.

The analytical expressions for the new method have also been applied to an investigation of the structure of the field winding slots and the effect they have on the harmonic fields. The results of this investigation have shown that for a slotted field geometry of a given spread angle the maximum flux density at the outermost slot is influenced by the actual slot shape and ratio of tooth width/slot width used. Simply selecting a 120° winding spread angle which eliminates the third special harmonic does not necessarily minimize the peak flux density at the winding.

An initial aim of the thesis was to present an implementation of a strict mathematical optimization technique which allows the optimum design parameters of the generator to be calculated. In order to optimize a machine design it is first necessary to describe and analyse the machine design problem.

In chapter 3, special attention was paid to the mechanical and electrical constraints which define the limits of the rotor design. These

constraints included bursting stresses, tip speed, superconductor capability, maximum flux density allowed in the stator core all of which have been specified and analysed. An analytical method of determining the tangential (hoop) and radial stresses due to centrifugal force was developed. The analytical expressions for the centrifugal stresses have been applied to the constrained optimisation problem, and it has been shown that, at least for material strength, overspeed factors, and dimensions determine the design of the inner rotor. It was also noted that the permissible stresses in the inner rotor body are at a maximum bursting speed of 1.6 to 1.7 times rated speed so as to ensure a sufficient safety factor in steady state operation.

Since the research into superconducting machines design was to use direct search methods, three direct search optimization procedures have been tested on mathematical functions in chapter 4. It was found that the direct search method is well suited to these problem and is effective for design problems for two reasons. Firstly since only two parameters are to be chosen (step size and convergence), much of the " art" encountered in using "hand" design is removed. Secondly, the amount of effort to use these procedures is relative low and problem preparation is usually simpler.

Consequently, other methods may be used in the optimization procedure (such as Powell's method) for providing computational gains and should be comparatively tested. The computer time for all mathematical test functions and design problems have been shown to be negligible, for example, in every case the optimum was found in less than 1 second. Although there is a chance that the methods may fail to reach the global optimum, the experience gained from numerous examples gives confidence that these procedures will be useful.

Chapter 5 shows non-linear programming is a practical and useful approach of optimizing machine design problem. Although this chapter

discussed the special case of optimizing flux distribution by selecting the field winding dimensions (r_{fi}, r_{fo}), the current density (J_f), and the dimensions of the environmental screen (r_{xi}, t_x), any property of the machine design problem such as power output, volume (or weight), or cost, can be optimized.

Chapter 5 shows that the optimal design is governed mostly by magnetic properties of the stator core and the allowable strength of the inner rotor materials, rather than the superconductor capability.

6.2 Recommendations for Future Work

6.2.1 Recommendations for design process

(1). Future work is required to minimize the higher localised flux concentration around the outermost slot by modifying the field winding design using the new analytical method developed in this thesis.

(2). The self inductance for a three-dimensional generator can be based on two-dimensional analysis if the former is corrected by using the effective length equation. This problem needs further detailed analysis.

(3). The electromagnetic forces on the outer rotor are the main outer rotor design requirements and are of particular interest when the generator is optimized. As a result, an analytical method is required to predict accurately the maximum critical forces which cause the outer rotor to be unstable and buckle during short-circuit operating period.

6.2.2 Recommendations for optimization process

Undeniably, the use of optimization techniques in superconducting machine design will continue to expand. It is worthwhile to guide this development in such way that the experience gained is beneficial to the entire range of superconducting machines. For this reason, the optimization has been discussed and described in the context of the total machine design process.

REFERENCES

Appleton, A.D. et al., 1975, 'Discussion on large superconducting a.c. generators', *International Conference Electrical Machines* , London, paper A4 sept. 1975.

Ammasai, N. et al., 1988, 'Operating cost optimization of speed changing induction motors', *IEE Proc.*, Vol. 135, pp 33-38.

Anderson, O.W., 1967, 'Optimum design of electrical machines', *IEEE Trans. PAS.*, Vol. PAS-86, pp 707-711.

Bandler, J.W. and Charalambous, D., 1972, 'Practical least p-th optimization of network', *IEEE Trans. MW*, Vol. 12, pp 837-840.

Bharadwaj, D.G. et al., 1979, 'Experience with direct indirect search methods applied to cage induction motor design optimization', *Electric Machines and Electromechanics*, Vol. 4 pp 85-93.

Box, M.J., 1966, 'Comparison of several current optimization methods and the use of the transformtions in constrained problems', *Computer J.*, Vol. 9, pp 67-77.

Box, M.J., et al., 1969, 'Non-linear optimization techniques', *I.C.I Monograph*, No. 5, Oliver and Boyed, Edinburgh.

Bratoljic, T., 1973, 'Turbogenerator with superconducting excitation winding',*Bulletin ASE.*, Vol. 64, pp 1040-1050.

Brooks, S.H., 1958, 'A discussion of random metods for seeking maxima', *Journal Operations Res. Soc.*, Vol. 6, pp 244-257. March 1986, pp 14-23.

Bumby, J.R., 1981, 'Superconducting a.c. generator with magnetic steel outer rotor', *IEE Proc.*, Vol. 128, pp 1-11.

Bumby, J.R., 1983, 'Superconducting rotating electrical machines', *Clarendon Press*, Oxford.

Corrol, C.W., 1961, 'The created response surface technique for optimizing non-linear, restrained system', *Operation Res.*, Vol. 9, pp 196-185.

Chari, M.V.K. and Haller, T.R., 1980, 'Steady state and short-circuit force on the stator windings of a superconducting geneartor', *IEEE on PAS*, Vol. PAS 99 pp 928-933.

Chidambarab, et al., 1982, 'Optimization of dual speed induction motors', *Electric Machines and Electromechanics*, Vol. 32, pp 239-244.

Edmonds, J., 1979, 'Superconducting generator technology, An overview', *IEEE Trans. on PAS*, Vol. MAG-15, No 1, pp 673.

Erlicki, M.S. and Appellbaum, J., 1965, 'Optimized parameter analysis of an induction machine', *IEEE Trans. on PAS*, Vol. PAS 84, No 11, pp 1017-1024.

Fiacco, A.V. and McCormick, G.P., 1964, 'The sequential unconstrained Minimization technique for non-linear programming', *Management Sci.*, Vol. 10 pp 601-617.

Fiacco, A.V. and McCormick, G.P., 1968, 'Nonlinear programming: sequential unconstrained Minimization techniques', *Wiley, New York*, 1968.

Gillet, R., et al., 1980, 'Superconducting generator development program', *Superconductivity conference.*, 1980.

Himmelbau, D.M., 1972, 'Applied non-linear programming', *McGraw-Hill* , New York, 1972

Hook, R., and Jeeves, T.A., 1961, 'Direct search solution of numerical and stastistical problem', *J. ACM, COMP.*, Vol. 8, pp 212-229.

Hughes, A., and Miller, T.J., 1977, 'Aanalysis of fields and inductances in air cored and iron cored synchronous machines', *IEE Proce.*, Vol. 124, pp 121-126.

Kirtley, J.L. and Furuyama, 1975, 'A design concept for large superconducting alternators', *IEEE Tans. on PAS*, vol. 94, no. 4, 1975.

Kirtley, J.L., 1976, 'Basic formulas for air core synchronous machines', *IEEE Conference*, paper 71, cp 155-PWR 1976.

Kirtley, J.L., 1988, 'Application of superconducting-High T_c and otherwise-To electrical power generators', *Electric Machines and Power System*, vol. 15 pp 121-134.

Kowalik, J. and Osborne, M.R., 1968, 'Methods for unconstrained optimization problems', *American Elsevier Publishing Co.*, New York.

Kuester, J.L. and Mize, J.H., 1973, 'Optimization technique with fortran', *McGraw-hill Publishing Co.*, New York

Lambrecht, D., 1981, 'Status of development of superconducting a.c. generators', *IEEE trans. on Magnetics*, Vol MAG-17, pp 1551-1559

Luck, D.L and Thullen, P., 1973, 'Double shielded superconducting winding', *U.S Patent* No. 3, 764, 85.

Maki, N., et at., 1980, 'Design and component of a 50 MVA superconducting generator', *IEEE Trans. on PAS*, Vol. PAS-99, pp 184-194.

Martinelli, G. and Morini, A., 1980, 'Study of the magnetic field superconducting alternators', *Archiv fur Elcktrotechnik*, Vol. 62 pp 141-151.

Martinelli, G. and Morini, A., 1981, 'Two dimensional winding models for calculation of magnetic field in superconducting turbogenerator', *Electric machines and electromechanics*, Vol. 6 pp 512-525.

Mcarther, D.S., 1960, 'Strategy in research-alternative methods for design of experiments', *I.R.E Trans. on E.M*, pp 34-39.

Menzies, R.W and Neal, G.W., 1979, 'Optimization program for large induction motor design', *Proc. IEE*, Vol. 122, No. 6

Miller, T.J. and Lawrenson, P., 1976, 'Penetration of transient magnetic fields through conducting cylindrical structure with reference to superconducting a.c. machines', *Proce. IEE*, Vol. 123, pp 437-443.

Minnich, S.H., et al., 1979, 'Design studies of superconducting generators', *IEEE on Maognetics*, Vol. MAG-15, pp 703-710.

Nagrial, M.H. and Lawrenson, P.J., 1979, 'Comparitive performance of direct search methods of minimization for design electrical machine', *Electric machines and Electromechanics*, Vol. 3, pp 315-324

Nelder, J.A and Mead, R., 1965, 'Simplex method for minimization', *Computer, J.*, Vol. 7, pp 1449-1454.

Powell, M.J.D., 1962, 'An iterative method for finding stationary values of a function of several variables ', *Computer, J.*, Vol. 5, pp 147.

Parker, J.H. and Towne, R.A., 1979, 'Design large superconducting turbine generator for electric utility application', *IEEE Trans. on PAS*, Vol. PAS-98, pp 2241-2249.

Pavithran, K.N., et al., 1987, 'Optimum design of an induction motor for operation with current source inverters', *Proc. IEE*, Vol. 134, pp 1-7

Ramarathnam, R., et al., 1973, 'A comparative study of minimization techniques for optimization of induction motor design', *IEEE Trans. on PAS*, Vol. PAS-86, pp 1448-1454.

Ross, J.S., 1976, 'The engineering discussion of large superconducting a.c. generator', *International Conference on Electric machines*, Vienna, 1976.

Ross, J.S. and Appleton, A.D., 1980, 'Progress in the development of superconducting a.c. generator', *CIGRE Report*, No. 11-01, Paris, 1980.

Sabrie, J.L., at et., 1983, 'Technical overview of French program', *IEEE Trans. on Magnetics*, Vol. Mag-3, No.3 1983.

Singh, et al., 1985, 'Experience in design optimization of poly phase induction motors using SUMT algorithm', *IEEE, Trans. PAS*, Vol. 102, pp 3379-3384.

Spang, H.A., 1962, 'Review of minimization techniques for non-linear function', *SIAM Review*, Vol. 4, No. 4 pp 343-365.

Spendley, W., et al., 1962, 'Sequential application of simplex designs in optimization and evolutionary operation', *Technometric*, Vol. 4, 441-461.

Spooner, E., 1973, 'Fully slotless turbo-genrators', *Proc. IEE*, Vol. 120, No. 12

Thullen, P., et al., 1971, 'An experimental alternator with superconducting rotating field winding', *IEEE on PAS*, Vol. PAS-90, pp 611-619.

Yamaguchi, K. et al., 1984, 'Superconducting rotor development for a 50 MVA generator', *IEEE on PAS*, Vol. PAS-103, pp 1795-1800

Wilde, D.J., 1964, 'Optimum seeking methods', *Prentice-Hall publishing*, New Jesy, 1964.

Woodson, H.H. et al., 1971, 'The application of superconductors in the field windings of large synchronous machines', *IEEE Trans. on PAS*, Vol. PAS-90, No 2, pp 620-627.

APPENDIX 1

FIELD ANALYSIS

A1.1 Assumption

To facilitate the two dimensional magnetic field analysis the following assumptions are made:

(1). The winding is assumed to be infinitely long in the axial z direction so that the vector potential has only the axial component A_z.

(2). The iron screen is infinitely long in the axial direction and its permeability is very large (i.e., $\mu_r = \infty$) and its conductivity is zero (i.e., ρ=0).

A1.2 Field Analysis by former Models

A1.2.1 Current Distribution

Assuming the winding to be represented by a current sheet at its mean winding radius (fig. A1.1) the current distribution could be represented as a Fourier series of currents

$$K(\theta) = \sum_{\substack{n=1 \\ n=odd}}^{\infty} \widehat{K}_n sinnp\theta \qquad A/m \tag{A1.1}$$

the magnitudes of current component are found by standard technique to be

$$\widehat{K}_n = \frac{N_f I_f}{\pi r_f} \frac{sin\frac{n\sigma_f}{2}.(-1)^{\frac{n-1}{2}}}{\frac{n\sigma_f}{2}} \qquad A/m \tag{A1.2}$$

but

$$k_{wn} = \frac{sin\frac{n\sigma_f}{2}.(-1)^{\frac{n-1}{2}}}{\frac{n\sigma_f}{2}} \tag{A1.3}$$

substituting eqn. (A1.3) into eqn. (A1.2), gives

$$\widehat{K}_n = \frac{I_f}{r_f}\left(\frac{N_f k_{wn}}{\pi}\right) \qquad A/m \tag{A1.4}$$

Therefore

$$K(\theta) = \sum_{\substack{n=1 \\ n=odd}}^{\infty} \frac{N_f I_f k_{wn}}{\pi r_f} sinnp\theta \tag{A1.5}$$

If the actual thickness of superconducting field winding is taken into account (fig. A1.2), then the amplitude of field current density (A/m^2) is obtained by Fourier analysis (see fig. A1.3)

$$J_f(\theta) = \sum_{\substack{n=1 \\ n=odd}}^{\infty} \widehat{J}_{f_n} sinnp\theta \qquad A/m^2 \tag{A1.6}$$

Where

$$\widehat{J}_{f_n} = \frac{2N_f I_f}{\pi(r_{fo}^2 - r_{fi}^2)} \frac{sin\frac{n\sigma_f}{2}.(-1)^{\frac{n-1}{2}}}{\frac{n\sigma_f}{2}} \qquad A/m^2 \tag{A1.7}$$

with the current density of the actual winding being

$$J_f = \frac{N_f I_f}{\sigma_f(r_{fo}^2 - r_{fi}^2)} \qquad A/m^2 \tag{A1.8}$$

substituting eqn. (A1.8) into (A1.7), gives

$$\widehat{J}_{f_n} = J_f\left(\frac{4sin\frac{n\sigma_f}{2}.(-1)^{\frac{n-1}{2}}}{n\pi}\right) \qquad A/m^2 \tag{A1.9}$$

Eqn. (A1.7) may be rearranged into the form

$$\widehat{J}_{f_n} = \frac{I_f}{r_f.t_f}\left(\frac{N_f k_{wn}}{\pi}\right) A/m^2 \tag{A1.9}$$

Where

$$r_f = \frac{(r_{fo} + r_{fi})}{2} \qquad (A1.10)$$

$$t_f = (r_{fo} - r_{fi}) \qquad (A1.11)$$

Comparing eqns. (A1.4) and (A1.9) establishes the relationships between the linear current density of the field winding current sheet (A/m) and the current density of the field winding thickness model as:

$$\widehat{K}_n = \widehat{J}_{fn} \times t_f \qquad A/m \qquad (A1.12)$$

A1.2.2 Vector potential Solution

The vector potential produced by the current sheet may be obtained from Laplace's equation expressed in cylindrical co-ordinate as:

$$\frac{1}{r}\frac{\partial}{\partial r}\left(r\frac{\partial A_z}{\partial r}\right) + \frac{1}{r}\frac{\partial^2 A_z}{\partial \theta^2} + \frac{\partial^2 A_z}{\partial z^2} = 0 \qquad (A1.13)$$

Assuming a constant vector potential in the axial direction, then

$$\frac{\partial A_z}{\partial z} = 0 \qquad (A1.14)$$

and equation (A1.13) reduces to :-

$$\frac{1}{r}\frac{\partial}{\partial r}\left(r\frac{\partial A_z}{\partial r}\right) + \frac{1}{r}\frac{\partial^2 A_z}{\partial \theta^2} = 0 \qquad (A1.15)$$

The solution for equation (A1.16), is given by

$$A_z(r,\theta) = \sum_{\substack{n=1 \\ n=odd}}^{\infty} (ar^{np} + br^{-np})(c.cosnp\theta + d.sinnp\theta) \qquad (A1.16)$$

The value of the constants a, b, c and d are determined according to the following boundary conditions:

1. at $r < r_f$ $\quad r \mapsto 0 \quad$ B_r, B_θ finite
2. at r=r_f (at the point where the current sheet exists):

   B_r (inside)=B_r(outside)

   $\Delta B_\theta = B_\theta$(inside)- B_θ(outside) = $-\mu_o \sum_{\substack{n=1 \\ n=odd}}^{\infty} \widehat{K}_n sinnp\theta$
3. at $r = r_{xi}$ (at the inner radius of stator environmental screen):

   If the environmental screen is an iron screen, $B_\theta = 0$, whilst if the environmental screen is conducting, $B_r = 0$.

The solutions of the magnetic field distributions are given by Hughes [Hughes, 1977]

In region [1] where $r < r_f$, the solution is

$$B_{1r_f} = \sum_{\substack{n=1 \\ n=odd}}^{\infty} \frac{\mu_o \widehat{K}_n}{2} \left(\frac{r}{r_f}\right)^{np-1} \left[1 \pm \left(\frac{r_f}{r_{xi}}\right)^{2np}\right] cosnp\theta \qquad (A1.17)$$

$$B_{1\theta_f} = - \sum_{\substack{n=1 \\ n=odd}}^{\infty} \frac{\mu_o \widehat{K}_n}{2} \left(\frac{r}{r_f}\right)^{np-1} \left[1 \mp \left(\frac{r_f}{r_{xi}}\right)^{2np}\right] sinnp\theta \qquad (A1.18)$$

In region [2] where $r_{xi} > r > r_f$, the solution is

$$B_{2r_f} = \sum_{\substack{n=1 \\ n=odd}}^{\infty} \frac{\mu_o \widehat{K}_n}{2} \left(\frac{r_f}{r}\right)^{np+1} \left[1 \pm \left(\frac{r}{r_{xi}}\right)^{2np}\right] cosnp\theta \qquad (A1.19)$$

$$B_{2\theta_f} = \sum_{\substack{n=1 \\ n=odd}}^{\infty} \frac{\mu_o \widehat{K}_n}{2} \left(\frac{r_f}{r}\right)^{np+1} \left[1 \mp \left(\frac{r}{r_{xi}}\right)^{2np}\right] sinnp\theta \qquad (A1.20)$$

The double sign ($\pm$) in the above equations indicate the effect of the environmental screen. The upper sign is for an iron environmental screen and the lower sign for a conducting environmental screen.

Winding thickness can now be accommodated by assuming the winding to be made up from a number of thin current sheets each of thickness dr_f when the linear current density of each sheet is given by

$$d\widehat{K}_n = \widehat{J}_{f_n} dr_f \qquad (A1.21)$$

Expressions for the magnetic fields of the thickness model in which the field coil is assumed to be uniformly distributed in a single slot per pole (i.e S=1) can now be derived by substiting $d\widehat{K}_n$ for $\widehat{K}_n$ in equations (A1.17) to (A1.20) and integrating with respect to the thickness dr_f of the field current sheet. The flux density components for three cylinderical regions are obtained:

For region 1 $(r < r_{fi})$

$$B_{r_f} = \int_{r_{fi}}^{r_{fo}} dB_{1r_f} \qquad (A1.22)$$

$$B_{\theta_f} = \int_{r_{fi}}^{r_{fo}} dB_{1\theta_f} \qquad (A1.23)$$

For region 2 $(r_{fi} < r < r_{fo})$

$$B_{r_f} = \int_{r_{fi}}^{r} dB_{2r_f} + \int_{r}^{r_{fo}} dB_{1r_f} \qquad (A1.24)$$

$$B_{\theta_f} = \int_{r_{fi}}^{r} dB_{2\theta_f} + \int_{r}^{r_{fo}} dB_{1\theta_f} \qquad (A1.25)$$

For region 3 $(r > r_{fo})$

$$B_{r_f} = \int_{r_{fo}}^{r_{fi}} dB_{2r_f} \qquad (A1.26)$$

$$B_{\theta_f} = \int_{r_{fo}}^{r_{fi}} dB_{2\theta_f} \qquad (A1.27)$$

The evaluation of the integrals in equations (A1.22-A1.27) are straightfoward but rather tedious, and so are not carried out here. However, the solution of magnetic field distribution for three regions was found and are reported in table 2.1. For example, the radial and tangential magnetic field components in region 1 ($r < r_{fi}$) can be writtern as:

For $np \neq 2$

$$B_{r_f} = \sum_{\substack{n=1 \\ n=odd}}^{\infty} \frac{\mu_o \hat{J}_{f_n}}{2(2-np)} r\left(\frac{r}{r_{fo}}\right)^{np-2}\left[1-\left(\frac{r_{fi}}{r_{fo}}\right)^{2-np} \pm \frac{2-np}{2+np}\left(\frac{r_{fo}}{r_{xi}}\right)^{2np}\left(1-\left(\frac{r_{fi}}{r_{fo}}\right)^{2+np}\right)\right] cosnp\theta \qquad (A1.28)$$

$$B_{\theta_f} = -\sum_{\substack{n=1 \\ n=odd}}^{\infty} \frac{\mu_o \hat{J}_{f_n}}{2(2-np)} r\left(\frac{r}{r_{fo}}\right)^{np-2}\left[1-\left(\frac{r_{fi}}{r_{fo}}\right)^{2-np} \pm \frac{2-np}{2+np}\left(\frac{r_{fo}}{r_{xi}}\right)^{2np}\left(1-\left(\frac{r_{fi}}{r_{fo}}\right)^{2+np}\right]\right. sinnp \qquad (A1.29)$$

For $np = 2$, i.e. the case when $n = 1$ and $p = 2$

$$B_{r_f} = \left(\frac{\mu_o \hat{J}_{f_1}}{2}\right) r\left[-ln\left(\frac{r_{fi}}{r_{fo}}\right) \pm \left(\frac{1}{4}\right)\left(\frac{r_{fo}}{r_{xi}}\right)^4\left(1-\left(\frac{r_{fi}}{r_{fo}}\right)^4\right)\right] cos2\theta \qquad (A1.30)$$

$$B_{\theta_f} = \left(\frac{\mu_o \hat{J}_{f_1}}{2}\right) r\left[-ln\left(\frac{r_{fi}}{r_{fo}}\right) \pm \left(\frac{1}{4}\right)\left(\frac{r_{fo}}{r_{xi}}\right)^4\left(1-\left(\frac{r_{fi}}{r_{fo}}\right)^4\right)\right] sin2\theta \qquad (A1.31)$$

The radial and tangential magnetic field components for thickness model can briefly expressed as:

$$B_r(r,\theta) = \sum_{\substack{n=1 \\ n=odd}}^{\infty} B_{r,n}(r) cosnp\theta \qquad (A1.32)$$

$$B_\theta(r,\theta) = \sum_{\substack{n=1 \\ n=odd}}^{\infty} B_{\theta,n}(r) sinnp\theta \qquad (A1.33)$$

A1.2.3 Machine inductances calculation

Once the magnetic fields are found, various self and mutual inductances are determined by calculating the winding flux linkages. This is a matter of integrating the flux density, $B_{(r,n)}(r)$, over appropriate winding area. Integrating over a two dimension winding distribution which varies sinusoidally in both dimension can be done as follows. By considering coil of constant turns, the flux linkages of these dN turns is found by integrating the radial of $B_{(r,n)}(r)$ over area A. The total flux linkages of the nth harmonic are then found by the flux linkages of the coil by multiplying the flux linkages of the coil by number of coils per winding and thus, the flux linkage, ψ, of the winding can easily be found by

$$\psi = p\lambda \int_{r_i}^{r_o} \int_{-\frac{\sigma}{2}}^{\frac{\sigma}{2}} \int_{\phi-\frac{\pi}{2}}^{\phi+\frac{\pi}{2}} K_w B_{(r,n)}(r) dr d\theta d\phi \qquad (A1.34)$$

Where

$$K_w = \frac{2N}{\sigma\left(r_o^2 - r_i^2\right)} \qquad (A1.35)$$

The term p appears in equation A1.34 because total flux is time flux linked by single coil. N is total number of turns in the winding. This process is straight forward but tedious. As result, the self and mutual inductanes for the winding are

$$L = \frac{\psi}{I} \qquad (A1.36)$$

and

$$M = \frac{\psi}{I} \qquad (A1.37)$$

substituting the expression for magnetic field in preceding section, self and mutual inductances are found and they are presented in table 2.2.

A1.3 Field Analysis accounting for slot geometry

It is assumed that the field winding under consideration has several slots i.e that $S \geq 1$, so that the field winding has, for every pole-pair, S slot-pairs separated by the geometrical angle α as shown figure 2.5.

The Fourier current density components of the field winding are now obtained by summing the individual slot components so that

$$J_{fs}(\theta) = \sum_{i=1}^{S} \sum_{\substack{n=1 \\ n=odd}}^{\infty} \hat{J}_{fs_{n_i}} sinnp(\theta \pm \alpha_i) \qquad (A1.38)$$

Where

$$\hat{J}_{fs_n} = \frac{N_{fs} I_{fs} k_{wn_s}}{\pi(r_{fso}^2 - r_{fsi}^2)} \quad A/m^2 \qquad (A1.39)$$

where

$$k_{wn_s} = \left(\frac{sin\frac{n\sigma_{fs}}{2}.(-1)^{\frac{n-1}{2}}}{\frac{n\sigma_{fs}}{2}}\right) \qquad (A1.40)$$

$$N_{fs} = \frac{N_f}{S} \qquad (A1.41)$$

$$\sigma_{fs} = \frac{\sigma_f}{S + (S-1)\frac{\sigma_{ft}}{\sigma_{fs}}} \qquad (A1.42)$$

but

$$Q = \frac{\sigma_{ft}}{\sigma_{fs}} \qquad (A1.43)$$

therefore

$$\sigma_{fs} = \frac{\sigma_f}{S + (S-1)Q} \qquad (A1.44)$$

Similarly, the flux density components corresponding to the S slot-pairs shown in figure 2.5 can be calculated as before. They have the same maximum of $B_{r,n}(r)$ and $B_{\theta,n}(r)$ but they are phase shifted because the slot-pairs in equation are spaced apart by α. Using the principle of superposition, the resultant radial and tangential magnetic field components are expressed as follows:

$$B_{r_T} = B_{r_1} + B_{r_2} + B_{r_3} + B_{r_4} + \ldots \qquad (A1.45)$$

$$B_{\theta_T} = B_{\theta_1} + B_{\theta_2} + B_{\theta_3} + B_{\theta_4} + \ldots \qquad (A1.46)$$

Where B_{r_T}=resultant radial flux density component

and B_{θ_T}=resultant tangential flux density component.

Using the above definition, the resultant of magnetic field components of field winding can be expressed as follows:

$$B_{r_T} = \sum_{i=1}^{S} \sum_{\substack{n=1 \\ n=odd}}^{\infty} B_{i_{r,n}}(r) cosnp(\theta \mp \alpha_i) \qquad (A1.47)$$

$$B_{\theta_T} = \sum_{i=1}^{S} \sum_{\substack{n=1 \\ n=odd}}^{\infty} B_{i_{\theta,n}}(r) sinnp(\theta \mp \alpha_i) \qquad (A1.48)$$

The above result can be easily be generalized for any symmetrical distribution S slot-pairs of saddle (conventional) type, or any configuration of the slot-pair distribution. The field winding as function of S slot-pairs are to be

independent as described above. However, the results generated by equations (A1.47-A1.48) are reported in table 2.4

Finally it worth mentioning that the above results can easily be generalized for three-phase armature windings. The procedure is exactly the same for these windings except that $(\theta - \alpha_i)$, J_{fs}, σ_{fs}, r_{fso}, and r_{fsi} are replaced by $(\theta - \alpha_i - \psi)$, J_{as}, σ_{as}, r_{aso}, and r_{asi}, the corresponding armature values.

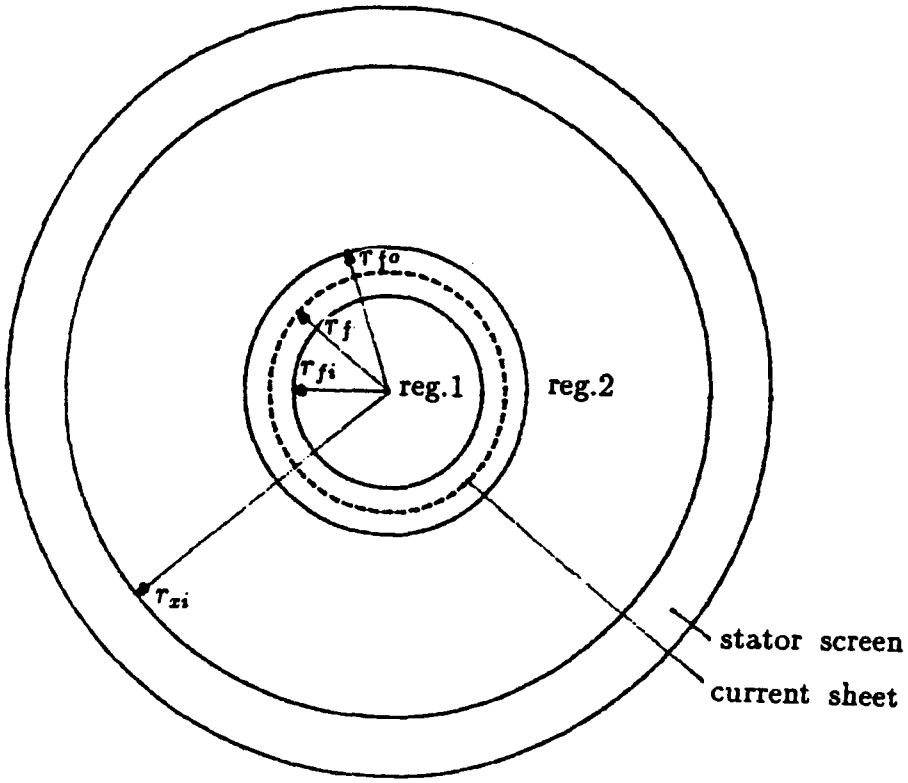

Fig.[A1.1] current sheet model for magnetic field calculation

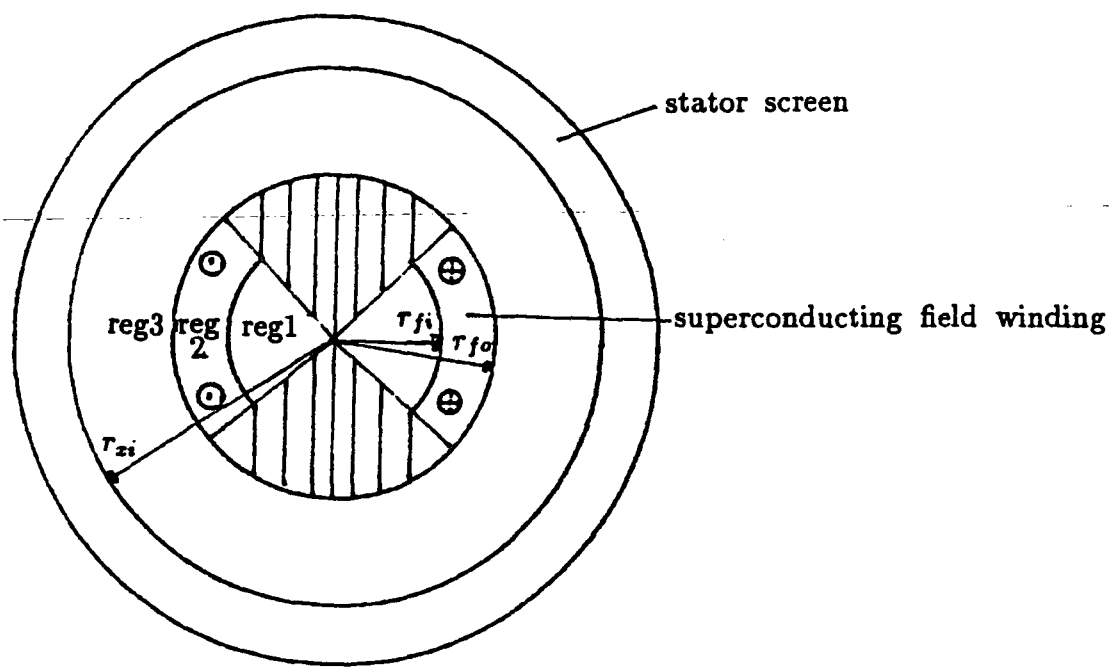

Fig.[A1.2] Thickness model for magnetic field calculation

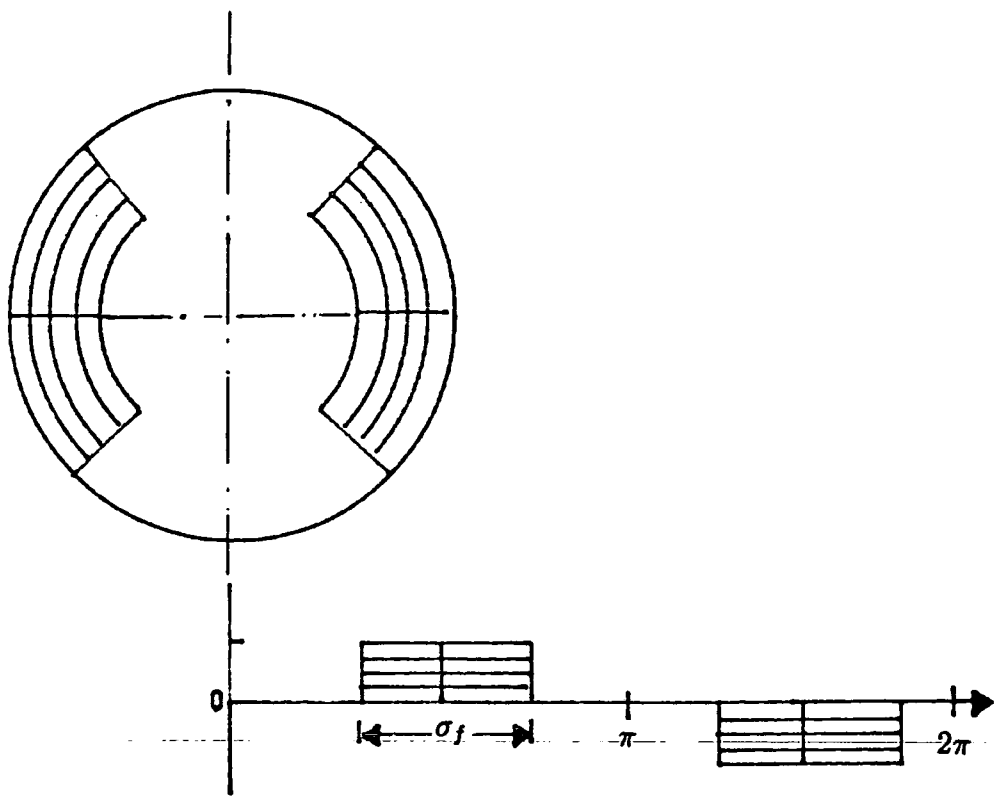

Fig.[A1.3] Distribution of field current density

APPENDIX 2

STRESS ANALYSIS

A2.1 Assumption

It is assumed in the analysis stress procedure that

(1). The material of the inner rotor body which carry the super-conducting winding is made of non-magnetic steel. At present the material adequately matches the following requirements of the inner rotor

(a). high strength

(b). high ductility

(c). non-magnetic properties

(d). low-thermal conductivity

(2). The field winding region is assumed to be a series of annular slots of constant width (i.e $\sigma_\theta = 0$).

(3). In this analysis the tresca criterion has been used to predict the failure of the material under the action of centrifugal forces. If the tresca criterion is obeyed for the slot region and has yield strength (T_o) and for the core region has yield strength (T), then the critical conditions must take the following form:

$$(\sigma_r)_{r=r_{fi}} \leq T_o \qquad (A2.1)$$

$$(\sigma_\theta)_{r=r_c} \leq T \qquad (A2.2)$$

$$(\sigma_\theta)_{r=r_{fi}} \leq T \qquad (A2.3)$$

(4). All pressure values are considered positive when compressive and negative tensile.

A2.2 Stress analysis

A2.2.1 General equations

Assuming plane strain the general basic equations consist of the following:

strain-stress:

$$\varepsilon_r = \frac{1}{E}\left[\sigma_r - \nu\sigma_\theta\right] \tag{A2.4}$$

$$\varepsilon_\theta = \frac{1}{E}\left[\sigma_\theta - \nu\sigma_r\right] \tag{A2.5}$$

$$\varepsilon_z = -\frac{\nu}{E}\left[\sigma_\theta + \nu\sigma_r\right] \tag{A2.6}$$

Where, in a cylinderical co-ordinate (r, θ, z), σ_r, σ_θ, and σ_z are the direct stresses, ε_r, ε_θ, and ε_z are the strains, E is Young's modulus, ν is Poisson's ratio.

Equilibrium:

The general equilibrium equations corresponding to axi-symmatric solid of revolution with centrifugal body force are expressed as follows

$$\frac{\partial\sigma_r}{\partial r} + \frac{\partial\sigma_z}{\partial z} + \frac{\sigma_r - \sigma_\theta}{r} + F_r = 0 \tag{A2.7}$$

$$\frac{\partial\sigma_\theta}{\partial\theta} = 0 \tag{A2.8}$$

$$\frac{\partial\sigma_z}{\partial r} + \frac{\partial\sigma_z}{\partial z} + \frac{\sigma_z}{r} + F_z = 0 \tag{A2.9}$$

A2.2.2 Analytical solution for stresses

Analytical solution for stress in the respective region can be analyzed in the following procedure

(i) Solution for core region

First consider the body of the inner rotor as a circular shape of uniform thickness rotating with constant speed ω rad/sec. The body force is centrifugal force figure 3.3.

$$F_r = \rho\omega^2 r \qquad (A2.10)$$

where ρ is the average density of the material of the inner rotor and the equilibrium equation (A2.7-A2.9) reduce to one only

$$\frac{\partial\sigma_r}{\partial r} + \frac{\sigma_r - \sigma_\theta}{r} + \rho\omega^2 r = 0 \qquad (A2.11)$$

The strain compatibility is represented by the usual expression

$$\varepsilon_r = r\frac{\partial\varepsilon_\theta}{\partial r} + \varepsilon_\theta \qquad (A2.12)$$

substituting for ε_r and ε_θ from the stress-strain equations A2.4-A2.5 into equation A2.12

$$\big(1+\nu\big)\big(\sigma_r - \sigma_\theta\big) = r\frac{\partial}{\partial r}\big(\sigma_\theta - \nu\sigma_r\big) \qquad (A2.13)$$

and from equation (A2.11) for $(\sigma_r - \sigma_\theta)$ giving:

$$r\frac{\partial}{\partial r}\big(\sigma_r + \sigma_\theta\big) = -\rho\omega^2 r^2\big(1-\nu\big) \qquad (A2.14)$$

Whence

$$\sigma_r + \sigma_\theta = -\rho\omega^2 \frac{r^2}{2}\left(1+\nu\right) + c_1 \qquad (A2.15)$$

Again, adding this to

$$\sigma_r - \sigma_\theta = -\frac{r\partial\sigma_r}{\partial r} - \rho\omega^2 r^2 \qquad (A2.16)$$

From equation (A2.11), it can be seen:

$$\frac{\partial\left(r^2\sigma_r\right)}{\partial r} = -\frac{\left(3+\nu\right)}{2}\rho\omega^2 r^3 + c_1 r \qquad (A2.17)$$

This can be integrated, giving

$$\sigma_r = -\frac{\left(3+\nu\right)}{8}\rho\omega^2 r^2 + A + \frac{B}{r^2} \qquad (A2.18)$$

$$\sigma_\theta = -\frac{\left(1+3\nu\right)}{8}\rho\omega^2 r^2 + A - \frac{B}{r^2} \qquad (A2.19)$$

$$\sigma_z = 0 \qquad (A2.20)$$

The arbitrary constants A and B are calculated by considering the boundary conditions for inner rotor case.

Boundary condition

For core regions of the inner rotor subjected to internal pressure p_i and external pressure p_o, figure 3.3, the boundary condition will be assumed to take the following form

$P = p_i$ at $r = r_c$ hence $\sigma_{r(r=r_c)} = -p_i$

$P = p_o$ at $r = r_{fi}$ hence $\sigma_{r(r=r_{fi})} = p_o$

By re-calling the stresses distribution equation (A2.18) and applying the above boundary conditions, the resulting expressions for A and B are obtained as follows:

$$B = \frac{r_{fi}^2 r_c^2 \left(p_o + p_i\right)}{\left(r_{fi}^2 - r_c^2\right)} + \frac{\rho\left(3+\nu\right)\omega^2 r_{fi}^2 r_c^2}{8} \qquad (A2.21)$$

$$A = \frac{2r_{fi}^2}{\left(r_{fi}^2 - r_c^2\right)} p_o + \frac{2r_c^2}{\left(r_{fi}^2 - r_c^2\right)} p_i + \frac{\rho\omega^2\left(3+\nu\right)\left(r_{fi}^2 + r_c^2\right)}{4} \qquad (A2.22)$$

ii. Solution for slot region

The slot region is subjected to internal pressure and fitted to the solid bore region, due to the interfance fit with solid core region figure 4.4. Consequently the tangential stress (σ_θ) will be equal to zero (according to the assumption shown in section A2.1)

$\sigma_\theta = 0 \quad$ at $r_{fi} \leq r \leq r_{fo}$

and by adopting the following boundary conditions:

$P = p_o \quad$ at $r = r_{fo} \quad$ hence $\sigma_{r(r=fo)} = 0$

$P = p_i \quad$ at $r = r_{fi} \quad$ hence $\sigma_{r(r_{fi})} = p_i$

Again, by re-calling the equilibrium equation (A2.11), and this would read

$$\frac{\partial\sigma_r}{\partial r} + \frac{\sigma_r - \sigma_\theta}{r} + \rho\omega^2 r = 0 \qquad (A2.23)$$

or

$$\frac{\partial\left(r\sigma_r\right)}{\partial r} - \frac{\sigma_\theta}{r} + \rho\omega^2 r^2 = 0 \qquad (A2.24)$$

But

$$\frac{\sigma_\theta}{r} = 0 \qquad (A2.25)$$

$$\frac{\partial(r\sigma_r)}{\partial r} + \rho\omega^2 r^2 = 0 \qquad (A2.26)$$

By intergrating equation (A2.26)

$$r\sigma_r + \frac{\rho\omega^2 r^3}{3} = A \qquad (A2.27)$$

$$\sigma_r = \frac{A}{r} - \frac{\rho\omega^2 r^2}{3} \qquad (A2.28)$$

Applying the boundary conditions, the constants A would be read

$$A = \frac{\rho_o \omega^2 r_{fo}^3}{3} \qquad (A2.29)$$

$$\sigma_{r_{(r=r_{fi})}} = -\frac{\rho_o \omega^2 r_{fi}^2}{3}\left[1 - \left(\frac{r_{fo}}{r_{fi}}\right)^3\right] \qquad (A2.30)$$

or

$$p_o = -\frac{\rho_o \omega^2 r_{fi}^2}{3}\left[1 - \left(\frac{r_{fo}}{r_{fi}}\right)^3\right] \qquad (A2.31)$$

iii. Solution for the inner rotor regions

Now the solution of the whole problem could easily be obtained by substituting the equation (A2.31) into equations (A2.21) and (A3.22), the constant A and B would read:

$$A = \omega^2\left[\frac{2r_{fi}\rho_o\left(r_{fo}^3 - r_{fi}^3\right)}{3\left(r_{fi}^2 - r_c^2\right)} + \frac{\rho\left(3+\nu\right)\left(r_c^2 + r_{fi}^2\right)}{4}\right] + \frac{2r_c^2 p_i}{\left(r_{fi} - r_c^2\right)} \qquad (A2.32)$$

or

$$A = \omega^2 r_{fi}^2 \Big[\frac{2\rho_o \big(y^3 - 1\big)}{3\big(1 - x^2\big)} + \frac{\rho\big(3 + \nu\big)\big(1 - x^2\big)}{4} \Big] + \frac{2x^2 p_i}{\big(1 - x^2\big)} \qquad (A2.33)$$

and

$$B = \frac{r_c^2 r_{fi}^2}{\big(r_{fi}^2 - r_c^2\big)} \Big[p_i + \omega^2 \Big(\frac{\rho_o \big(r_{fo}^3 - r_{fi}^3\big)}{3 r_{fi}} + \frac{\rho\big(3 + \nu\big)\big(r_{fi}^2 - r_c^2\big)}{8} \Big) \Big] \qquad (A2.34)$$

or

$$B = \frac{x^2 r_{fi}^2}{\big(1 - x^2\big)} \Big[p_i + \omega^2 r_{fi}^2 \Big(\frac{\rho_o \big(y^3 - 1\big)}{3} + \frac{\rho\big(3 + \nu\big)\big(1 - x^2\big)}{8} \Big) \Big] \qquad (A2.35)$$

Where

Ω is critical speed, $\Omega = \omega \times r_{fi}$

x is radii ratio, $x = \frac{r_c}{r_{fi}}$

y is radii ratio, $y = \frac{r_{fo}}{r_{fi}}$

ρ is rotor body density

ρ_o is slot/tooth effective density

Finally, substitute equations (A2.33) and (A2.35) into (A2.19), The resulting expressions for hoop stress at r_c and r_{fi} will read in normalized form as follows:

$$\sigma_{\theta_{(r=r_c)}} = \frac{1}{12(1 - x^2)} \{ 12\big(1+x^2\big) p_i + 8\omega^2 r_{fi}^2 \rho_o \big(y^3 - 1\big) + 3\omega^2 r_{fi}^2 \rho \big(1 - x^2\big) \big[\big(1-\nu\big) x^2 + \big(3+\nu\big) \big] \} \qquad (A2.36)$$

$$\sigma_{\theta_{(r=r_{fi})}} = \frac{1}{12(1 - x^2)} \{ 24 p_i x^2 + 4\omega^2 r_{fi}^2 \rho_o \big(y^3 - 1\big)\big(1+x^2\big) + 3\omega^2 r_{fi}^2 \rho \big(1 - x^2\big) \big[\big(1-\nu\big) + \big(3+\nu\big) x^2 \qquad (A2.37)$$

But

$$\Omega = \omega \times r_{fi}$$

and according to the following critical conditions

$$\sigma_{r_{(r=r_{fi})}} \leq T_o$$

$$\sigma_{\theta_{(r=r_c)}} \leq T$$

$$\sigma_{\theta_{(r=r_{fi})}} \leq T$$

Then, equations A2.30, A2.36, and A2.37 may be written as

At $r = r_{fi}$

$$T_o \geq -\frac{\rho_o \Omega^2}{3}\left[1 - y^3\right] \qquad (A2.38)$$

At $r = r_c$

$$T \geq \left(\frac{1}{12(1-x^2)}\right)\{12\left(1+x^2\right)p_i + 8\Omega^2\rho_o\left(y^3-1\right) + 3\Omega^2\rho\left(1-x^2\right)\left[\left(1-\nu\right)x^2+\left(3+\nu\right)\right]\} \qquad (A2.39)$$

At $r = r_{fi}$

$$T \geq \left(\frac{1}{12(1-x^2)}\right)\{24p_i x^2 + 4\Omega^2\rho_o\left(y^3-1\right)\left(1+x^2\right) + 3\Omega^2\rho\left(1-x^2\right)\left[\left(1-\nu\right)x^2+\left(3+\nu\right)\right]\} \qquad (A2.40)$$

From equations A2.38 and A2.39, the inner rotor bursting speed must always be subject to the constraint

$$\Omega \leq -\left[\frac{3T_o}{\rho_o\left(1-y^3\right)}\right]^{1/2} \qquad (A2.41)$$

and

$$\Omega \leq \left[\frac{12T\left(1-x^2\right)-12\left(1+x^2\right)p_i}{8\rho_o\left(y^3-1\right)+3\rho\left(1-x^2\right)\left[(1-\nu)x^2+\left(3+\nu\right)\right]}\right]^{1/2} \qquad (A2.42)$$

and

$$\Omega \leq \left[\frac{12T\left(1-x^2\right)-24x^2p_i}{4\rho_o\left(y^3-1\right)\left(1+x^2\right)+3\rho\left(1-x^2\right)\left[(1-\nu)x^2+\left(3+\nu\right)\right]}\right]^{1/2} \qquad (A2.43)$$

APPENDIX 3

PUBLICATIONS

3.1. Introduction

Two papers will be published in connection with the research presented in this thesis. They are as follows,

Paper 1 : Safi, S.K. & Bumby, J.R., *A Two-Dimensional Analysis of the Space Harmonic Magnetic Fields in a Superconducting a.c. Generator.*, Electric Machines and Power System, Paper to be published 1990.

Paper 2 : Safi, S.K. & Bumby, J.R., *Application of Optimization Methods in the Design of a Superconducting a.c. Generator Rotor.*, Paper in preparation.